LABORATORY ANALYSIS OF HYPERCONCENTRATIONS

By

Pierre Y. Julien and Yongqiang Lan

Colorado State University

February 1989

CER88-89PYJ-YL11

LABORATORY ANALYSIS OF HYPERCONCENTRATIONS

By

Pierre Y. Julien and Yongqiang Lan

Colorado State University

February 1989

CER88-89PYJ-YL11

ACKNOWLEDGMENTS

The authors are grateful to Professor E. V. Richardson, who not only demonstrated great enthusiasm and interest in this study but also supported Mr. Y.Q. Lan during the course of his Ph.D. studies at Colorado State University.

TABLE OF CONTENTS

LIST OF FIGURES

LIST OF TABLES

LIST OF SYMBOLS

a_1	empirical constants
A	Conversion coefficient in definition of concentration.
A_1, A_2	constants
A, B, C	Integration constants in velocity distribution.
A_n, B_n,	Integration constants in velocity distribution.
C_D	drag coefficient
C_n,C'_n,	Integration constant in velocity distribution.
C_v	Volumetric sediment concentration
C_{vm}	maximum attainable concentration for maximum viscosity.
C_{vo}	critical concentration for the formation of Bingham plastic fluid.
C_w	sediment concentration by weight.
d	particle diameter in microns.
dP	percentage of the volume of a certain particle diameter to the total particle volume.
d_f	apparent floc diameter.
d_{app}	apparent particle diameter.
du/dy	rate of shear
D	Particle diameter
D_{50}	diameter of particles of which 50% is finer.
D_i	graded particle diameter
D_m	Maximum possible particle diameter
D_s	diameter of suspended particles
D_u	hypothetical diameter of the unsheared envelope surrounding the sphere with a uniform thickness defined by Valentik and Whitmore.
D_v^*	non-dimensionized dispersive parameter
E	measure of elastic properties
f	Fanning friction coefficient.
f_D	Darcy-Weisbach friction factor.
f_T	Tomita's defined friction factor.

F_D	drag force on a particle
F_{KM}	Krieger and Maron coefficient.
g	acceleration of gravity
G	constant.
h	height of stationary cylinder emmerged in fluid in the viscometer.
H	flow depth in open channel.
He	particle Hedstrom number
k	roughness thickness of the wall.
k	constant.
k_b	ratio of the volume of bonded particle to that of unbonded particle.
k_1, k_2	coefficients.
K	constant
K'	coefficient in Metzner and Reed's generalized relation
L	measure of length.
m	exponent
n	flow behavior index or power law exponent.
n'	coefficient in Metzner and Reed's generalized relation.
n"	$= \frac{d(\ell nT)}{d(\ell nN)}$,
N	speed of rotating cylinder, rps.
O_p	orientation of particle in suspension
p	hydraulic pressure, pressure head or hydraulic head.
P_x	pressure gradient = -dP/dL.
ΔP	pressure drop over length L.
$\overline{P}$	plasticity number defined by Plessis and Ansley.
Q	Total discharge of hyperconcentrated flow.
r	regression coefficient.
r	radial coordinate in cylindrical coordinate system.
R	diameter of pipe

R	diameter of stationary plate in the cone-and-plate viscometer.
R	hydraulic radius in open channel.
Re	conventional Reynolds number.
Re_B	Bingham Reynolds number
$(Re_B)_c$	critical Bingham Reynolds number below which laminar flow is present.
Re_c	Clapp's defined Reynolds number .
Re_{MR}	Metzner and Reed generalized Reynolds number.
Re_{pl}	generalized Reynolds number for power law fluids.
Re_{pl}	power law Reynolds number.
$(Re_p)_2$	Ryan and Johnson's defined Reynolds number.
Re_T	Tomita's defined Reynolds number.
R_i	diameter of inner cylinder of rotational concentric viscometer.
R_o	diameter of outer cylinder of rotational concentric viscometer.
$s=R_o/R_i$	
s_p	surface area per unit volume of the actual particle.
s_o	surface area per unit volume of a sphere or cube of equivalent dimension = 6/d.
S	channel slope.
t	time
T	torque
T_D^*	dimensionless turbulent/dispersive ratio
Tr	Trask sorting coefficient
u	velocity of flow or particle
u^+	dimensionless velocity.
U_*	friction velocity.
U_m	maximum flow velocity.
U_o	velocity of approaching fluid near a particle
V	cross-sectional average velocity.
V_p	average volume of particle

x	coordinate along downstream direction.
y	upward distance above channel bed or wall.
y^+	dimensionless coordinate.
y_2^+	coefficient.
y_0	thickness of flow "plug"
Y	yield number.
z	Rouse number = $\frac{\omega_0}{\beta\ kU_*}$
z_k	modified Rouse number
α	angle of internal friction.
α	ratio or factor.
α_1, α_2	coefficients
β	generalized viscosity = $K'8^{n'-1}$.
β_1, β_2	coefficients
θ	spring deflection
θ	angle of slope in open channel.
σ	standard deviation.
σ_z	Inclusive Graphic Standard Deviation or Sorting coefficient.
ϵ	coefficient.
ϵ_s	diffusion coefficient for sediment
ϵ_w	diffusion coefficient for water
ρ	density of fluid
ρ_m	density of water-sediment mixture.
ρ_s	density of sediment particle
ℓ	mixing length of fluid.
ℓ_m	mixing length of suspension.
κ	von Karman constant.
λ	linear sediment concentration.
θ_b	coefficient of the pores caused by particle collisions.

δ	thickness of bonded water on particle surface
δ	boundary layer thickness
γ_s	unit specific weight of particles
γ_f	unit specific weight of mixture formed by water and fine particles
ω	settling velocity of particle in suspension
ω_0	settling velocity of single particle in an infinite mass of fluid.
Φ	particle diameter scale defined as Log_2D.
ψ_1	first shape factor of particle
ψ_1	second shape factor of particle.
ψ_p	shape factor of particle
Ω	angle between the cone and the plate
η	dynamic viscosity of fluid or coefficient of rigidity.
η_p	consistency index or power law coefficient.
ξ	dimensionless distance = y/R or y/H.
ζ	turbulent-dispersive parameter.
ν	kinematic viscosity of fluid.
μ	dynamic viscosity of fluid.
μ_a	apparent dynamic viscosity.
μ_e	effective dynamic viscosity.
μ_∞	limiting dynamic viscosity.
τ	shear stress in general.
τ_0	boundary shear stress
τ_y	yield shear stress
τ_w	wall shear stress
τ^*	dimensionless excess shear stress
χ	dimensionless parameter = τ_y/τ_w.
Ξ	Coles' wake flow function.
Π	Coles' wake strength coefficient.

INTRODUCTION

Flowing water has the capacity to carry varying amounts of sediment depending on the availability of sediment and the forces exerted by water on sediment particles. The amount of sediment transported ranges from virtually none at all in a crystal clear stream to over 50 percent by volume in mudflows as experienced at Mount St. Helens. Flows with high suspended sediment concentration are common in many part of the United States. Hyperconcentrations and mudflows have been observed in the San Francisco Bay area, in rivers downstream of Mount St. Helens, in Utah, in the Southwestern United States, and in other semi-arid areas throughout the world. In many cases when floods occur sediment concentrations are quite high with flow properties and sediment transport being considerably different than expected from existing methodologies.

The presence of suspended sediment and wash load (fine sediments carried in suspension with a particle size smaller than most sediment particles found in the bed of a stream) significantly affects the flow velocity and the sediment transport capacity of natural streams. When concentrations of sediments are low, effects are negligible, but at higher concentrations both the physical and dynamic characters of the fluid flow are different from clear water flow. The viscosity and specific weight of the fluid are increased, and turbulence intensity, velocity, sediment concentration distributions, flow resistance, and sediment transport capacity are changed. When the fluid become more viscous, the fall velocity of sediment particles in suspension decreases which allows them to remain in suspension for longer periods and total sediment transport rates are markedly increased. Fluid flow and sediment transport are affected by fine material in suspension even at fairly moderate concentrations. This effect

increases with increasing concentration such that at extremely high concentrations, including hyperconcentrated flows or mudflows, the mechanics of movement and flow properties are completely different from clear-water flow. Sediment mixtures have been observed to stop flowing due to high viscosity and yield stress and as yet no new relations or theory have been developed to fully explain these observations.

This document stems from the far reaching goals of the ASCE Task Committee on Analysis of Laboratory and Field Sediment data accuracy and availability. With the general purpose to assemble and evaluate sedimentation data from laboratory and field investigations with regard to accuracy and availability, the problem of hyperconcentrations has also been included in the evaluation procedure. This document issued from a compilation of existing technology on laboratory analysis of hyperconcentrated flows has been prepared to provide guidelines for the analysis of hyperconcentrations. Among the topics to be examined figure the definition and classification of hyperconcentrations. The terminology used in defining hyperconcentrated flow is rather complex and reflects the multitude of physical processes involved. The role played by particles of various sediment sizes is to be examined with respect to the cohesive properties of clay particles. The rheological behavior of hyperconcentrations is completely altered by the presence of large concentrations of sediment particles and small proportions of cohesive sediment particles. Laboratory measurements of rheological properties are essential to dissociate between yield, viscous, turbulent and dispersive stresses. In hyperconcentrations, the settling velocity of particles can be significantly reduced owing to the non-Newtonian behavior of water-sediment mixtures. The effect of hyperconcentration on velocity profiles and resistance to flow is also to be investigated.

I. DEFINITIONS AND CLASSIFICATIONS

I-1. Terminology

The following terminology is frequently referred to in this study:

Hyperconcentrated flow — defined as a highly sediment-laden flow in which the presence of fine sediments materially affects fluid properties and bed material transport compared with the flow without an appreciate quantity of fine sediments. From this definition it appears that hyperconcentrated flow includes flows changing from water-floods to landslides. In the next two sections, it may be seen that some investigators exclude mud/debris flow and landslide from hyperconcentrated flows.

Mudflows — A mudflow is a flowing mass of predominantly fine-grained earth material that possesses a high degree of fluidity during movement. The degree of fluidity is revealed by the observed rate of movement or by the distribution of the resulting deposit. If more than half of the solid fraction of such a mass is coarser than sand, the term "debris flow" is preferable. In general, the water content of mudflow ranges from 10-60% according to various measurements. With an increase in water content, mudflows grade into loaded and clear streams; with a decrease in water content, they grade into earthflows and dry landslides.

Mudflows possess a remarkable ability to transport very large masses of rock; this ability is in large part due to a relatively high specific gravity and the high viscosity.

Landslides — Landslide is defined as a rapid downward movement under the influence of gravity of a mass of rock, earth, or artificial fill on a slope (see Varnes, 1958). The motion may be either that of a slide, flow, or fall, acting singly or together. All are forms of slope failure arising

from a high shearing stress along a potential surface of rupture which exceeds the shearing resistance along a potential surface.

Homogeneous flow — Homogeneous flows represents the flow regime in which the particles being transported are so small that the fall velocities are insignificant compared with the vertical motion of fluid, thus, the vertical distribution of sediment particles is nearly uniform.

Heterogeneous flow — Heterogeneous flow is defined as the regime in which all solids are in suspension, but the vertical sediment concentration gradient is not uniform.

I-2. Definition of Concentration

Sediment concentration is defined as the amount of sediment in a unit amount of carrying water, usually expressed in volume or in weight. The common unit for expressing suspended sediment concentration is the milligram per liter computed as 1,000,000 times the ratio of the dry weight of sediment in grams to the volume of water-sediment mixture in cubic centimeters. Other units, such as parts per million (ppm) or percent by weight, and percent by volume, have been used in the past to express suspended sediment concentration. In the analysis of hyperconcentrated flows, it is more convenient to use percent by volume as the measure of concentration. The conversion among these units is tabulated as follows;

concentration, in milligrams per liter

$$= A \times (\text{weight of sediment} \times 10^6)/\text{weight of water-sediment mixture}$$

$$= A \times \text{ppm}$$

$$= A \times C_w \times 10^6$$

$$= (\text{kg/m}^3) \times 10^3$$

$$= A \times (\rho_s C_v / (\rho + (\rho_s - \rho)\, C_v)) \times 10^6 \qquad (1.1)$$

in which the factor, A, is given by Table 1-1 and is based on specific weights of water and sediment of 1.00 g/cm^3 and 2.65 g/cm^3, respectively, C_w is the sediment concentration measured by weight and ρ and ρ_s are the densities of water and sediment, respectively.

I-3. Classification of Hyperconcentrated Flows

The presence of suspended sediment affects the flow of natural streams. When concentrations of suspended sediment are low, the effects are negligible. At high concentration, however, both the physical and dynamical characters of the flows vary with different composition of sediments. These flow patterns are generally distinguished by different names, such as waterfloods, mud floods, mud flows, landslides, debris flows, etc; depending on what kind of classification schemes is used by the authors.

The classification schemes of hyperconcentrated flows vary from engineers, geologists, geomorphologists and researchers in different part of the world. Generally such flows have been classified (Bradley and McCutcheon, 1985) according to: (1) triggering mechanism, (2) sediment composition, and (3) rheological and kinematic behaviors.

Classification by flow triggering mechanism include groupings for lahars, till flows, semi-arid mountain mud flows, and alpine mud flows. Lahars are of volcanic origin and can be induced by related earthquakes, rapid melting of snow and ice, conversion of pyroclastic flows and dry avalanches to water borne flows, breaking or ejection of crater lakes, and saturation and failure of avalanches or debris dams (Higgins, et al., 1983). Excessive rainfall can mobilize flows of material on volcano slopes which are also classified as lahars. The flow may be hot or cold (Costa, 1984). Till flows originate in sediments on or near glacier, back-wasting of slopes composed of sediment and stagnant ice, melting of debris-lahar ice, and

Table 1-1. Factors A in Eq. 3.11 for Computation of Sediment Concentration in Milligrams per Liter When Used with 10^6 Times Ratio of Weight of Sediment to Weight of Water-Sediment Mixture[a]

$\frac{\text{Weight of sediment}}{\text{Weight of sediment and water}} \times 10^6$	A	$\frac{\text{Weight of sediment}}{\text{Weight of sediment and water}} \times 10^6$	A
(1)	(2)	(3)	(4)
0- 15,900	1.00	322,000-341,00	1.26
16,000- 46,900	1.02	342,000-361,000	1.28
47,000- 76,900	1.04	362,000-380,000	1.30
77,000-105,000	1.06	381,000-398,000	1.32
106,000-132,000	1.08	399,000-416,000	1.34
133,000-159,000	1.10	417,000-434,000	1.36
160,000-184,000	1.12	435,000-451,000	1.38
185,000-209,000	1.14	452,000-467,000	1.40
210,000-233,000	1.16	468,000-483,000	1.42
234,000-256,000	1.18	484,000-498,000	1.44
257,000-279,000	1.20	499,000-513,000	1.46
280,000-300,000	1.22	514,000-528,000	1.48
301,000-321,000	1.24	529,000-542,000	1.50

[a]Based on density of water of 1.000 g/ml, plus or minus 0.005 in the range of temperature $0^{\circ}C$-$29^{\circ}C$, dissolved solids concentration between 0 ppm and 10,000 ppm, and the specific gravity of sediment of 2.65. After ASCE "Sedimentation Engineering", 1975.

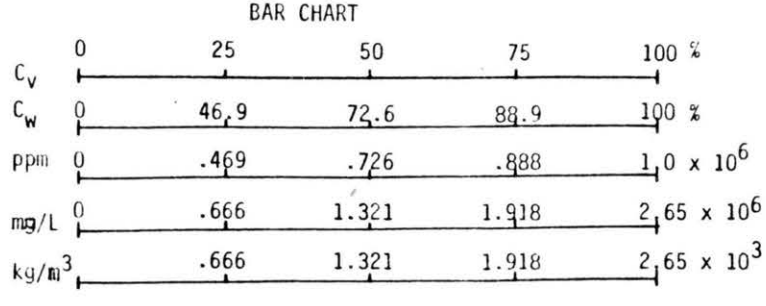

erosion and mobilization of sediment by a catastrophic release of meltwater (Costa, 1984). Semi-arid mountain mud flows and alpine mud flows are triggered by the slumping or slipping of unconsolidated materials on steep slopes (Higgins, et al., 1983). Such movement usually occurs following soil saturation during fairly intense, short-duration rainfall events.

While the above classifications have descriptive value, there is some overlap and lack of coverage, most notably for flows that are generated on lower gradient slopes. Consequently, classification by sediment content holds some advantage over schemes which are based on such a qualitative methodology. The most common classification schemes based on sediment content are given in Table 1-2 and some disagreements concerning terms and definitions are illustrated. These disagreements are mainly caused by the different composition of sediment samples used in the studies by different authors. Obviously, the physical and dynamic properties of flow with high concentration are affected not only by the sediment concentration, but also by the sediment size distribution, fine grain content, chemical properties, etc. For instance, with the same sediment concentration, flow with larger content of fine sediment has higher yield shear stress and its sediment concentration profiles are more uniform. This is why most hyperconcentrated flows with coarse materials in suspension in Japan are defined as debris flows or begin as debris flows, while most flows with fine materials in China tend to be fine-grained hyperconcentrated flows that grade into mud flows. Therefore, only sediment concentration is not sufficient to separate flow patterns.

One of the disagreements is the division between hyperconcentrated flows and mud or debris flows. In this range the National Research Council (O'Brien and Julien, 1984) introduces a new term, mud flood, whereas hyperconcentrated flow may be more descriptive. Pierson and Scott (1985)

Table 1-2. Classification of Flow with High Concentration (after Bradley and McCutcheon, 1985)

Sources	Sediment concentration in volume (S.G. = 2.65) 10 20 30 40 50 60 70 80 90 100
Beverage, and Culbertson (1966)	high | extremely high | hyperconcentrated flow | mud flow
Costa (1984)	water flood | hyperconcentrated flow | debris flow
NRC from O'Brien and Julien (1984)	water flood | mud flood | mud flow | landslides
Takahashi (1981)	debris grain flow | fall, landslides, creep sturzstorm, pyroclastic flow
Chinese investigators (Fan, Dou, 1980)	debris flow hyperconcentrated flow
Pierson and Costa (1984)	stream flow: hyperconcentrated slurry flow: (debris current) debris and mud flows solifunction granular flow: sturz-storm, debris avalanche, earth flow soil creep

have defined mud flows as having the strength by virtue of particle contact to hold interstitial water when the flow comes to a halt. Mud flow deposits are uniform and poorly sorted. They define hyperconcentrated flows where the sediment load separates into a suspended and bed load components. The fluid medium separates into two phases and sediment deposits are stratified or sorted. Pierson and Scott measured this transition between hyperconcentrated and mud flows for a 1982 lahar at Mt. St. Helens at 59 percent by volume. This value is just below the 60 percent division assigned by Beverage and Culbertson (1964). Costa (1984) estimates the division between hyperconcentrated flow and debris flow at 47 percent by volume but notes that this can not be precisely defined. He refers to measurements of maximum concentrations by volume for hyperconcentrated flows ranging from 38 to 45 percent. The NRC assigns a fairly limited range for mud floods and mud flows. O'Brien and Julien (1984) seem to indicate that this arises because landslides are delineated over an extensive range, based on minimum and maximum packing of sediment particles. The packing of uniform spheres varies from 53 to 74 percent by volume while the packing of non-uniform silts, sands, and gravels ranges from 45 to 88 percent by volume. Evidently the lubricating action of interstitial water is ignored in assigning a range of 50 to 90 percent by volume to landslides. Furthermore, there are a number of observations of mud or debris flows in channels that fall within this range and thus dispute this classification. Fan and Dou (1980) note that concentration of 78 percent by volume have been observed in tributaries of the Yellow River, and 82 percent by volume in the Jiangjia Ravine debris flow. Fei (1983) notes measurements of 83 percent concentration by volume in the Yellow River. Costa summarizes debris flow concentrations falling in the range of 50 to 79 percent for flows in

Wrightwood Canyon in California, Rio Riventado in Costa Rica, Hunshui Gully in China, Bullock Creek in New Zealand, and Mayflower Gulch in Colorado.

Pierson and Costa (1984) classified flows according to concentration and kinematic behaviors to avoid problems of using concentration as a single variable. The division between stream flow and slurry is assumed to be the transition from Newtonian and non-Newtonian behaviors. The break between slurry flow and granular flow is primarily a function of particle size and gradation. As of yet neither class can closely associated with specific concentration. Sediment size distribution, shape, cohesion or composition all seem to be important factors in such classification scheme.

Since hyperconcentrated flow is such a complex flow phenomenon that a satisfactory classification is not available. As indicated by Bradley and McCutcheon (1985), no single classification will describe all the components or describe the flow as channel geometry and sediment availability change in the downstream direction. Based on limited field evidence, the Beverage and Culbertson (1964) classification scheme seems to be more useful than the NRC scheme. The proposal by Pierson and Costa may be even more descriptive than that of Beverage and Culbertson, but the transition between hyperconcentrated flow and slurry flow remains difficult to estimate.

I-4. Sediment Size Distribution

Many observations in flumes and some observations in rivers and deltaic deposits show that sediment size in hyperconcentrated flows is finer than that in mudflows or debris flows. A typical example is given by Pierson and Scott (1985) from the analysis of mudflows and hyperconcentrated flow from the Mt. St. Helens (Figure 1-1).

Field evidences indicate that there is a significant difference for sediment size distribution between debris/mud flows and hyperconcentrated

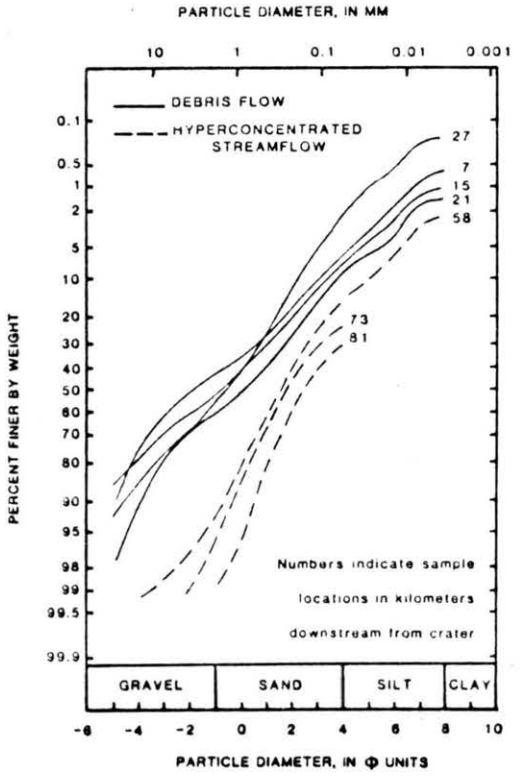

Figure 1-1. Particle Size Distribution Curves of Flow Samples from the First Flood Surge (Gray Lahar Unit) Collected Progressively Further Downstream (after Pierson and Scott, 1985).

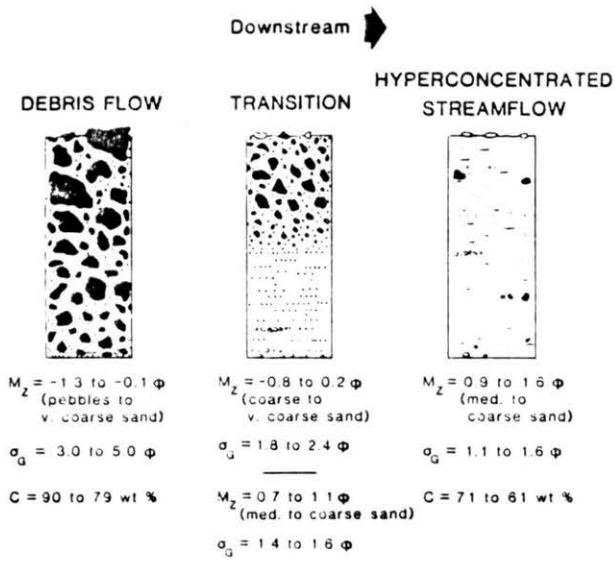

Schematic representation of deposit facies in the three main reaches. Ranges in mean grain size (M_z), sorting (σ_G), and sediment concentration by weight (C) are indicated. The M_z and σ_G values represent Graphic Mean and Graphic Standard Deviation (Folk, 1965). The scale gives particle diameter in terms of the negative logarithm to the base 2 of the diameter in millimeters (after Pierson & Scott, 1985).

flows. Debris flows are characterized by poorly sorted deposits supporting coarse angular clasts (including pebbles) in a fine-grained matrix, while hyperconcentrated flow deposits are generally better sorted and may show stratification. Furthermore, they lack a fine grained matrix, levees, terminal lobate features, large clasts and have no preferred orientation of woody debris.

The best parameters for distinguishing between debris and hyperconcentrated flows are sorting, kurtosis and percent clay. The sorting was determined by measuring the Inclusive Graphic Standard Deviation (Folk and Ward, 1957), σ_z, or the Trask sorting coefficient, Tr, which are defined respectively as;

$$\sigma_z = \frac{\Phi_{84} - \Phi_{16}}{4} + \frac{\Phi_{95} - \Phi_5}{6.6} \tag{1.2}$$

$$Tr = \sqrt{\frac{D_{75}}{D_{25}}} \tag{1.3}$$

in which Φ is defined as the particle diameter scale in terms of the negative logarithm to the base 2 of the diameter in millimeters ($\Phi = \log_2 D$). It was reported (Costa and Jarrett, 1981; Pierson and Scott, 1985; etc.) that the Trask Sorting coefficient is much higher for debris and mudflows than for hyperconcentrated flow. Debris flows have kurtosis values near 1.0 indicating even sorting between the middle and extreme parts of the distribution curve. Hyperconcentrated flows are better sorted in the middle part of the distribution than at the extremes. The amount of clay in the debris flow deposits is greater than the amount necessary to exhibit yield strength. Hyperconcentrated flows do not have the necessary clay percentage to have a yield strength.

Sediment size distributions of mud flows and debris flows are also different although these flows have all been used to describe a flow regime with sweeping variations in the concentrations of solid materials. It is generally accepted that mudflow is simply a variety of debris flow in which the mud, although not necessarily quantitatively predominant, endows the mass with specific properties and modes of behavior which distinguish it from flows of debris devoid of mud. Besides, debris flows have greater gravel content (larger than 50 %) than mudflow (Varnes, 1978).

I-5. Types of Sediment Transport

Grain movement in flows with hyperconcentration differs considerably from that in clear water flow because of the frequent interaction of particles in the suspension. Generally, moving particles can be classified into: (1) contact load or bed load; (2) suspended load; and (3) neutral buoyant load; etc.

Contact load is described as the transport of bed material in contact with bed surface either as rolling, sliding and jumping. Its submerged weight is counterbalanced by the impact caused by mutual collisions with bed particles. When the flow intensity (or flow velocity) is low, contact load may have frequent contact with the bed surface. When the flow intensity increases to a certain value, the movement of the grains will prevail in the layers below the surface, provided that the drag is large enough to overcome the frictional resistance of the surface layer. The particles moving or rolling in terms of this thin layer are thus called laminated load. In an ordinary sediment-laden flow, laminated load usually does not exist. Even if it does exist, it is relatively unimportant unless the slope of the river channel is larger than 1 percent (Qian and Wan, 1986).

Suspended load relates to sediment particles held in suspension by the interaction of vortices in turbulent flow with the particles and the interaction between particles. In most cases, potential energy from the flow is required to maintain the movement of suspended particles originated from turbulent energy.

Neutral buoyant load exists in non-Newtonian flow because of the yield shear stress. The settling velocity of fine grains is zero and no relative sediment movement will occur unless the shear stress of the flow is greater than the yield shear stress. Consequently, particles with a certain submerged weight can be kept stationary without segregation with water owing to the existence of the yield stress. The maximum diameter of neutral buoyant particles D_m can be determined by the following formula:

$$D_m = k \tau_y/(\gamma_s-\gamma_f) \tag{1.4}$$

where k is a constant, τ_y is the Bingham plastic yield shear stress, γ_s is the specific weight of particles, and γ_f is the unit weight of mixture formed by water and particles finer than one fiftieth of D_m. Experiments indicates that the constant K has an average value of 10 (Qian and Wang, 1984). In fact, the neutral buoyant particles and water mix together to form a homogeneous fluid and moves in its entirety.

II. RHEOLOGY OF HYPERCONCENTRATIONS

II-1. Fundamentals

Purely viscous, single-phase fluids and pseudohomogeneous multiphase fluid mixture that are stable even in the absence of turbulence may be classified in accordance with the nature of their response to shearing stresses under conditions resulting in unidirectional laminar flow. In other words, these fluid mixtures can be classified in accordance with their constitutive or rheological equation, namely,

$$\tau = f(\frac{du}{dy}) \tag{2.1}$$

where τ is the shearing stress imposed on the fluid which is subjected to strain at a rate du/dy, which is the velocity gradient or the rate of shear. For purely viscous fluids this equation describes the rheology of the fluid. The graphical representation of the equation is known as the rheogram for the fluid.

In the completely general case the functional relationship between the velocity gradient and the imposed shear stress is not a simple one. This is particularly evident with disperse multiphase mixtures as generally happened in hyperconcentrated flows. In general terms, then, we may expect the shearing stress within a fluid to be related not only to the rate of shear but to all other factors which determine the concentration and resistance of particles or particle agglomerates. This may be expressed as:

$$\tau = f(\frac{du}{dy}, C_v, V_p, O_p, \psi_p, K_{PF}, K_{PD}, K_{PA}, K_{PM}, t, E) \tag{2.2}$$

where C_v, V_p, O_p, ψ_p are respectively, the concentration, average volume, orientation, and the shape of the particles or agglomerates at time t after the start of shearing;

K_{PF} and K_{PD} are coefficients descriptive of the rate of formation or destruction of particles or agglomerates;

K_{PA} and K_{PM} are coefficients descriptive of the rate of alignment or misalignment of the particles or agglomerates in the direction of the shear stress;

E is measure of the elastic properties of the composite system.

Although considerable effort has been expended in the search for exact relationship among the variables which characterize the rheological behavior of fluids and fluid systems, thoroughly satisfactory constitutive equations have so far been derived only for the simplest case, the so-called Newtonian fluid. One of the major problems is the difficulty of determining, either theoretically or experimentally, the independent effect of each of the many influencing factors. On the other hand, it is possible, through reference to Equation 2.2, to explain qualitatively certain limiting forms of rheological behaviors, and this serves as a basis of classification.

Fluids are classified into various rheological types on the basis of the form of their rheological equations or rheograms. The scheme of classification is shown in Figure 2-1.

The major division is between fluids that are described as purely viscous and those that exhibit both viscous and elastic properties. Purely viscous fluids are those which, on removal of the shearing force, do not recover from any deformation they may have undergone under its action. The coefficients of any terms involving E in Equation 2.2 are zero. Viscoelastic fluids are those which, on removal of the shearing force, do, in fact, recover from the deformation they have undergone during the

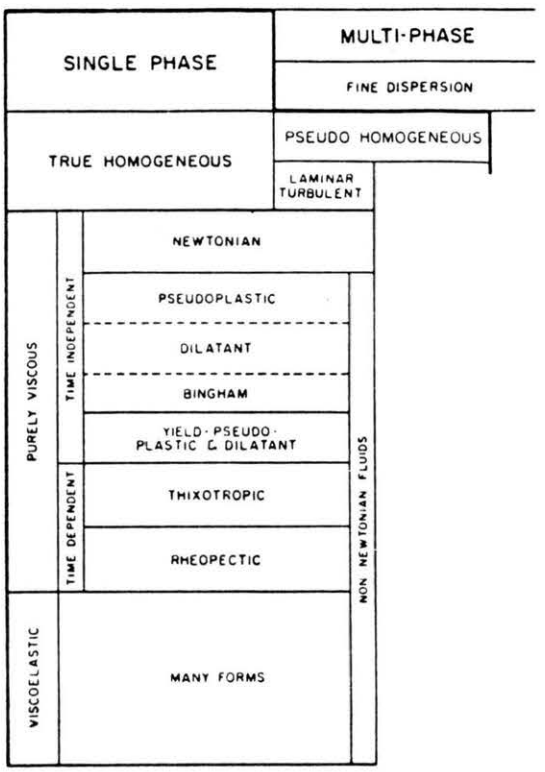

Figure 2-1. Rheological Classification of Complex Mixtures that Behave as Single-Phase Systems (after Grovier and Aziz, 1972)

shearing action. Viscoelastic fluids may be considered as substances intermediate between purely viscous fluids, on the one hand, and purely elastic solids, which recover fully from deformation up to their yield stresses, on the other hand. The coefficients of terms involving E in Equation 2.2 are not all zero. In hyperconcentrated fluids, visco-elastic characteristics are generally not found and therefore in the following chapter we will not present the rheology of viscoelastic sediment-fluid mixtures. Interested readers may refer to Govier and Aziz's book (1972).

The purely viscous fluids may be divided into the categories of time-independent and time-dependent. The first category includes those fluids which, if they exhibit development of structure or orientation of particles, have rates K_{PF}, K_{PD}, K_{PA}, and K_{PM} which are sufficiently high that, for all intents and purposes, the fluids attain an equilibrium condition immediately. Such high values of the rate constants are equivalent to a situation where the coefficients of all terms involving t in Equation 2.2 are zero. The time-dependent category includes those other fluids that have lower rates of development or decay of structure or orientation, take a measurable time to attain their equilibrium conditions, and those behavior therefore depends both upon the rate constants and duration of shear measured from a time of known condition. The coefficients of terms involving t in Equation 2.2 are not all zero.

The time-independent group of purely viscous fluids may be subdivided into several different types. The first category is that for which the rheological behavior is such that the rheogram passes through the origin of the τ and du/dy coordinates. This means that the fluid responds to the smallest applied shearing stress or that there is no "yield" strength required to be overcome before flow commences. In the language of Equation 2.2, this means that the rate constants are all high, that the coefficients

of terms involving E and t are all zero, and that C_p=0, or if C_p= 0, V_p, ψ_P, and O_p are such that the particles or agglomerates offer no resistance to the initiation of movement of the fluid. Within this "no yield" category are the Newtonian, the pseudoplastic, and the dilatant fluids.

The second category of purely viscous fluids is that for which a finite shearing stress is required before flow commences. The rheogram for these fluids does not pass through the origin of coordinates but intercepts the τ axis at a finite value known as the yield stress and characteristic of the fluid. In terms of Equation 2.2, this means that the rate constants are all high, that the coefficients of all terms involving E and t are zero, but that C_p=0 and V_p, ψ_p, and O_p are such that the particles or agglomerates offer a finite resistance to the initiation of movement of the fluid. In this "yield stress" category of fluids are the Bingham fluids and the Yield pseudoplastics.

The time-dependent group of purely viscous fluids includes the thixotropic and the rheopectic fluids. These are similar to the pseudoplastic or yield-pseudoplastic fluids except that their behavior is dependent upon the duration of shear. In Equation 2.2 the rate constants, or some of them, are not high, the coefficients of all terms involving E are zero, the coefficients of all terms involving t are not zero, and C_p, V_p, ψ_p, and O_p, or one or more of them, change with time. Details will not be given in this report because this type of flow merely occurs in hyperconcentrated flows or is not important.

In the following sections, typical time-independent purely viscous fluid models of hyperconcentrations, including Newtonian, pseudoplastic, Bingh-plastic, dilatant, yield-pseudoplastic, yield-pseudodilatant, and quadratic, are discussed. The rheograms of these fluids are illustrated in Figure 2-2. Some of the empirical models which have been proposed for

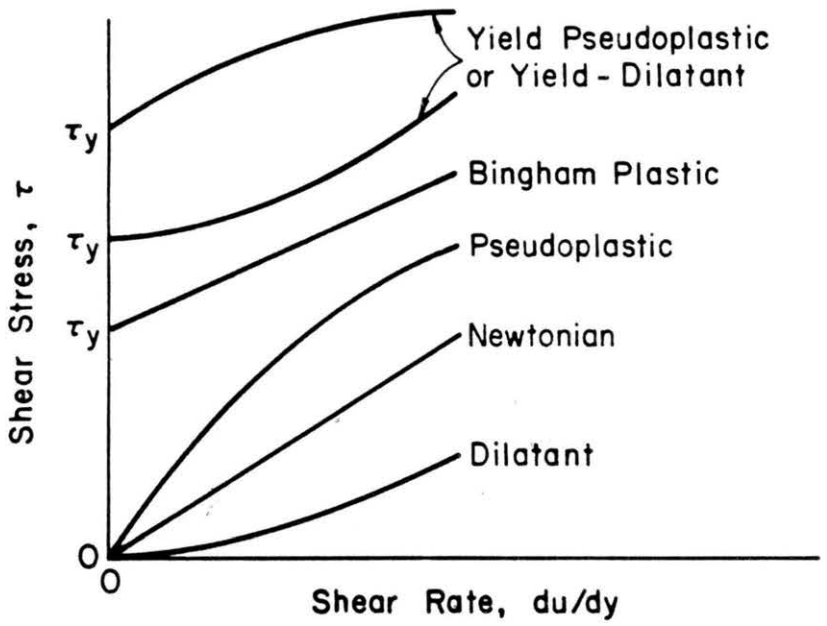

Figure 2-2. Flow Curves on Arithmetic Coordinates for Various Types of Time-Independent Fluid

relating shear stress to shear rate in these substances are given in Tables 2-1 and 2-2, respectively, for those without and with a yield stress.

II-2. Rheological Models of Fluids Without a Yield Stress

2.2.1. **Newtonian** Model

Newtonian fluids are so named because their rheological behavior follows the postulation of Newton that fluids might be expected to respond to an applied shearing stress by flowing in a manner such that the velocity gradient is strictly proportional to the applied stress. Newton postulated this for all fluids subject only to the restriction that the stress not be so high as to cause turbulence within the fluid. The Newton hypothesis is represented by the constitutive or rheological model (Schlichting, 1955)

$$\tau = \mu \frac{du}{dy} \tag{2.12}$$

where μ is the kinematic viscosity of the fluids and du/dy is the velocity gradient or the rate of shear.

In fact, hyperconcentrated fluids in the field generally do not follow the Newtonian model due to the existence of sediments and turbulence in the suspension. With no sediment or very limited sediments in the clear fluids, the rheological model can be described as

$$\tau = \mu \frac{du}{dy} + \rho \ell^2 \left(\frac{du}{dy}\right)^2 \tag{2.13}$$

where ℓ is Prandtl's mixing length and ρ is the mass density of the fluid. For laminar flow, the second term on the right hand of Equation 2.3 disappears.

Table 2-1. Rheological Models of Hyperconcentrations Without a Yield Stress

Equation	Model	Form	Reference
2.3	Power law or Ostwald-de Waele (pseudoplastic or dilatant)	$\tau = \eta_p \left(\frac{du}{dy}\right)^n$	Reiner (1949)
2.4	Ellis	$\tau = \frac{1}{A+B\tau^{\alpha-1}} \left(\frac{du}{dy}\right)$	Reiner (1960)
2.5	Prandtl-Eyring	$\tau = A \sinh^{-1}\left[\frac{1}{B}\left(\frac{du}{dy}\right)\right]$	Eyring (1936) Prandtl (1928)
2.6	Reiner-Phillippoff	$\tau = \mu_\infty + \frac{\mu_o - \mu_\infty}{1+(\tau/A)^2}\left(\frac{du}{dy}\right)$	Phillippoff (1935)
2.7	Sisko	$\tau = A\left(\frac{du}{dy}\right) + B\left(\frac{du}{dy}\right)^n$	Sisko (1958)

Table 2-2. Rheological Models of Hyperconcentrations with a Yield Stress

Equation	Model	Form	Reference
2.8	Bingham-plastic	$\tau = \tau_y + \eta\left(\frac{du}{dy}\right)$	Bingham (1922)
2.9	Herschel-Bulkley (yield-pseudoplastic or yield-pseudodilatant)	$\tau = \tau_y + \eta_p\left(\frac{du}{dy}\right)^n$	Herschel and Bulkley (1926)
2.10	Quadratic	$\tau = \tau_y + \eta\frac{du}{dy} + \zeta\left(\frac{du}{dy}\right)^2$	O'Brien and Julien 1985)
2.11	Rabinowitch-Mooney	$f(\tau) = \frac{du}{dy}$	Rabinowitch (1929)

2.2.2. **Pseudoplastic** Model

Pseudoplastic fluids are those fluids for which an infinitesimal shear stress will initiate motion, and for which the rate of increase in shear stress with velocity gradient decreases with increasing velocity gradient. This type of behavior is widely encountered in solutions or suspensions in which large molecules or fine particles for loosely bounded aggregates or alignment groupings that are stable and reproducible at any given shear rate, but which rapidly and reversibly break down or reform with increase or decrease in shear rate. There is no single or simple form of constitutive equation that accurately describes the rheological behavior of pseudoplastic fluids, although several empirical equations are useful over limited ranges of velocity gradient. These equations include the power law which will be discussed later, the Prandtl-Eyring equation (Eyring, 1936; Prandtl, 1928), the Ellis equation (Skelland, 1967), the Reiner-Philippoff equation (Philippoff, 1935), the Sisko equation (Sisko, 1958), and Cross equation (Cross, 1965).

The widely used power law in engineering calculations is described by

$$\tau = \eta_p \left(\frac{du}{dy}\right)^n \tag{2.3}$$

where η_p is the consistency index or power law coefficient and n is the flow behavior index or power law exponent. The flow behavior index, n, is readily determined as the slope of a plot of τ versus (du/dy) on logarithmic coordinates. The value of n is less than unity for pseudoplastics.

The power law fits experimental data for many pseudoplastics at intermediate velocity gradient and over a range of 10 to 100 folds, but fails both at very low and very high velocity gradients (Govier and Aziz, 1972).

2.2.3. **Dilatant** Fluid Model

Dilatant fluids are those fluids for which an infinitesimal shear stress will start motion, but for which the rate of increase in shear stress with velocity gradient increases as the velocity gradient is increased. Mathematically they are similar to the pseudoplastic model and indeed the empirical equations for pseudoplastics apply to the dilatants with appropriately different values of certain rheological constants. With reference to the power law, the flow behavior index, n, is greater than unity for dilatant fluids and less than unity for pseudoplastics.

Dilatant fluids are much less common than pseudoplastics and dilatancy is observed only in certain ranges of concentration in suspensions of irregularly shaped solids in liquids and generally restricted to high shear rate ranges (Metzner and Whitlock, 1958). For example, it was found that in a highly sheared grain dispersion the shear stress, while neglecting the viscous shear stress, can be described by a dilatant model with the flow behavior index, n, equal to 2 (Bagnold, 1954; Takahashi, 1978, 1980). Unfortunately, the application of this model to actual hyperconcentrated flows was not convincing.

II-3. Rheological Models of Hyperconcentrations with a Yield Stress

2.3.1. **Bingham-Plastic** Model

The Bingham fluid is to some extent a limiting or idealized case. It is a fluid for which a finite stress is required to initiate motion and for which there is a linear relationship between the shearing stress in excess of the initiating stress and the resulting velocity gradient. The constitutive equation for a Bingham fluid is

$$\tau - \tau_y = \eta \frac{du}{dy} \tag{2.8}$$

where τ_y=the yield shear stress,

η =viscosity of the mixture or the coefficient of rigidity.

Materials that behave as, or nearly as, Bingham plastics include pseudohomogeneous suspensions of ultrafine or fine particles in liquids at intermediate concentrations. Included among the suspensions which, within a range of concentration and especially at low shear rates, behaves as Bingham fluids are water suspensions of clay slurry or mud, fly ash, finely divided minerals, quartz, metallic oxides, and sewage sludge.

Bingham-plastic model has long been used by many researchers (Thomas, 1963; du Plessis and Ansley, 1967; Valentik and Whitmore, 1965; Fan and Dou, 1980; Wan, 1982; Mills, 1983; Higgins, et al., 1983; Cao, et al., 1983; Hou and Yang, 1983; etc.) in analyzing hyperconcentrated flows, especially flows with high fine-sediment concentration (for instance, mud or debris flows by most Chinese investigators). For narrow range of shear rates or low shear rate as happened in open channel hyperconcentrated flows, Bingham-plastic model has been successfully applied.

2.3.2. **Yield-Pseudoplastic** Model

In many hyperconcentrated suspensions there exists a yield stress, as in the case of Bingham plastics, but the relationship between the shearing stress in excess of that initiating flow and the resulting velocity gradient is not linear. Commonly the relationship exhibits convexity to the shear stress axis, the fluids showing this behavior may be called yield-pseudoplastics. (In the less common case when the curve is concave to the shear stress axis the fluid could be described as yield-dilatant.) Many clay-water and similar suspensions behave as yield-pseudoplastics, particularly at intermediate levels of concentration. A widely used yield-pseudoplastic model is given by

$$\tau = \tau_y + \eta_p \left(\frac{du}{dy}\right)^n \qquad (2.9)$$

where η_p, and n are the characterizing coefficients. This three-parameter equation, first proposed by Herschel and Bulkley (1926), was strongly supported by Chen (1983,1985) in modelling mud flows. Chen reported that Equation 2.9 is a generalized model that can cover the spectrum of Newtonian, Bingham-plastic, pseudoplastic, dilatant and power law models depending on how the yield stress, τ_y, the consistency index, η_p, and flow behavior index, n, are chosen.

2.3.3. **Quadratic** Model

Based upon physical reasoning, the shear stress encountered in fluids with large concentration of sediments should include components to describe: (1) cohesion between particles; (2) internal friction between fluid layers and sediment particles; (3) turbulence; and (4) impact of particles. The resulting yield-dilatant model proposed by O'Brien and Julien (1985) can be written in a quadratic form:

$$\tau = \tau_y + \eta \frac{du}{dy} + \zeta \left(\frac{du}{dy}\right)^2 \qquad (2.10)$$

where η is the dynamic viscosity and ζ is the turbulent-dispersive parameter. In Equation (2.10) the third term on the right hand side is referred to as the turbulent-dispersive stress combining the effects of turbulence and the effects of dispersive stress induced by the collisions between sediment particles. The conventional expression for the turbulent stress in sediment-laden flows combines with Bagnold's dispersive stress relationship because both stresses are proportional to the second power of

the rate of shear. The combined turbulent-dispersive parameter, ζ, can be written as:

$$\zeta = \rho_m \ell_m^2 + a\rho_s \lambda^2 D_s^2 \tag{2.14}$$

where ρ_m and ℓ_m are the density and mixing length of the suspension, D_s is the diameter of suspended particle, a is the empirical parameter defined by Bagnold, and ρ_s is the density of sediment particles, and λ is the linear concentration defined as the ratio of central distance between two particles and the diameter of the particles in suspension. λ can be expressed as a function of sediment concentration as

$$\lambda = \left[(C_{vm}/C_v)^{1/3} - 1 \right]^{-1}$$

where C_{vm} is the maximum obtainable concentration with a value of .65 for natural sediment and .74 for sperical particle.

Equation 2.10 has been tested against data from Govier et al. (1957), Savage and McKeown (1983) and Bagnold (1954). It is claimed that Equation 2.10 is a sound physically-based rheological model for hyperconcentrated flows (Julien and Lan, 1989).

2.3.4. **Rabinowitch-Mooney** Relations

Instead of trying to develop a rheological relation to predict the shear stress as a function of shear rate and other parameters, Rabinowitch-Moonay's relation states that shear rate can be expressed as a function of shear stress. The constitutive equation is written as

$$f(\tau) = \frac{du}{dy} \tag{2.11}$$

which was first developed by Herzog and Weissenberg (1928) and later emphasized by Rabinowitch and Mooney actually.

Many rheological equations, including the equations said above, and the Metzner and Reed's equation for viscoelastic fluids, can all be classified in to this relation.

2.3.5. **Metzner and Reed**'s Generalized Equation

A generalized approach applicable to the laminar pipe flow of any time-independent fluid has been developed by Metzner and Reed (1955), based on the Rabinowitsch equation in the form of Equation 2.15

$$-\left(\frac{du}{dr}\right)_r = \frac{8V}{D}\left[\frac{1+3n'}{4n'}\right] \tag{2.15}$$

where $$n' = \frac{d\ \ell n(D\Delta P/4L)}{d\ \ell n(8V/D)}$$

The coefficient n' is determinable from the slope of a log-log plot of $D\Delta P/4L$ versus $8V/D$ where $\Delta P/L$ is the pressure gradient at a flow velocity V in a pipe or capillary tube of diameter D under laminar flow conditions. The shear stress on the wall of the pipe of capillary tube, on the other hand, is obtained easily from force balance as,

$$\tau_w = \frac{D\Delta P}{4L} \tag{2.16}$$

Equation 2.15 has been verified by Metzner and Reed (1955) for a variety of non-Newtonian fluids including pseudoplastic, yield-pseudoplastic, and Bingham-like fluids over an intermediate range of Metzner and Reed Reynolds number Re_{MR} which is defined as

$$Re_{MR} = D^{n'} V^{2-n'} \rho/\beta \tag{2.17}$$

where $\beta = K'8^{n'-1}$

and K′ is defined in the equation

$$\frac{D\Delta P}{4L} = K'\left(\frac{8V}{D}\right)^{n'} \tag{2.18}$$

The Metzner and Reed generalized equation has been also verified for dilatant materials by Grisky and Green (1971). The generalization of Metzner and Reed are of great value in instances where the rheological behavior of the fluids is not adequately described by one of the simpler constitutive equations, or when one is involved in the direct scale-up from data taken in a small diameter pipe.

III. RHEOLOGICAL MEASUREMENTS AND ANALYSIS

Most engineers are familiar, at least in a general way, with the techniques of obtaining and interpreting laboratory data to determine the viscosity of a Newtonian fluid, but the measurement and interpretation of the rheological properties of non-Newtonian fluids and mixtures are less well understood. Skelland (1967) discusses these matters clearly and precisely. Here only a brief review will be given with emphasis on data interpretation rather than details of apparatus.

III-1. Viscometric Equipments

Three different types of apparatus are in common use for measuring viscosity or other rheological properties. Each of these is designed to create conditions of laminar shear and to permit the measurement of quantities from which the shear stress and the rate of shear may be determined. The types are the following [Skelland,1967]:

a. The **capillary viscometer** is a device that causes a sample of fluid to flow at a measured rate in laminar motion under a measured pressure gradient through a precision bore capillary tube of known diameter and length. A schematic illustration of this viscometer is shown in Figure 3-1(a). Precautions are taken to maintain constant temperature conditions, and corrections are applied for entrance and kinetic energy effects, and effective slip near the tube wall. This viscometer has the advantage of mechanical simplicity and of permitting the attainment of high rates of shear. On the other hand, the sample is subjected to a rate of shear that varies from zero at the axis of the capillary to a maximum at the wall. Also ordinary capillary viscometer do not permit the same sample of fluid to

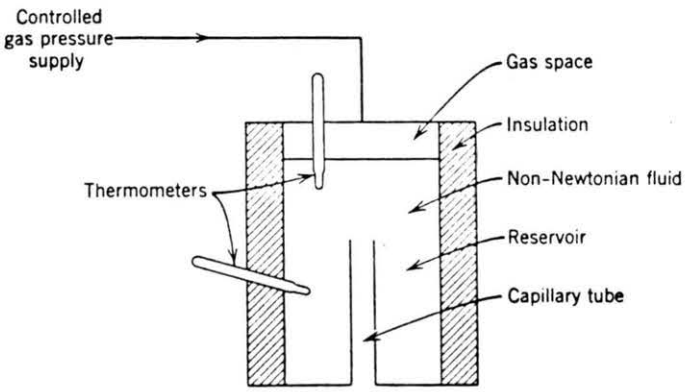

a) Schematic Diagram of a Modified Capillary Tube Viscometer

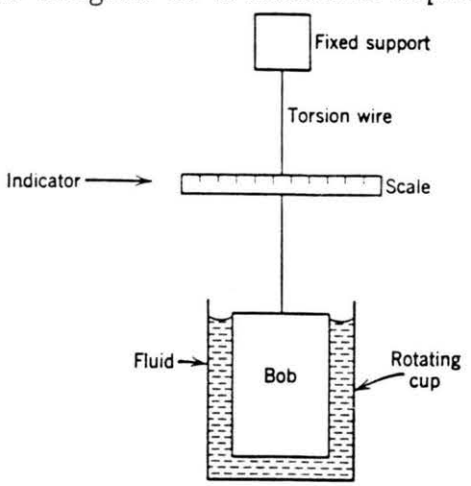

b) Schematic Diagram of the Concentric Cylinder Rotary Viscometer

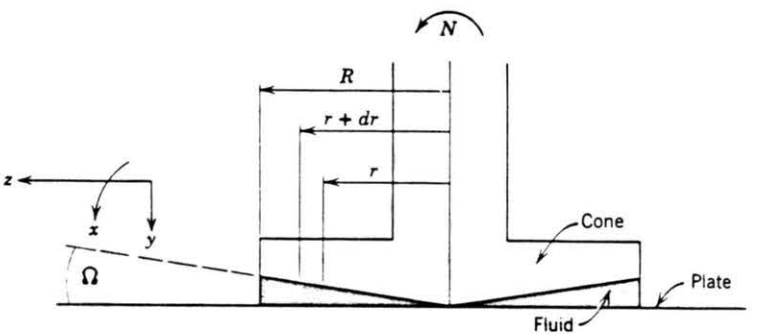

c) Schematic Diagram of the Cone-and-Plate Viscometer

Figure 3-1. Schematic Diagram of Three Different Types of Viscometers (after Skelland, 1967)

be subjected to sustained flow and thus are not suitable for measuring the behavior of time-dependent fluids.

b. The **concentric cylinder** or **rotational viscometer** permits a sample of fluid placed in the annular space between a stationary and a rotating cylinder to be subjected to shear, and the torque acting upon the stationary cylinder to be measured, as shown schematically in Figure 3-1(b). Generally, the outer cylinder is rotating and the inner one is stationary, which ensures the stable condition of flows required in the test. The rate of shear is determinable from the geometry of the system and the speed of the rotating cylinder. The shear stress is obtained from the measured torque. A variant of the design involves the use of a single rotating cylinder, which may be immersed in a sample of the fluid in any suitable container. Again precautions must be taken to ensure laminar flow and constant temperature, and end-effect corrections may be required.

The rotational viscometer is suitable for use over a wide range of rates of shear (although not the highest). With a small annular gap the shear rate is nearly constant through the fluid and this, coupled with the fact that a particular sample can be subjected to sustained shear, makes it a most useful instrument for the study of the viscous properties of non-Newtonian fluids.

c. The **cone-and plate viscometer** or the similar parallel-plate viscometer is designed to subject a sample of fluid maintained in the narrow space between a rotating, flat, circular plate and an inverted cone or a parallel plate to laminar shear, as shown schematically in Figure 3-1(c). Generally, in the absence of strong secondary flows, these instruments are useful over a reasonable range of shear rates and are ideal for the study of viscous properties of non-Newtonian fluids at low and moderate shear rates. For the cone-and plate geometry, the angle between the cone face and the

flat plate is normally less than 1 degrees. Measurements of the rotational speed and the torque permit the calculation of the rate of shear and the shear stress. Precautions are required to ensure isothermal conditions and the absence of secondary flows, but end effect corrections are usually negligible. One of the chief differences resulting from the cone-and-plate and the parallel-plate arrangements is the near constancy of the rate of shear in the cone-and-plate geometry. This allows a direct calculation of shear rate and shear stress without the necessity of differentiating the torque-rotational speed data, as must be done with the parallel-plate geometry. It should be noted, however, that the analysis for the cone and plate is only approximate for situations where elastic effects are present, and that secondary flows may cause errors in the interpretation of the data. The secondary flows are minimized by using small cone angles and low rotational speeds. A detailed discussion of these effects and indications of the range of utility of the cone-and -plate viscometer has been presented by Ginn and Metzner (1969). Generally, for an unknown fluid it is not possible to predict the magnitude of the secondary flows in the cone-and-plate geometry and the parallel plate device is preferable. Notwithstanding this, the cone-and-plate data of Ginn and Metzner and of Meister and Biggs (1969) show excellent agreement with capillary tube data and suggest that, with proper corrections for inertial effects, a cone-and-plate instrument with a cone angle of less than 2 degrees will give results suitable for most applications.

III-2. Determination of Rheograms

The interpretation of the laboratory measurements for engineering use involves the calculation of points to define the rheogram or flow curves for the fluid and, in the case of viscoelastic fluids, the calculations of the

normal stresses. This means the calculations of the rates of shear from the measured data and the corresponding shear stresses, and the normal stress difference in the case of viscoelastic fluids, and requires a complete understanding of the details of the flow of the fluids in the instrument.

3.2.1. Capillary Viscometer

With the **capillary** viscometer, the measured data related to the viscous properties, after application of any appropriate corrections, are:

Q = volumetric flow rate,

D = inside diameter of capillary,

L = effective length of capillary, and

ΔP = pressure drop due to laminar friction over length L.

The average fluid velocity is

$$V = 4Q/\pi D^2 \tag{3.1}$$

Under conditions of steady, fully developed flow through the vertical capillary tube the following force balance applies:

$$(\pi D^2/4)\Delta P = \pi DL\tau_w \tag{3.2}$$

or

$$\tau_w = \frac{D\Delta P}{4L} \tag{3.3}$$

where τ_w is the shearing stress at the wall of the capillary. The rate of shear of the capillary wall may be determined from the general equations of Rabinowitsch (1929) and Mooney (1931), i.e., Equation (2.15). The slope, n', may vary and the applicable value should be used for each value of 8V/D. For Newtonian fluids n' =1.

The interpretive procedure is, therefore,

a. to calculate τ_w from the data after any appropriate corrections, and Equation 3.3,

b. to plot τ_w versus 8V/D on logarithmic coordinates and determine n' as a function of 8V/D;

c. to calculate $(-\frac{du}{dr})_w$ from Equation 2.15;

d. to plot τ_w versus $(-\frac{du}{dr})_w$ on lines or logarithmic coordinates as preferred, and

e. if desired, to fit an appropriate one of the constitutive equations to the data to determine the expected rheological parameters.

3.2.2. Cylindrical Viscometer

The viscous property data obtained with a **concentric cylindrical** viscometer are:

R_i = diameter of the inner cylinder or the bob assumed to be stationary,

R_0 = diameter of the outer cylinder or the rotating cup,

θ = spring deflection being a measure of the torque on the stationary cylinder,

h = height of stationary cylinder immersed in fluid, corrected for end effect,

N = speed of rotating cylinder, sec^{-1}.

Neglecting end effects at the base of the bob, a simple force balance yields the following equation to calculate the torque acting upon the stationary bob;

$$\tau_{Ri}(\pi R_i h)(R_i/2) = T = K\theta \tag{3.4}$$

or

$$\tau_{Ri} = \frac{2K\theta}{\pi R_i^2 h} \tag{3.5}$$

where T is the torque on the stationary cylinder, τ_{Ri} is the shear stress on the stationary bob, and K is a suitable spring constant.

The relationship between the rate of shear and the geometry of the system is given by an equation due to Krieger and Maron (1954);

$$\left(\frac{du}{dr}\right)_{Ri} = \frac{4\pi N}{1 - s^2} F_{KM} \tag{3.6}$$

where $s = R_0/R_i$.

F_{KM} = the Krieger-Maron correction factor,

$$F_{KM} = 1 + \frac{s^2 - 1}{2s^2}\left[1 + \frac{2}{3}\ell n\ s\right]\left[\frac{1}{n''} - 1\right] + \frac{s^2 - 1}{6s^2}\ell n\ s\left[\left(\frac{1}{n''} - 1\right)^2 + \frac{d(1/n'' - 1)}{d\ \ell n\ T}\right] \tag{3.7}$$

$n'' = d(\ell n\ T)/d(\ell n\ N)$ is the slope of a logarithmic plot of T versus N.

When n' is constant, or nearly so, the equation simplifies somewhat and may be approximately by a series expansion.

Calderbank and Moo-Young (1959) have calculated values of F_{KM} from the approximate equation for series of values of s and n". These are given by Skelland (1969). For Newtonian fluids, n" =1 and F_{KM}=1.

If the annular gap between cup and bob is made very small (i.e., $s \rightarrow 1.0$), the shear rate approaches a constant value across the annulus and is given by

$$\frac{du}{dr} = 2\pi RN/(R_0 - R_i) \tag{3.8}$$

The procedure for interpreting data from the concentric cylinder viscometer is, therefore,

a. to calculate τ_{Ri} from θ, Equation 3.5 and the appropriate value of K;

b. to plot θ versus N on logarithmic coordinates and determine n" as a function of N;

c. to calculate F_{KM} for the value of s and N of interest from Equation 3.7;

d. to calculate $(\frac{du}{dr})_{Ri}$ from Equation 3.6 with appropriate values of N, s and F_{KM};

e. to plot τ_{Ri} versus $(\frac{du}{dr})_{Ri}$ on arithmetic or logarithmic coordinates as preferred, and

f. if desired, to fit an appropriate one of the constitutive equations to the data.

For **rotating cylinder viscometer**, the procedure is the same as for the concentric cylinder instrument except that the shear rate at the surface of the rotating cylinder is given by

$$\frac{du}{dr} = 4\pi N/n" \tag{3.9}$$

3.2.3. Cone-and-Plate Viscometer

The interpretation of the viscous behavior data from the **cone-and-plate** viscometer is easiest of all. The data consist of

R = diameter of the stationary plate,

Ω = angle between the cone and plate,

N = rotational speed of cone, rps,

θ = spring deflection being a measure of the torque on the plate.

The rate of shear at a radius r is given by

$$(\frac{du}{dr})_r = \frac{2\pi rN}{r\tan\Omega} \approx \frac{2\pi N}{\Omega} \tag{3.10}$$

since for small angles $\tan\Omega \approx \Omega$. As mentioned earlier, for the range of cone angles employed, the rate of shear is essentially independent of r, i.e., is constant through the fluid.

If $T = K\theta$ is the torque (where K is a suitable spring constant), then from a force balance, and since τ is constant under the constant rate of shear, we have

$$T = 2\pi\tau\int_0^R r^2 dr \tag{3.11}$$

from which

$$\tau = \frac{3K\theta}{2\pi R^3} \tag{3.12}$$

From these relations the interpretation procedure is

a. to calculate τ from the deflection, and spring constant using Equation 3.11;
b. to calculate $\frac{du}{dr}$ from the cone speed and Equation 3.12;
c. to plot τ versus $\frac{du}{dr}$ on arithmetic or logarithmic coordinates as preferred;
d. if desired, to fit an appropriate one of the constitutive equations to the data.

III-3. Analysis of Rheograms

3.3.1. Determination of Yield Stress

Yield stress, as it is defined, is the minimum shear stress required to initiate motion in the sediment suspension. It can be evaluated graphically as the shear stress at zero shear rate from the rheogram obtained hereby. Here precautions must be taken to ensure data points in the low shear rate

region, otherwise yield stress may be over/under estimated considerably because rheological relationship of the suspension at low shear rate region may not follow the same at high shear rate region. Figure 3-2 shows typical rheograms of mud and bentonite suspensions from O'Brien and Julien (1985) and Engelund and Wan (1984) illustrating this particular phenomena.

In hyperconcentrated flow (including mud and debris flows) study, a few empirical equations have been supposed to relate the yield stress to the concentration of the sediment particles, mostly basing upon the assumption that the suspension behaves as a Bingham fluid. The first equation was developed by Arrhenius and later extended by Thomas (1963)

$$\tau_y = k_1 C_v^3 \tag{3.13}$$

where k_1 is constant characterizing the suspension and dependent on the particle size and shape and electrolyte concentration. Thomas has studied the dependence of k_1 on the shape and size of particle, he finds

$$k_1 = (\frac{210}{d^2})\psi_1 \tag{3.14}$$

where k_1 is in units of lbf/ft^2, d is the particle diameter in microns, and ψ_1 is a shape factor given by

$$\psi_1 = \exp[0.7(s_p/s_0 - 1)] \tag{3.15}$$

where s_p = surface area per unit volume of the actual particles,

s_0 = surface area per unit volume of a sphere or cube of equivalent dimension = 6/d

These equations appear suitable for particles of irregular crystalline shape but not for spheroidal particles for which ψ_1 is approximately 0.1.

Thomas (1963) has extended the above work on dispersed ultrafine and fine particles to cover flocs of such particles of overall dimensions up to 115 microns. He shows that

$$\tau_y = k_1 \alpha^4 C_v^3 \tag{3.16}$$

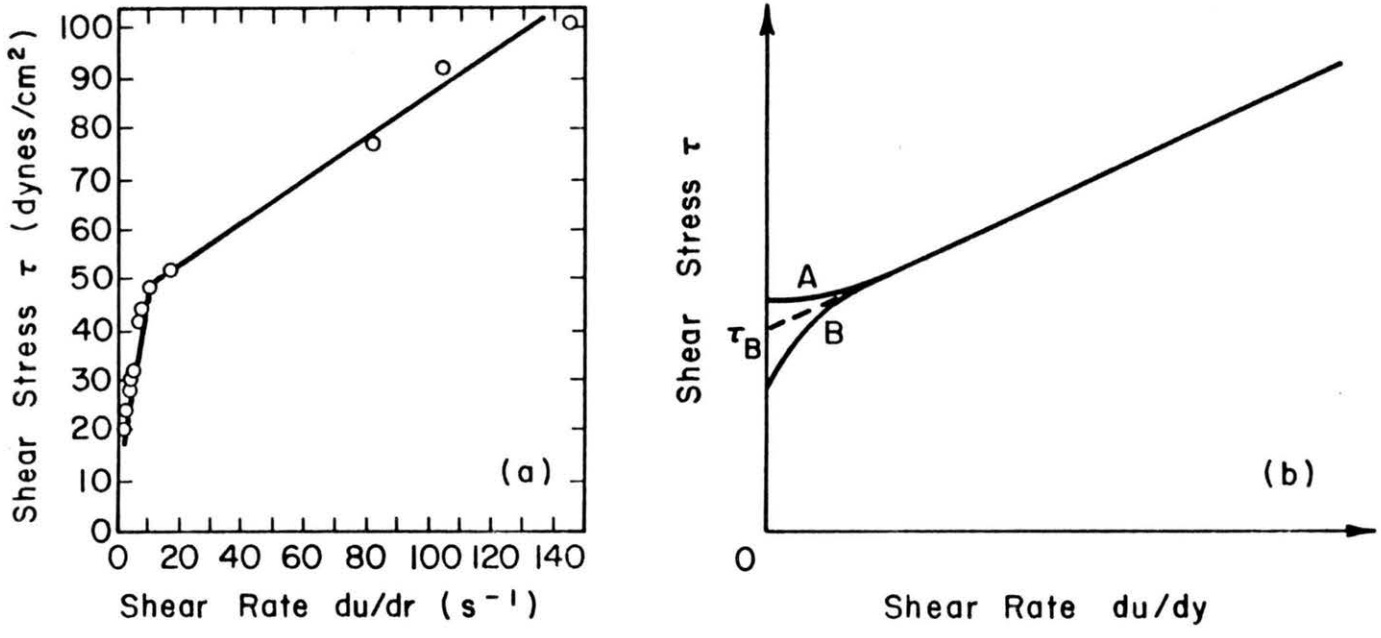

Figure 3-2. Rheograms for Clay Suspension. (a) Aspen Natural Soil (after O'Brien and Julien, 1988). (b) A - Bentonite Suspension; B - Kaoline Suspension (after Engelund and Wan, 1984)

where $k_1 = 1.55\times10^{-2}$ lbf/ft^2,

α = ratio of the volume of immobilized dispersing fluid to the volume of solids related approximately to the particle and flocs apparent diameters through the equation

$$d_f/d_{app} = (1+\alpha^2) \tag{3.17}$$

where d_f = apparent floc diameter and d_{app}=apparent particle diameter given by

$$d_{app} = d(s_0/s_p)\exp(-0.5\ln^2\sigma) \tag{3.18}$$

where σ = logarithmic standard deviation.

Street (1958) and Thomas (1963) suggested an exponential relationship between yield stress τ_y and sediment concentration by volume. Such relation has been later verified by many researchers (Qian et al., 1980; O'Brien et al., 1988) through studies of mudflow, debris flow or clay suspensions. This exponential relation is generally expressed as

$$\tau_y = \alpha_2 e^{\beta_2 C_v} \tag{3.19}$$

where coefficient α_2 and β_2 depend on the type and concentration of particles in the mixture. A summary of the results is given by O'Brien and Julien (1988) in Table 3-1.

Similar formula has been given by Fei (1983),

$$\tau_y = a \exp[M(C_v-C_{vo})/C_{vm}] \tag{3.20}$$

where C_{vo} is the critical concentration for the formation of Bingham fluid,

C_{vm} is the maximum attainable concentration for maximum viscosity, and

$M = \begin{cases} 8.45 & \text{for sediment slurry} \\ 6.87 & \text{for coal slurry} \end{cases}$

When the suspension does not appear to show Bingham properties, the above equations can not be applied to calculate the constitutive parameters of the mixture.

Table 3-1. Yield Stress and Viscosity of Mudflow Matrices (after O'Brien and Julien, 1988)

	$\tau_y = \alpha_2 e^{\beta_2 C_v}$		$\eta = \alpha_1 e^{\beta_1 C_v}$	
Source (1)	α_2 (dynes/cm²) (2)	β_2 (3)	α_1 (poises) (4)	β_1 (5)
(a) Relationships Found in Field				
Aspen pit 1	1.81×10^{-1}	25.7	3.60×10^{-2}	22.1
Aspen pit 4	2.72	10.4	5.38×10^{-2}	14.5
Aspen natural soil	1.52×10^{-1}	18.7	1.36×10^{-3}	28.4
Aspen mine fill	4.73×10^{-2}	21.1	1.28×10^{-1}	12.0
Aspen natural soil source	3.83×10^{-2}	19.6	4.95×10^{-4}	27.1
Aspen mine fill source	2.91×10^{-1}	14.3	2.01×10^{-4}	33.1
Glenwood 1	3.45×10^{-2}	20.1	2.83×10^{-3}	23.0
Glenwood 2	7.65×10^{-2}	16.9	6.48×10^{-1}	6.2
Glenwood 3	7.07×10^{-4}	29.8	6.32×10^{-3}	19.9
Glenwood 4	1.72×10^{-3}	29.5	6.02×10^{-4}	33.1
(b) Relationships Found in Literature				
Iida (1938)	--	--	3.73×10^{-5}	36.6
Dai et al. (1980)	2.60	17.48	7.5×10^{-3}	14.39
Kang and Zhang (1980)	1.75	7.82	4.05×10^{-2}	8.29
Qian et al. (1980)	1.36×10^{-3}	21.2	--	--
	$\sim 5.0 \times 10^{-2}$	~15.48	--	--
Chien and Ma (1948)	5.88×10^{-2}	19.1~32.7	--	--
Fei (1981)	1.66×10^{-1}	25.6	--	--
	$\sim 4.7 \times 10^{-3}$	~22.2	--	--

3.3.2. Determination of Viscosity

The viscosity or the coefficient of rigidity of Bingham suspension can also be expressed as a function of solid particle concentration by volume. A widely applied formula is

$$\mu_r = (1-\xi C_v)^{-m} \tag{3.21}$$

where μ_r is the ratio of the viscosity of the suspension to that of clear water at the same temperature, ξ is a coefficient related to the size, shape and composition of the sediments in suspension, and m is an exponent with a common value of 2.5. Considering that both the particles themselves and the bonded water, which is strongly attached to the surface of fine grains with a thickness of δ, contribute to the viscosity of the suspension, Fei (1983) derived the same formula and an equation to calculate the coefficient ξ,

$$\xi = 1 + 6\alpha\delta\Sigma(\Delta P_i/D_i) \tag{3.22}$$

where α is a coefficient and ΔP_i is the percentage of particles with diameter D_i. If we let $C_{vm}=1/\xi$, μ_r becomes infinity when $C_v=C_{vm}$. C_{vm} is then called the maximum concentration for maximum viscosity. And Equation 5.22 can be rewritten as

$$\mu_r = (1-C_v/C_{vm})^{-m} \tag{3.23}$$

where m equals 2.5, which is exactly the same formula as used by Landel et al. (1963) to calculate the viscosity of Newtonian suspension of fine particles.

Thomas (1963) also related the viscosity of the suspension to the sediment concentration in an exponential form as,

$$\mu_r = \exp(k_2 C_v) \tag{3.24}$$

where k_2 is a coefficient given by

$$k_2 = 2.5 + 14\psi_2/\sqrt{d} \tag{3.25}$$

in which ψ_2 is a second shape factor defined as

$$\psi_2 = \sqrt{s_p/s_0} \quad , \tag{3.26}$$

and d, s_p, s_0 are as defined above.

A more general regression relation has been given in a similar exponential form as Equation (3.19), i.e.

$$\eta = \alpha_1 e^{\beta_1 C_v}$$

which is popularly used all over the world (Thomas, 1963; Dai and Wan, 1980; O'Brien, 1986; O'Brien and Julien, 1988, etc.). A summary of tested results by O'Brien and Julien for the coefficients α_1 and β_1 is also given in Table 3-1.

"Apparent viscosity" of a non-Newtonian fluid, μ_a, is defined as the ratio of shear stress to the corresponding shear rate, that is,

$$\mu_a = \tau/(du/dy) \tag{3.27}$$

Generally the apparent viscosity of a suspension is a function of particle size and shape, composition of solid particles, and shear rate applied to the fluid. For Bingham plastic fluids, μ_a is independent of the shear rate, while for pseudoplastic fluids, μ_a declines from μ_0 at du/dy=0. asymptotically to a limiting value μ_∞ as du/dy $\rightarrow \infty$.

3.3.3. Dispersive Shear Stress

Dispersive shear stress was introduced by Bagnold (1954) to denote the shear stress induced by interparticle collisions in the suspension when the solids concentration is high. It is included in the turbulent-dispersive shear stress term in the quadratic model (Eq. 2.10). The theoretically derived expression for the dispersive shear stress is

$$\tau_D = a_1 \rho_s (\lambda D_i)^2 \left(\frac{du}{dy}\right)^2 \sin\alpha \tag{3.28}$$

where α is the angle of internal friction, and the other parameters are as defined before (Equation 2.14). Equation 3.28 is based on the assumption that uniformly dispersed, spherical particles of equivalent mass exchange

momentum in an elastic collision and viscous stresses in the suspension are negligible. This assumption may not be true since collisions between non-uniform, angular particles of different sizes, traveling through a fluid at different velocities , are generally inelastic, which implies that a calibration is required in the equation. On the other hand, the proportional coefficient a_1 in the equation is a variant being a function of sediment concentration (Bagnold, 1954) and possibly flow velocity in the open channel flows (Takahashi, 1980).

Bagnold used a flexible rubber inner cylinder wall in his concentric cylindrical viscometer to measure the shear stress of hyperconcentrations under high rates of shear. At low rates of shear, viscosity dominates and the stresses are linearly proportional to the shear rate. Under high rate of shear, Bagnold suggested that the dominant shear stress can be contributed to interparticle friction and collisions. In this grain inertia region, both the normal and shear stresses depend on the second power of the shear rate. The rheograms he obtained from neutral buoyant suspension are presented in Figure 3-3(c). It was from the high shear region where the slope of rheogram is two in the log-log graph, that the dispersive shear stresses were determined. The coefficient a_1 obtained thus by Bagnold are functions of concentration λ as shown below

λ	a_1
<14	0.034
14.5	0.043
17.0	0.17

although suspension with concentration $\lambda > 14$ is unrealistic in natural stream; while Takahashi gave different values of a_1 from different discharge of inertial flows generated in a flume (Takahashi, 1980)

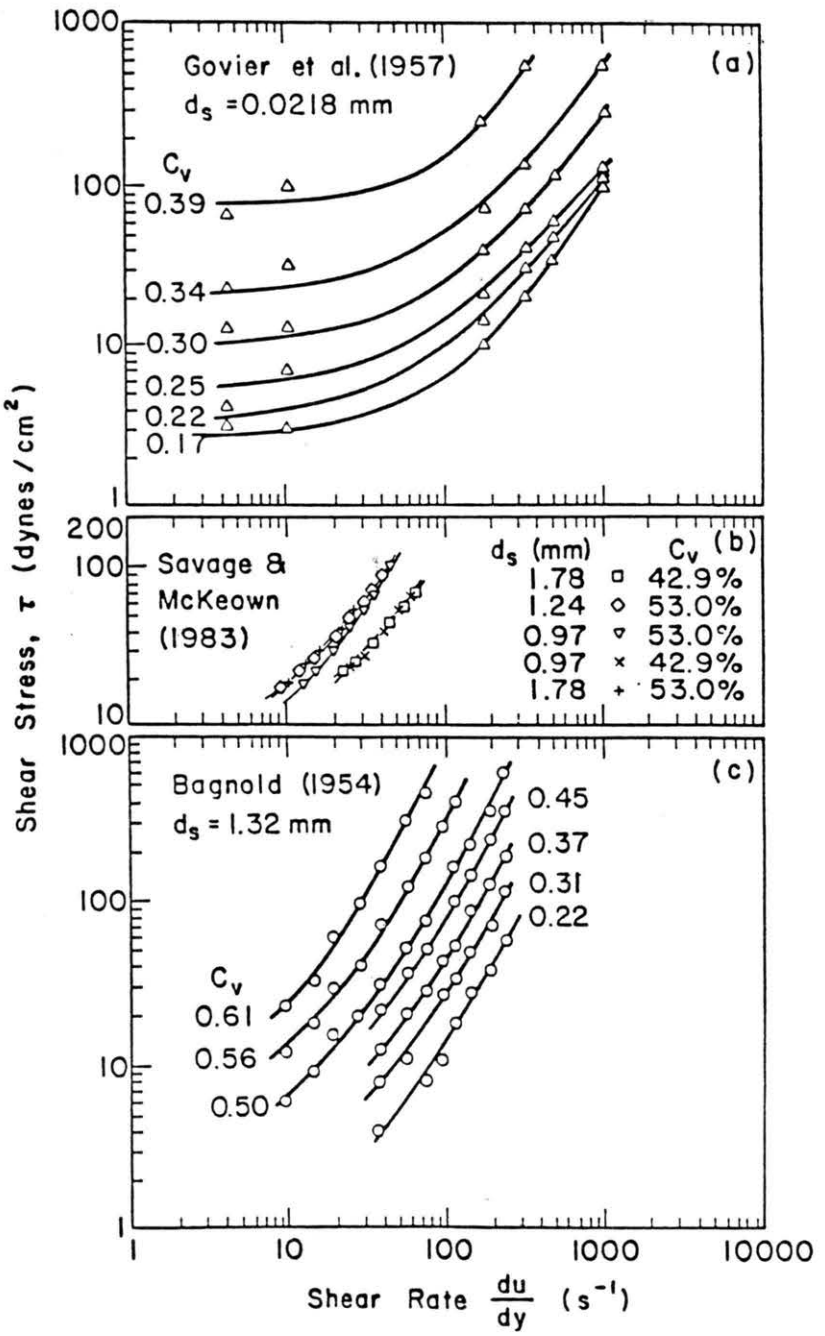

Figure 3-3. Shear Stress Versus Shear Rate from Experiments (after Julien and Lan, 1989)

Q(ℓ/s)	a_1
2.1	0.5
1.5	0.35

with no measurement on sediment concentration.

Equation 3.28 has been utilized by Lowe (1976), Takahashi (1978, 1980), and Savage (1979) and Savage and McKeown (1983) to investigate momentum exchange in grain flows. Takahashi (1980) applied it to open channel mud and debris flows to predict the flow velocity distributions, but the results were not convincing due to the unreasonable ignorance of other shear stress components such as turbulence in the suspensions. Obviously this simulation will be improved if the total shear stress set to equal to the sum of dispersive stress, viscous stress and turbulent stress, as described in the Quadratic rheological model (Equation 2.10).

3.3.4. Example of Analysis of Rheogram Using the Quadratic Model

The rheological properties of hyperconcentrated sediment mixtures have been studied by Julien and Lan (1989) using the quadratic model (Eq. 2.10) and experimental data sets from Bagnold (1954), Govier et al. (1957), and Savage and McKeown (1983). Despite the dissimilarities of sediment sizes, types and rates of shear, it is found that Eq. 2.10 fits these three data sets extremely well, as shown in Figure 3.3. The parameters τ_y, η, and ζ thus obtained for each data set are compiled in Table 3-2, which indicates that these three parameters increase with increasing sediment concentration.

Equation 2.10 can be rearranged to give its linearized dimensionless form, that is,

$$\tau^* = 1 + (1 + T_a^*)\, a\, D_v^* \tag{3.29}$$

Table 3-2. Coefficients, τ_y, η and ζ as Functions of Sediment Concentration and Types of Sediment (after Julien and Lan, 1989)

1. Govier et al.'s (1957)

d_s mm	0.0218	0.0218	0.0218	0.0218	0.0218	0.0218
C_v %	39.7	34.1	30.3	24.9	21.8	16.8
τ_y dynes/cm^2	78.4	20.7	9.84	5.00	3.20	2.61
η poises	.351	.290	.137	.093	.067	.0315
ζ g/cm	3.15×10^{-3}	2.4×10^{-4}	1.28×10^{-4}	3.10×10^{-5}	3.8×10^{-5}	6.34×10^{-5}

2. Savage and McKeown's (1983)

d_s mm	0.97	0.97	1.78	1.78	1.24
C_v %	42.9	53.0	53.0	42.9	53.0
τ_y dynes/cm^2	1.96	1.75	3.59	0.14	6.61
η poises	.715	.975	1.34	.882	.983
ζ g/cm	5.8×10^{-3}	2.55×10^{-3}	1.88×10^{-2}	2.72×10^{-3}	2.63×10^{-2}

3. Bagnold's (1954)

d_s mm	1.32	1.32	1.32	1.32	1.32	1.32	1.32
C_v %	60.6	57.0	51.1	45.6	38.5	32.0	23.0
τ_y dynes/cm^2	8.15	6.72	3.00	4.20	2.93	2.18	0.00
η poises	0.75	.485	.300	.185	.126	.083	.067
ζ g/cm	.0342	.0224	.0088	.0048	.0025	.00144	.00064

in which the three dimensionless parameters are defined as

$$(1)\quad \tau^* = \frac{\tau - \tau_y}{\eta \left(\frac{du}{dy}\right)}, \qquad \text{dimensionless excess shear stress;}$$

$$(2)\quad D_v^* = \frac{\rho_s \lambda^2 d_s^2}{\eta} \left(\frac{du}{dy}\right), \quad \text{dimensionless dispersive/viscous ratio; and}$$

$$(3)\quad T_D^* = \frac{\rho_m \ell_m^2}{a \rho_s \lambda^2 d_s^2}, \qquad \text{dimensionless turbulent/dispersive ratio.}$$

When τ^* is plotted versus D_v^* in Figure 3.4, it is observed that data sets from Bagnold, Govier et al., and Savage and McKeown can fit in a straight line together. Besides, it's clear that the parameters D_v^* can be used to delineate particular cases of the quadratic model. The results shown in Figure 3.4 indicate that τ^* is sufficiently close to unity when $D_v^* < 30$ to justify the use of Bingham plastic model. On the other hand, τ^* exceeds four when D_v^* is roughly larger than 400, which indicates that in this region the turbulent-dispersive stress is dominant.

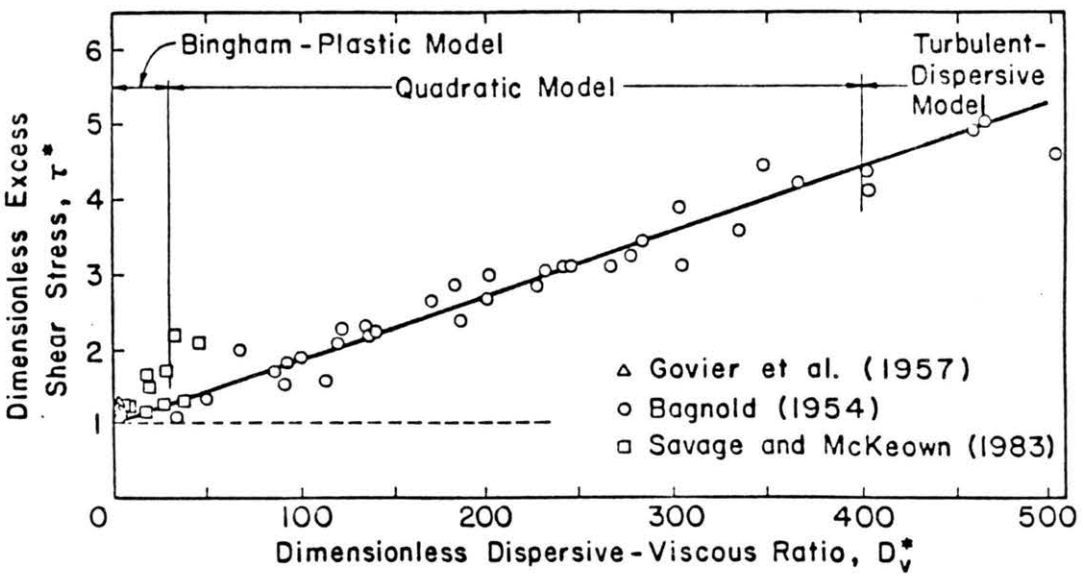

Figure 3-4. Dimensionless Plot of Shear Stress Versus Dispersive-Viscous Ratio (after Julien and Lan, 1989)

IV. SETTLING VELOCITY

The settling velocity of a given particle in a sediment-laden flow is expected to be different from that of the same particle in clear water because of the mutual interaction between particles and of a hydrodynamic interference between particles and the suspending medium, even without fine sediment. Generally, one might expect hydrodynamic interference, interparticle collision, and interaction to be the rule rather than the exception at volumetric concentrations in excess of 2 or 3 percent, and where the particles do not agglomerate the settling velocity is reduced. The magnitude of settling velocity reduced then depends upon the total sediment concentration, fine sediment concentration, and physical properties of sediment particles, etc.

IV-1. Settling in Mixtures of Fine and Coarse Particles

With both fine and coarse particles in suspension the settling properties of particles become much more complicated. Collisions and flocculation might occur after the sediment concentration reaches a certain value. Generally three categories of settling are to be expected according to the concentration as well as the sediment constituent, which is represented by the concentration for maximum viscosity. These categories are:

category 1, restricted settling of discrete particles and discrete flocs;

category 2, settling of discrete particles in suspension with flocculent structure;

category 3, slow settling of flocculent structure as a whole.

In category 1, the fine particles gather into flocs but the flocculent structure has not developed yet. Coarse particles and flocs freely settle in discrete form with interference between them. In category 2, flocculent structure starts to be formed by the fine particles and yield shear stress appears. Coarse particles, while settling across the flocculent structure, are subject to a large drag by the latter. In category 3, all the particles transform into neutral buoyant load. The flocculent structure prevents the coarse particles from settling freely and all the particles settle slowly as an entirety. Following an increase in concentration the settling of sediment will gradually transform from category 1 to category 2, and then to category 3. The coarser the sediment constituent, the higher the concentration at which transition takes place.

Over the past few decades, investigations on the settling velocity of particles in hyperconcentrated flow concentrated on category 1, leaving a blank in the studies of categories 2 and 3. And clearly, most of these studies are based on the assumptions that the suspension has Bingham fluid properties. Among these studies, Pazwash's, Valentik and Whitmore's, Plessis and Ansley's, and Ansley and Smith's retain most attention.

4.1.1. **Plessis** and **Ansley**'s Method (1967)

Plessis and Ansley treated semi-theoretically the drag force of Bingham fluid on various boundary geometry. First the yield force was obtained by integrating the yield stress over the surface of the sphere and then the submerged weight of the particles was again assumed to be the counterbalanced by the stokes drag force and the yield force. The derived expression for drag coefficient, C_D, is written as

$$C_D = \frac{24}{Re_B} + \frac{2\pi\tau_y}{\rho\omega^2} \tag{4.1}$$

where C_D is related to the fall velocity of particles in the suspension, ω, as

$$\omega^2 = \frac{4}{3}\frac{gD}{C_D}\left(\frac{\gamma_s - \gamma}{\gamma}\right) \tag{4.2}$$

For generality, Plessis and Ansley expressed C_D as;

$$C_D = f\left[\frac{He + Re_B}{Re_B^2}\right] = f(\bar{P}) \tag{4.3}$$

in which He is the particle Hedstrom number defined as $\rho D^2 \tau_y/\eta^2$ and Re_B is the Bingham Reynolds number defined as $\rho D\omega/\eta$, $\bar{P}$ was called the plasticity number in their study. With experimental data from a concentric cylindrical viscometer, Plessis and Ansley obtained by least square analysis that

$$C_D = 5.306\bar{P}^{.48} \tag{4.4}$$

with a regression coefficient r = .96.

Ansley and Smith (1967) combined in a little different manner from that of Plessis and Ansley the two dimensionless terms, i.e., Re_B and He, into a single parameter. They expressed the dynamic state of the Bingham fluid around a moving sphere in the ratio of a characteristic inertia to the sum of a viscous stress and a yield stress as

$$C_D = f\left(\frac{\rho\omega^2}{\frac{\eta\omega}{D} + K\tau_y}\right) = f\left(\frac{Re_B^2}{Re_B + KHe}\right) \tag{4.5}$$

The parameter, K, in the above expression was treated as the ratio of the contribution of the yield stress and viscous stress terms to the drag of the sphere. The value of K was determined to be $7\pi/24$ by a flow model which is composed of the field envelop sheared around the sphere. As a matter of fact, Equations (4.4) and (4.5) are the same kind.

4.1.2. Valentik and Whitmore's Method (1965)

In this method, Valentik and Whitmore attempted to resolve the problem by assuming that a moving sphere is surrounded by a concentric sphere of influence, that is, the concept of "the unsheared envelope". According to them, the submerged weight of a sphere in clay suspension is counterbalanced by two forces, yield force and drag force, which is expressed by

$$\frac{\pi D_u^2}{4} \tau_y + C_D \frac{\pi D_u^2}{4} \left(\frac{1}{2} \rho \omega^2\right) = (\rho_s - \rho) \frac{\pi D^3}{6} \tag{4.6}$$

in which D_u is the hypothetical diameter of the unsheared envelope surrounding the sphere with a uniform thickness. Generally, D_u has a value ranging from .9D to 1.6D. Then the drag coefficient is expressed as

$$C_D = \frac{4}{3} \frac{gD}{\omega^2} \left(\frac{D}{D_u}\right)^2 \left(\frac{\rho_s - \rho}{\rho}\right) - \frac{2\pi\tau_y}{\rho\omega^2} \tag{4.7}$$

4.1.3. Pazwash's Method (1970)

Pazwash's approach toward this problem is no other than Plessis and Ansley's. For the drag on a sphere in a Bingham fluid flow, he assumed that the Stokes creeping motion is valid with η instead of μ. He postulated that

$$F_D = \iint_S (\tau_0 \sin\theta + p\cos\theta) dS \tag{4.8}$$

and $$\tau_0 = \tau_y + \eta r \frac{d}{dr}\left(\frac{u}{r}\right) \tag{4.9}$$

in which τ_0 is the boundary shear stress; p is the pressure on the boundary; and r is the radius of the sphere. The drag coefficient was obtained by

$$C_D = \frac{24}{Re_B} + \frac{\pi \tau_y}{\rho U_0^2/2} \tag{4.10}$$

in which U_0 is the velocity of approaching Bingham fluid, $\tau_y/(\frac{1}{2}\rho U_0^2)$ was designated as "The Plasticity number". Equation 3.14 was generalized by an empirical factor, K_p, which depends on the shape of the boundary, as

$$C_D = \frac{24}{Re_B} + \frac{2K_p He}{Re_B^2} \tag{4.11}$$

4.1.4. **Evaluation of Each Method**

A straightforward way to evaluate a method is to compare the results of calculations with the actual measurements in hyperconcentrated fluids. Here, the method of Valentik and Whitmore is discarded from this evaluation, since it is not directly related to the fall velocity prediction and its physical reasoning was pointed out to be unrealistic (Woo, 1986). The data obtained by Valentik and Whitmore, along with data obtained by Pazwash, Plessis and Ansley, Xu and Wu, however, were used for the evaluation of other methods. On the other hands, it is easily observed that the abovementioned three formulations to calculate the drag coefficient C_D are essentially the same, they all can be written as

$$C_D = f\left(\frac{Re_B + KHe}{Re_B^2}\right) \tag{4.12}$$

with which K is 1.0 in Plessis and Ansley's method, $7\pi/24$ in Ansley and Smith's method, and 1.5 in Pazwash's method. Therefore comparison of only one of these methods with the measurements is necessary. Herein, Ansley and Smith's method is chosen to compare with experimental measurements in Figure 4-1. The data points scatter below the Newtonian curve although the correlation using Pazwash's data only appears to be improved. The scattering appears to be due primarily to the inaccuracy of experimental data, namely τ_y and η, rather than the inadequacy of the equations as pointed by Pazwash (1970). As applied by many researchers, τ_y and η were determined by drawing a straight line passing through the experimental points in the rheogram of the suspension in a certain region of shear rate. This may overestimate or underestimate these coefficients if the rheogram of the suspension do not possesses a straight outline, i.e., the suspension can not be strictly described as Bingham fluid, for instance the kaoline suspension used by Valentik and Whitmore. This implies that only adequate rheological model can accurately evaluate the settling velocity of particles in hyperconcentrated flows. Unfortunately, the rheology of hyperconcentrated which is to be discussed in the last chapter is not well simulated up to now, which makes it difficult to determine the settling velocity of particles accurately.

IV-2. Settling in Mixtures of Coarse Particles

The gross settling of uniform coarse grains generally obeys the formula:

$$\omega/\omega_0 = (1-C_v)^m \tag{4.13}$$

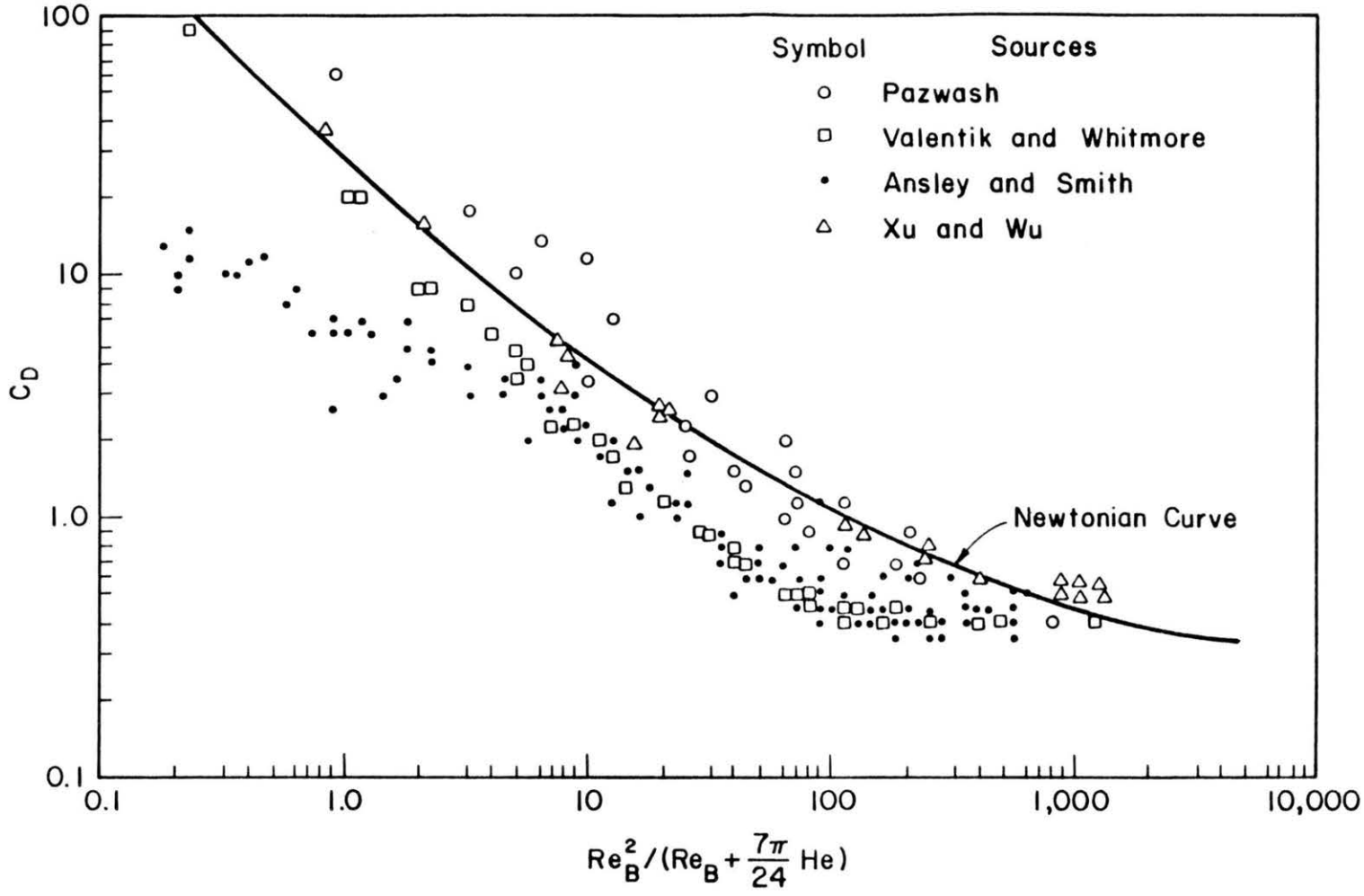

Figure 4-1. Ansley and Smith's Correlation Using All Data

in which ω is the gross settling velocity, ω_0 the settling velocity of a single particle in an infinite mass of fluid and the exponent m is a function of the Reynolds number $Re=\omega_0 D/\nu$, in which D is the diameter of sediment particles and ν is the kinematic viscosity of clear water. According to Richardson and Zaki's study (1954), m approaches a maximum constant value of 4.46 for Reynolds number smaller than .4 and approaches a minimum of .3 when Re is greater than $10^3 \sim 10^4$. Other researchers reported higher m value as shown in Figure 4-2, which implies that the exponent m is not only a function of grain Reynolds number but also a function of other factors. Yue (1983) contends that m should decrease with concentration. It appears that the scattering of experimental points in Figure 4-2 is yet to be properly explained.

In nonuniform suspensions, Equation (4.13) may not apply. After considering the effects of bonded water on the particle surface on the mixture's properties, Chu (1982) developed a new formula to calculate the gross settling velocity of a swarm of non-flocculated particles for high concentration, which is expressed as;

$$\frac{\omega}{\omega_0} = [1 - \theta_b K_b C_v]^{3.5} \tag{4.14}$$

where K_b is the ratio of the volume of bonded particles to that of unbonded particles and θ_b is the coefficient of the pores caused by collision between particles. Commonly, θ_b is taken to be 1.4 and K_b is expressed as

$$K_b = 1 + 6 \int_0^1 (\delta/D)\, dP \tag{4.15}$$

in which δ is the thickness of the bonded water on the particle surface, δ = 1 mm according to Woodruff's experiments and dP is the percentage of the

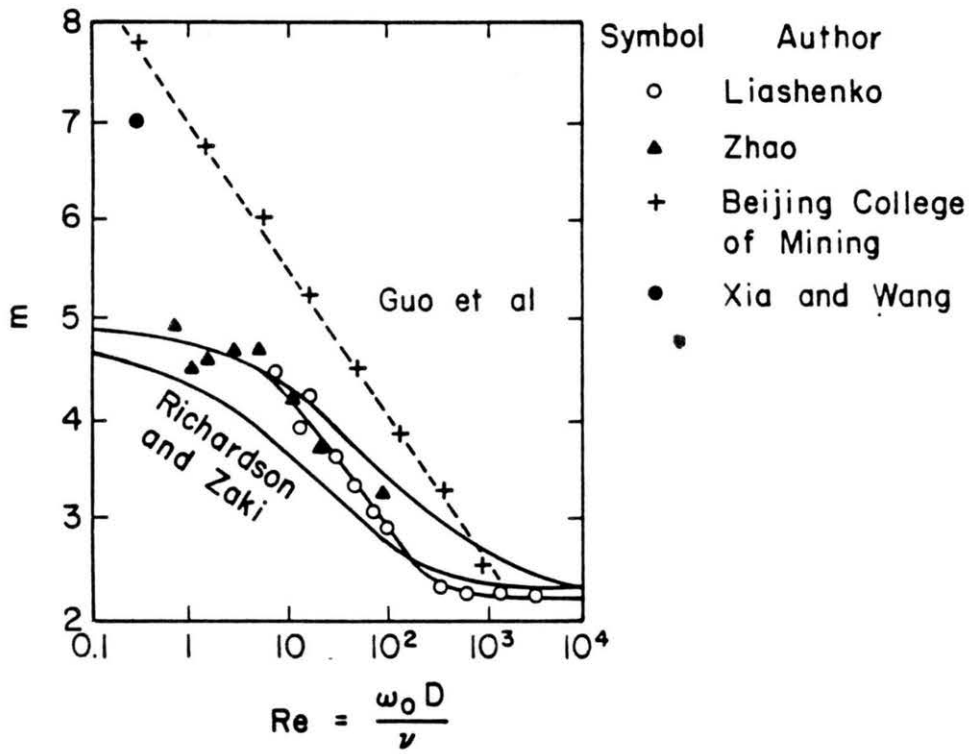

Figure 4-2. Exponent m in Eq. (4.13) as a Function of Particle Reynolds Number (after Qian and Wan, 1986)

volume of a certain particle diameter to the total particle volume. Then Equation (4.14) becomes

$$\omega/\omega_0 = \{1 - 1.4\ [1 + 6\ \int_0^1 (\delta/D)dP]C_v\}^{3.5} \qquad (4.16)$$

or for convenience of application

$$\omega/\omega_0 = \{1 - 1.4\ [1 + 6\Sigma(\delta/D_i)\Delta P_i]C_v\}^{3.5} \qquad (4.17)$$

Equation (4.17) was compared with experimental data from various investigators and the result is shown in Figure 4-3. It is suggested that Equation 4.17 can predict the settling velocity of non-uniform particles without flocculation extremely well.

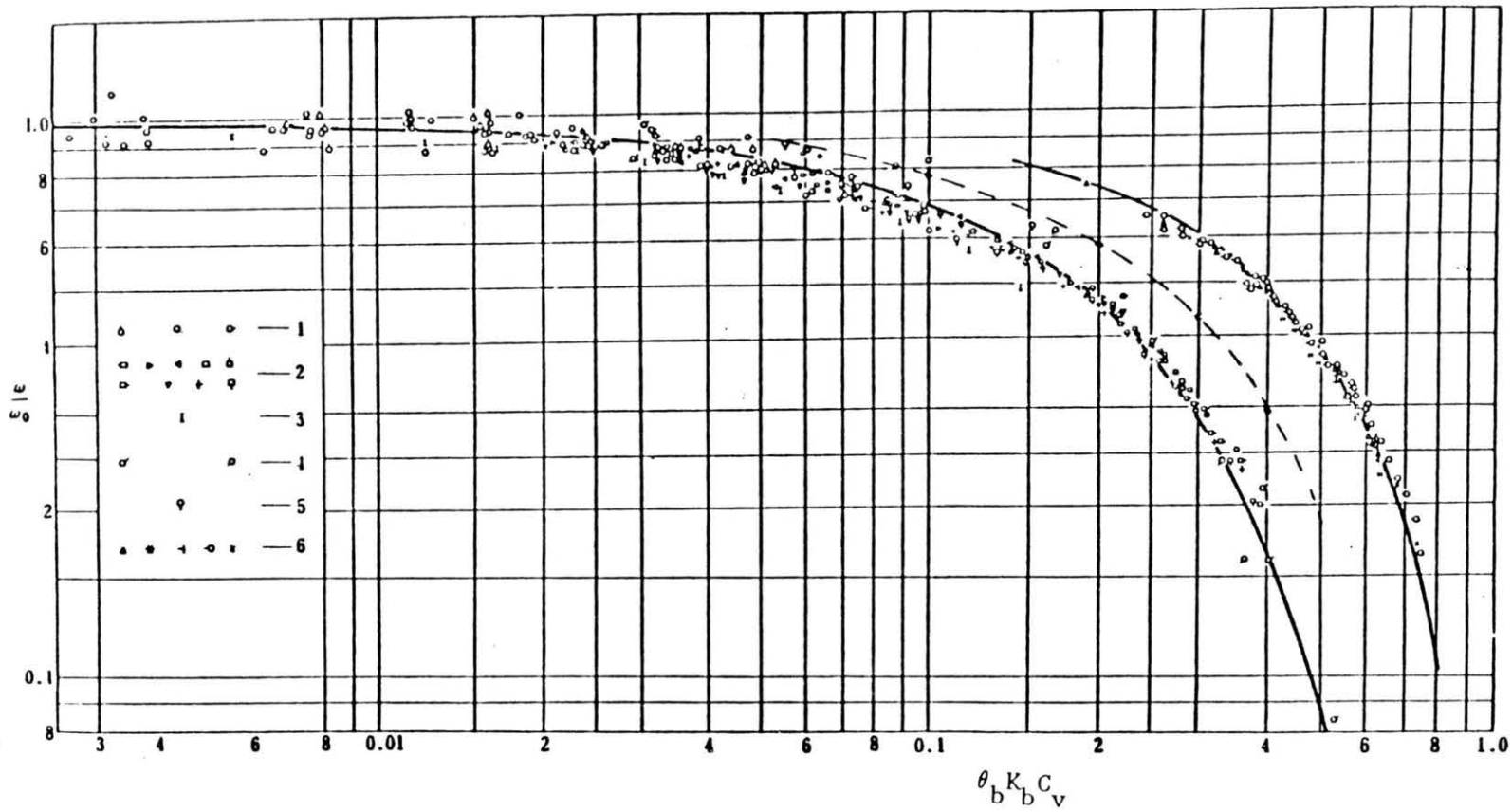

Figure 4-3. Comparison of Eq. 4.17 with Experimental Data. The Curve on the Right of the Above Figure is for the Case that no Fine Materials in the Suspension (After Chu, 1982)

V. VELOCITY DISTRIBUTIONS OF HYPERCONCENTRATED FLOWS

As long as sediment particles exist in the flows the velocity distribution does not obey the general laws applying to clear water flows due to the interactions between particles and the fluids. The interactions between particle and fluids not only change the viscosity of the suspension, cause yield stress, destroy or damp the turbulent eddies, but also may turn the suspension into multiphase flows. Investigations into this area are still very limited and empirical. So a thorough understanding of velocity distribution of hyperconcentrated flows cannot be presented in this chapter. Instead, this chapter will emphasize on the review of field observed velocity distributions and the general laws fitted by different types of hyperconcentrated flows. Similar to clear water flows, the hyperconcentrated flows will be divided into laminar, transition, and turbulent flows from low flow regime to high flow regime. Also pipe flows and open channel flows are distinguished. In the pipe flows, the treatment is restricted to steady-state isothermal flow in plain pipes.

V-1. Steady-State Laminar Flows

5.1.1. Laminar Flows in Pipes

For steady-state isothermal hyperconcentrated flows in plain pipes, a simple force balance on a cylindrical element of radius r and length dL yields,

$$-\pi r^2 dP - 2\pi r \tau dL = 0 \tag{5.1}$$

from which

$$\tau = -\frac{r}{2}\frac{dP}{dL} \tag{5.2}$$

and when r = R

$$-\pi R^2 dP = 2\pi R \tau_w dL \tag{5.3}$$

where τ and τ_w denote the shear stress at radius r and R, respectively. Combining Equation 5.2 and Equation 2.11 then yields velocity distribution after appropriate integration. Typical results, for Bingham-plastic, pseudo-plastic, yield-pseudoplastic, dilatant fluids, etc., are given in Table 5-1, where the parameters are defined in Chapter 2. Other results for other fluids are referred in Skelland (1967) and Govier and Aziz (1972). In Figures 5-1 to 5-3, velocity profiles corresponding to these typical fluids models are drawn.

In application to hyperconcentrated sediment flows, velocity distributions of Bingham-plastic and yield-pseudoplastic fluids are the most widely accepted. The former is suitable for flows with high content of fine sediments (for instance slurry mud flow and debris flows, etc.) and the later is for flows with coarse materials (for example the debris flows described by many Japanese researchers such as Takahashi, 1980, etc.).

In those flows with a yield stress, a core region with a constant velocity near the centerline of the pipe exists. This core flow region is called "plug flow" of which the thickness is proportional to the yield stress and inversely proportional to the pressure gradient along the pipe. As the flow in the pipe develops from laminar flow to turbulent flow this "plug flow" will disappear gradually.

Table 5-1. Velocity Profiles of Hyperconcentrated Laminar Flows in Pipes

Equation	Model	Velocity Distributions
5.4	Bingham-plastic	$u = \frac{1}{\eta}\left[-\frac{dP}{4dL}(R^2 - r^2) - \tau_y(R-r)\right]$ $r_p < r < R$
		$u = \frac{1}{\eta}\left[-\frac{dP}{4dL}(R^2 - r_p^2) - \tau_y(R-r_p)\right]$ $0 < r < r_p$
		$r_p = 2\tau_y/(-\frac{dP}{dL})$
5.5	Yield-pseudoplastic	$u = \frac{(1/\eta_p)^{1/n}}{(-dP/2dL)}\frac{n}{1+n}\left[(-\frac{R}{2}\frac{dP}{dL} - \tau_y)^{\frac{1+n}{n}}\right.$
		$\left. - (-\frac{r}{2}\cdot\frac{dP}{dL} - \tau_y)^{\frac{1+n}{n}}\right]$
		for $r_p < r < R$. For $0 < r < r_p$, $u = u(r = r_p)$ in which r_p is given as above.
5.6	Pseudopastic or dilatant	$u = \left[-\frac{1}{2\eta_p}\frac{dp}{dL}\right]^{1/n}(\frac{n}{1+n})\left[R^{\frac{1+n}{n}} - r^{\frac{1+n}{n}}\right]$
5.7	Quadratic model	$u = -\frac{\eta}{2\zeta}(R-r) + \frac{1}{2\zeta^2}(-\frac{dL}{dp})\left\{\left[\eta^2 - 4\zeta(\tau_y\right.\right.$
		$\left.\left. + \frac{R}{2}\frac{dp}{dL})\right]^{3/2} - \left[\eta^2 - 4\zeta(\tau_y + \frac{r}{2}\frac{dp}{dL})\right]^{3/2}\right\}$
		for $r_p < r < R$; for $0 < r < r_p$, u_p is given by Equation 6.7 with $r = r_p$.

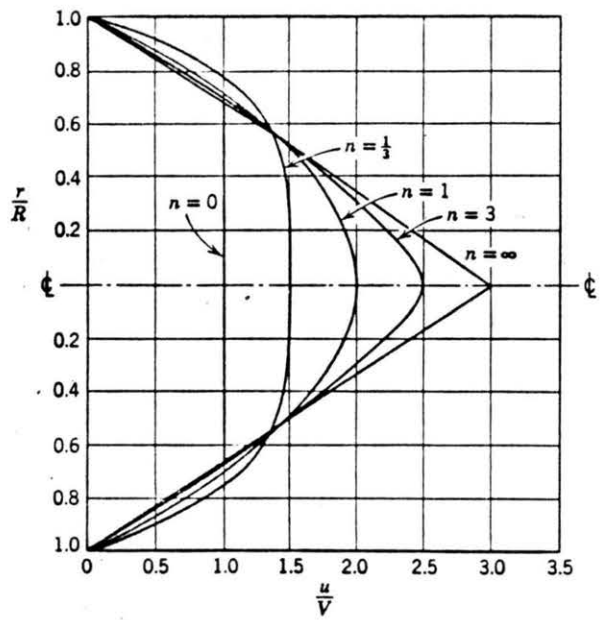

Figure 5-1. Velocity Distributions for Power Law Fluids in Laminar Flow Through Tubes

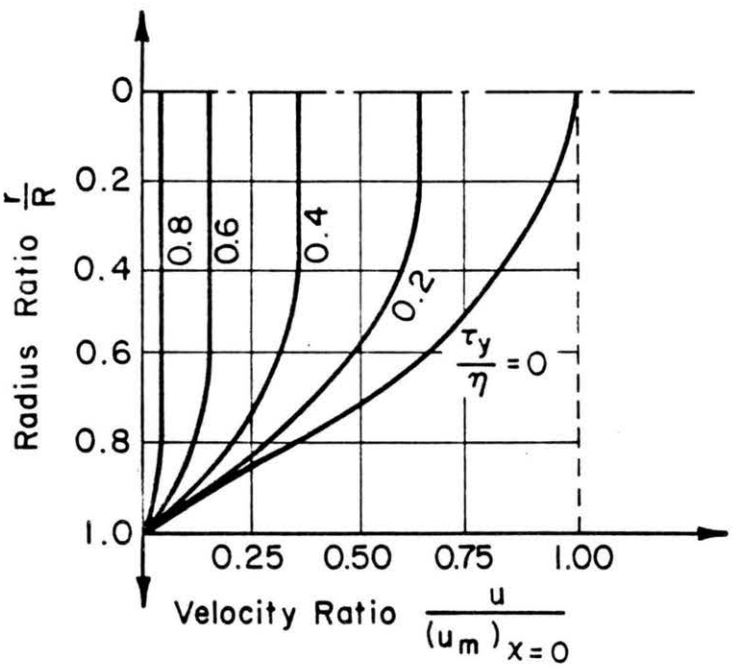

Figure 5-2. Velocity Profiles of Laminar Bingham Plastic Fluid in Pipes

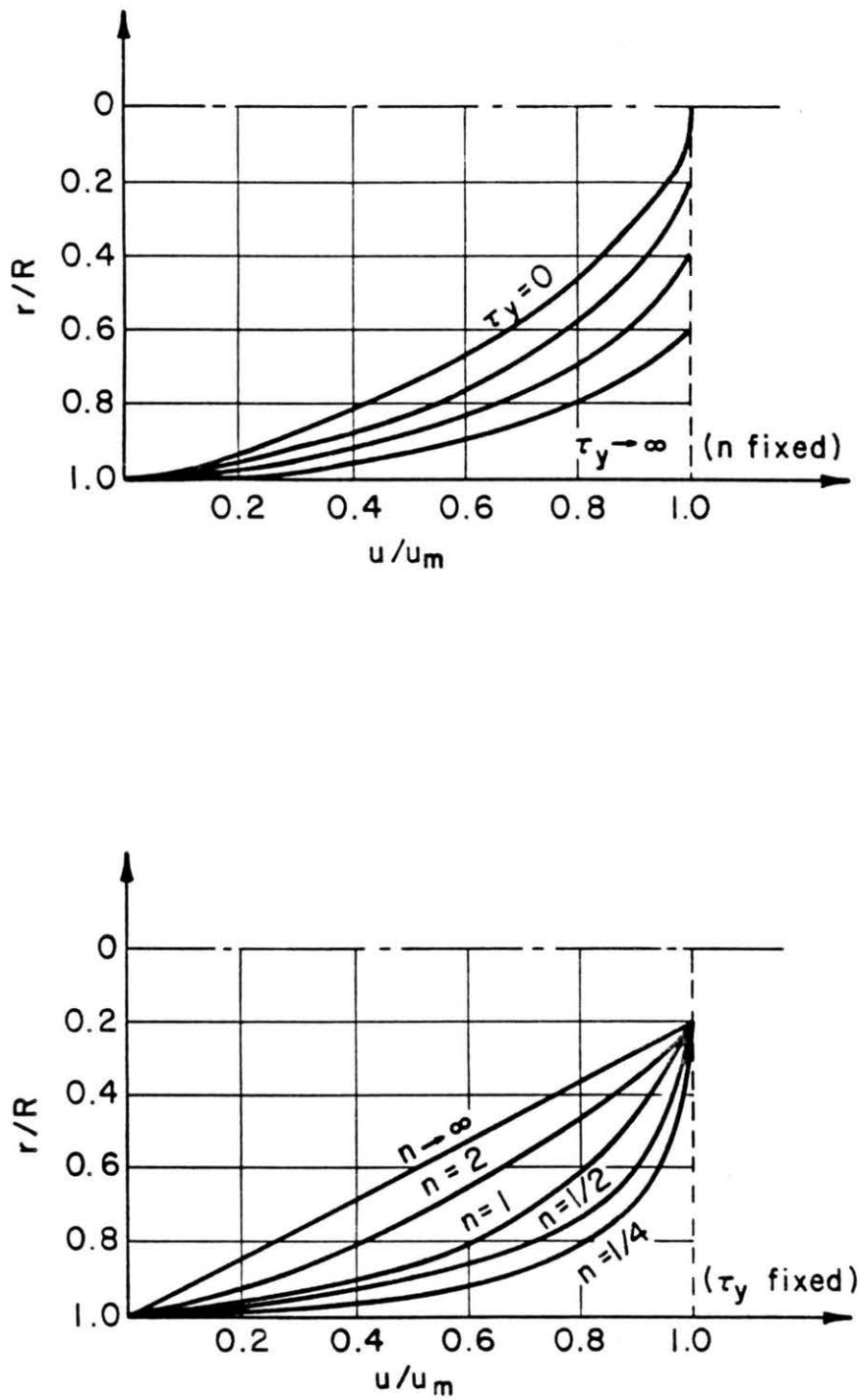

Figure 5-3. Velocity Profiles of Laminar Yield-Pseudoplastic Fluid in Pipes

5.1.2. Laminar Flows in Open Channels

Velocity distributions of steady-state laminar flows in open channels are more complicated than that in pipes due to the complexity of its geometric boundary. The problem can be solved by combining the continuity equation, equations of motion, and the appropriate rheological equations of the suspensions. From authors' knowledge, no theoretical analysis has been accomplished up to now even to the two-dimensional flows. For a one-dimensional laminar motion of an incompressible hyperconcentrated fluid, the equation of motion of the suspension is described by

$$\frac{\partial u}{\partial t} + u\frac{\partial u}{\partial x} = g\sin\theta - \frac{1}{\rho_m}\frac{\partial p}{\partial x} + \frac{1}{\rho_m}\frac{\partial \tau}{\partial y} \tag{5.8}$$

where ρ_m is the density of the mixture, u is the velocity in the downstream x-direction, p is the internal pressure, g is the gravitational acceleration, $\sin\theta$ is the channel slope and y is the upward distance above the channel bed perpendicular to the flow. For a uniform one-dimensional flows, Equation 5.8 can be simplified to

$$\tau = \rho_m g(H-y)\sin\theta = \rho_m g(H-y)S \tag{5.9}$$

from which the velocity distributions of hyperconcentrated suspensions can be derived after combining with the appropriate rheological equations. Typical results, for Bingham-plastic, pseudoplastic, yield-pseudoplastic, dilatant, and quadratic, are given in Table 5-2. These velocity distributions can be easily illustrated in accordance with Figures 5-4 to 5-7.

Table 5-2. Velocity Profiles of Hyperconcentrated Laminar Flows in Open Channels

Equation	Model	Velocity Distribution
5.10	Bingham-plastic	$u = \frac{1}{2\eta\rho_m gS}(\tau_0-\tau_y)^2$, $y_0<y<H$; $u_0 = \frac{\tau_0}{\eta}\left[y - \frac{1}{2}\frac{y^2}{H}\right] - \frac{\tau_y}{\eta}y$, $0 < y < y_0$ where $y_0 = \frac{1}{\rho_m gS}(\tau_0-\tau_y)$ and $\tau_0 = \rho_m gHS$.
5.11	Pseudo-plastic	$u = \left(\frac{\rho_m gS}{\eta_p}\right)^{1/n}\frac{n}{1+n}\left[H^{\frac{1+n}{n}} - (H-y)^{\frac{1+n}{n}}\right]$
5.12	Yield-pseudoplastic	$u = \frac{\eta_p H}{\tau_0}\frac{n}{1+n}\left[\left(\frac{\tau_0-\tau_y}{\eta_p}\right)^{\frac{1+n}{n}} - \left(\frac{\tau_0-\tau_y}{\eta_p} - \frac{\tau_0}{\eta_p}\frac{y}{H}\right)^{\frac{1+n}{n}}\right]$ for $0<y<y_0$; for $y_0<y<H$, $u=u(y=y_0)$ in which y_0 is defined as above.
5.13	Quadratic	$u = -\frac{\eta}{2\zeta}y + \frac{H}{12\zeta^2\tau_0}\left\{\left[\eta^2-4\zeta(\tau_0-\tau_y)\right]^{3/2} - \left[\eta^2 + 4\zeta\tau_y - 4\zeta\tau_0(1-y/H)\right]^{3/2}\right\}$ for $0<y<y_0$; for $y_0<y<H$, u is given by equation 5.13 with $y=y_0$.

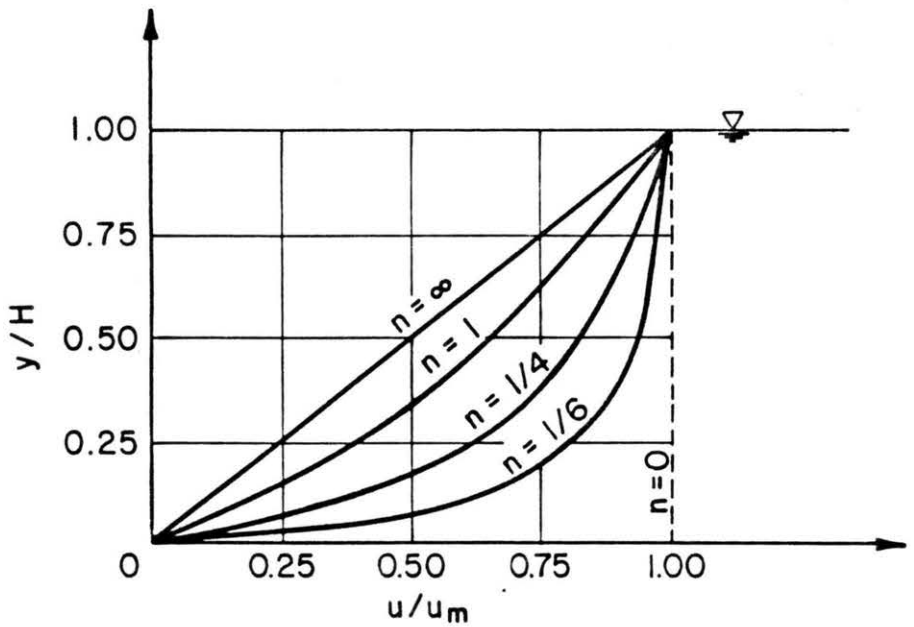

Figure 5-4. Velocity Profiles of Laminar Pseudoplastic Fluid in Open Channel (Uniform Suspension)

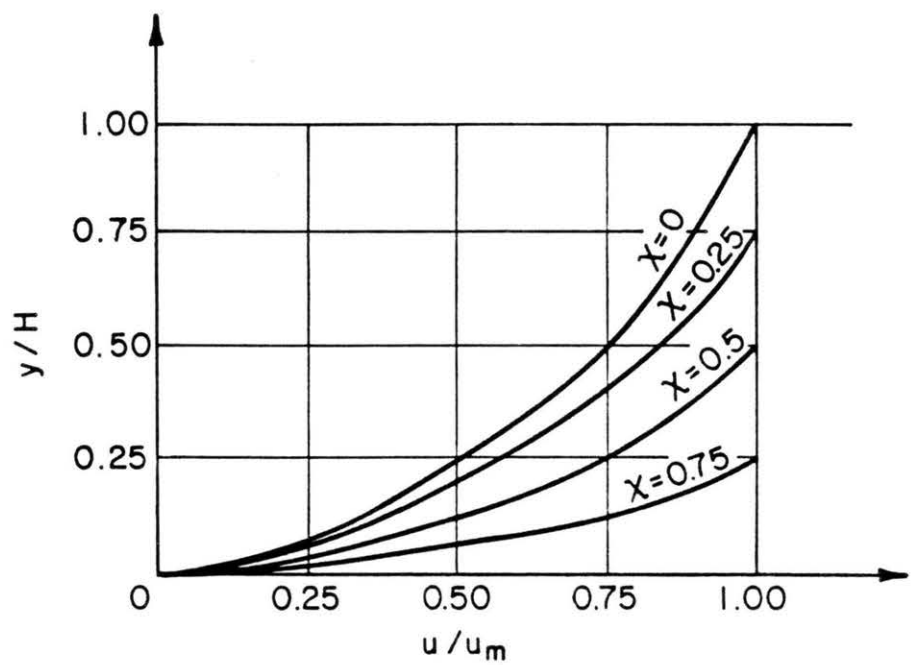

Figure 5-5. Velocity Profiles of Laminar Bingham Plastic Fluid in Open Channel (Uniform Suspension)

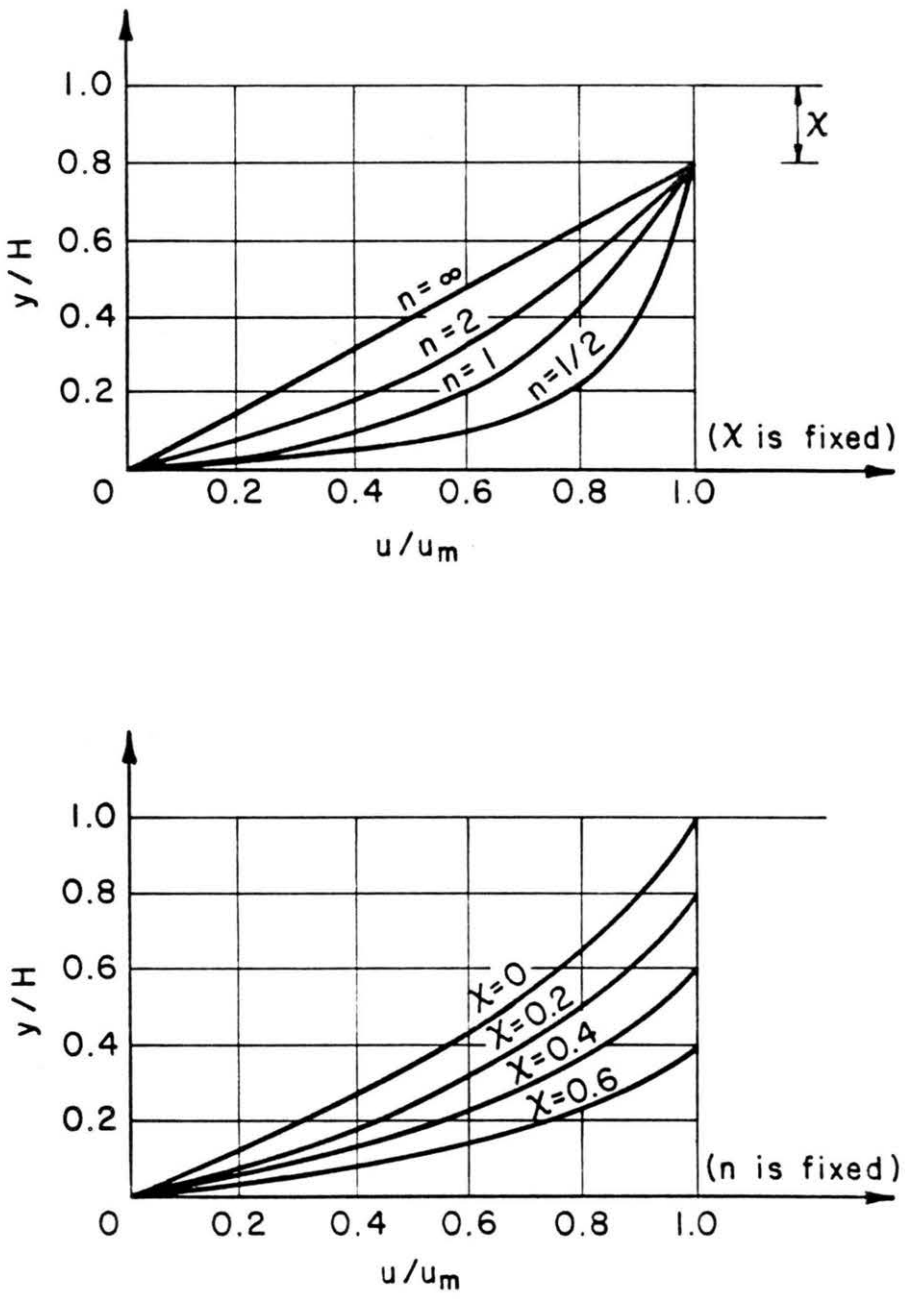

Figure 5-6. Velocity Profiles of Laminar Yield-Pseudoplastic Fluid in Open Channel (Uniform Suspension)

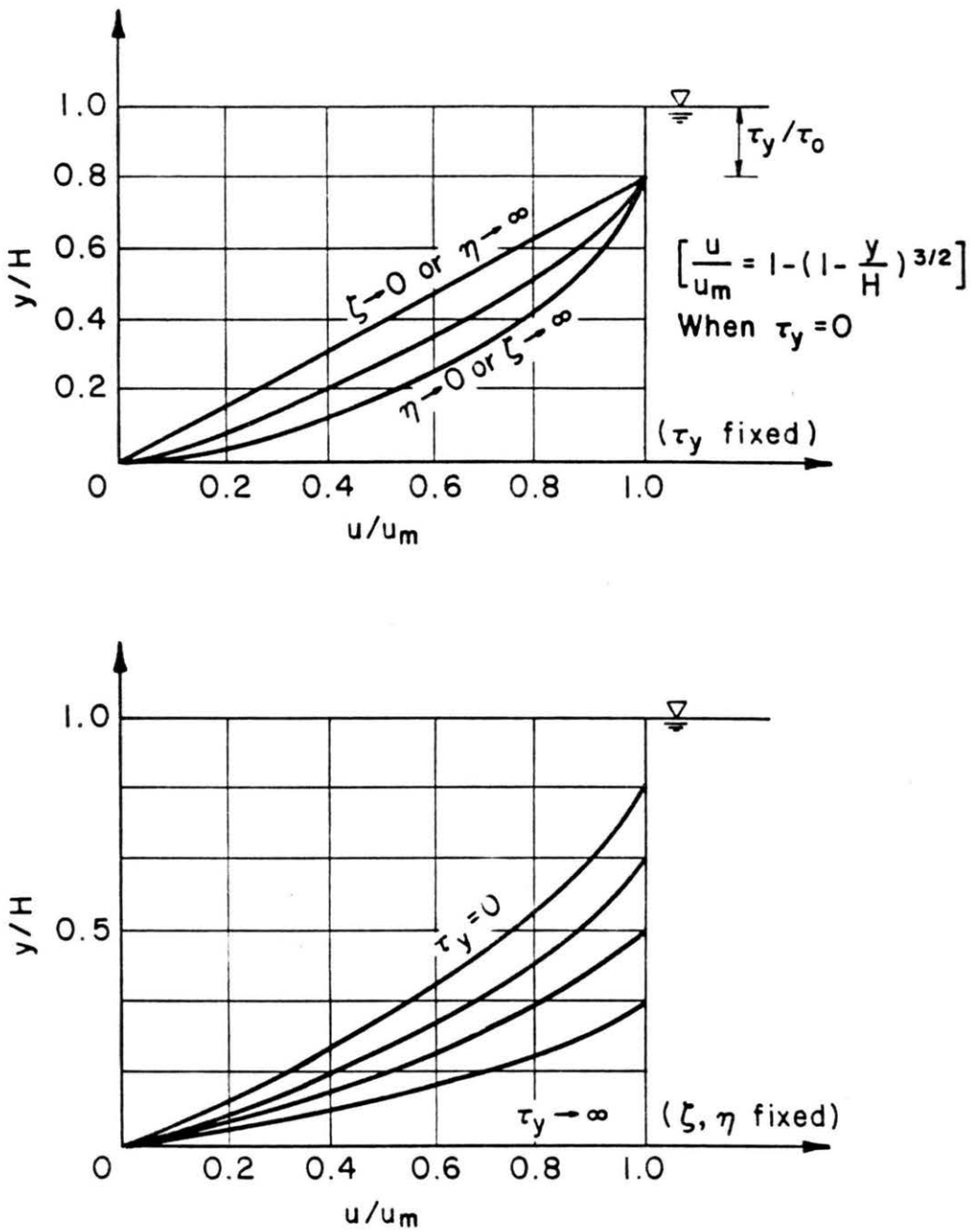

Figure 5-7. Velocity Profiles of Quadratic Fluid in Open Channel (Uniform Suspension)

V-2. Steady-State Turbulent Flows

Studies on turbulent flow of non-Newtonian or hyperconcentrated fluids have been rather limited, partly because turbulence is encountered less frequently with these materials than with Newtonian systems. In the early years contributions to this area include those from Dodge and Metzner (1959), Tomita (1959), and Clapp (1961) to power law fluids, that of Torrance (1963) to power law, Bingham, and Yield-pseudoplastic fluids. In the recent years, a lot of efforts have been attributed to study the effects of sediment concentration on the turbulent intensity as well as velocity distributions of sediment-laden flows (Einstein and Chien, 1955; Coleman, 1981; Woo, 1986; Lau, 1983; Parker and Coleman, 1986; etc.). Although the flows these researchers investigated are hardly considered to be typical hyperconcentrated non-Newtonian flows, their results gave a lot of implications how velocity profiles change with sediment concentration in the flows.

In turbulent flows of hyperconcentrated fluids, the flow region is also assumed to be composed of laminar sublayer, transition (or buffer) zone and turbulent core as applied to Newtonian fluids. The effects of turbulence are considered to be negligible in the laminar sublayer, but the effects of turbulence and viscous shear are of the same order of magnitude in the transition zone. The effects of viscosity are assumed to be negligible in the turbulent core. However, the effects of dispersive shear is assumed to be as important as other major terms in the equation.

5.2.1. Log Law Velocity Distribution of Hyperconcentrated Flows

It has been evidently proved that in flow with high sediment concentration the logarithmic law of wall for the velocity distribution is still applicable, that is,

$$u^+ = A\ Lny^+ + B \qquad (5.14)$$

where u^+ is the dimensionless velocity defined as u/U_*, y^+ is the dimensionless distance from the wall, and A and B are integration constants. Generally, y+, A and B are functions of flow regime and rheological properties of the fluids. For Newtonian turbulent flow,

$$A = \frac{1}{\kappa},$$

$$y^+ = yU_*/\nu,$$

and $B = 5.5$

For high sediment-laden flows, early researches (Vanoni, 1946, Einstein and Chien, 1955; Vanoni and Nomicos, 1960; etc.) indicates that the von Karman constant κ of the suspension decreases as sediment concentration increases. The relationship between these two parameters can be well described by the well-known graphs by Einstein and Chien (1955, Fig.15) and by Vanoni and Nomicos (1960), based on Vanoni's disputable hypothesis that the turbulence is damped by the sediments.

On the other hand, Coleman (1981) re-examined the data from earlier experiments to show that the change in κ was caused by the incorrect interpretation of the logarithmic velocity distribution to the outer flow region where the log law is not really valid. He was able to quantify the effect of suspended sediment on the flow in terms of the wake strength coefficient of the velocity profile, which was first used by Coles (1956) to describe the deviation of velocity from the logarithmic law in turbulent flow. This velocity distribution is given by

$$u^+ = \frac{1}{\kappa} Lny^+ + B + \frac{\Delta U}{U_*} + \frac{\Pi}{\kappa} \Xi(y/\delta) \qquad (5.15)$$

where Π is the Coles' wake strength coefficient. The function $\Xi(y/\delta)$ denotes Coles' wake flow function, which is normalized to have the properties $\Xi(1)=1$, and $\Xi(0)=0$ and δ denotes the boundary layer thickness. The term $\Delta U/U_*$ denotes the downshift in the velocity distribution because of wall roughness.

Coleman used Equation 5.14 to examine von Karman constant κ from straight line fitting to experimental velocity profiles in the lower 15% of the flow, in the region where the wake flow terms are negligible and not out in the more central regions of the flows. He observed that κ is essentially a constant over a wide range of flow conditions from sediment-free flows to flows carrying a near capacity load of suspended sediment. Also Coleman showed that the wake strength coefficient Π for uniform non-separating flows varies directly with the gross-flow Richardson number as shown in Figure 5-8 (Fig. 4 in the original paper).

The finding that κ is not dependent on sediment concentration is far-reaching and important as claimed by Coleman. However, the invariance of κ is accompanied with a wake flow function which requires further investigations (Julien and Lan, 1988). Also, the effect of sediment should be concluded in the changes of viscosity, coefficient B and possibly the rheological model. When the rheology of the sediment-water suspension turns to be non-Newtonian fluids as behaved in most hyperconcentrated flows, the rheological properties of the suspension are more important in formulating the velocity profiles of the flows. This will be demonstrated in the following sections.

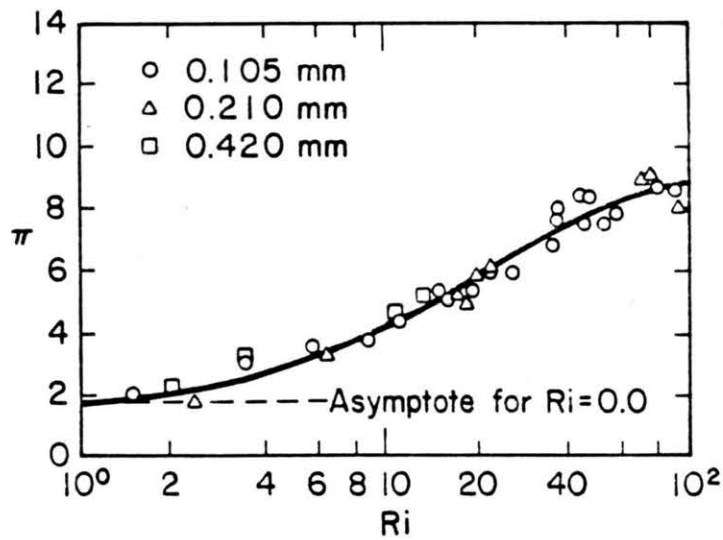

Figure 5-8. Relation Between Cole's Strength Coefficient and Richardson Number (after Coleman, 1981)

Dodge and Metzner's Formulations.

Dodge and Metzner (1955) carried out a semitheoretical analysis of the turbulent flow in smooth pipes of non-Newtonian fluids described by the power law. His results can be expressed in a log-law form as

$$u^+ = A_n \mathrm{Ln} y^+ + B_n \tag{5.16}$$

where y^+ is defined differently as

$$y^+ = Z\xi^n = \frac{y^n (U_*)^{2-n} \rho}{\eta_p}$$

$$Z = R^n \rho (U_*)^{2-n} / \eta_p$$

$$\xi = y/R$$

and R is the diameter of the pipe. In Equation 5.16, A_n and B_n are integration constants depending on the component n of the power law. In the turbulent core, the constants A_n and B_n are given by

$$A_n = 5.66/n^{0.75}$$

$$B_n = -.566/n^{1.2} + \frac{3.475}{n^{0.75}} [1.96 + 0.815\ n - 1.628\ n\mathrm{Log}\ (3 + \tfrac{1}{n})] \tag{5.17}$$

Bogue and Metzner (1963) reviewed the earlier work of Dodge and Metzner and proposes as an improvement on Equation 5.16. They concluded that within the range studied ($0.45 \leq n \leq 1.0$), the turbulent non-Newtonian velocity profiles are substantially the same as those for Newtonian fluids when

expressed either in terms of U/V versus ξ or in terms of $(U_{max} - u)/U_*$ versus ξ, as shown in Figures 5-9 and 5-10. The interested reader is referred to the original work for details.

Clapp's Equations

Clapp (1961) proposes the following rheological relationship for turbulent power-law fluid flows;

$$\tau = \eta_p \left(\frac{du}{dy}\right)^n + \rho \ell^2 \left(\frac{du}{dy}\right)^2 \tag{5.18}$$

to derive a universal velocity profile for the turbulent power-law fluid flows in a smooth tube after following analogous analysis to the Prandtl and von Karman approach to Newtonian fluids. The results are

Laminar sublayer: $0 < y^+ < 5^n$

$$u^+ = (y^+)^{1/n} \tag{5.19}$$

Buffer layer: $5^n < y^+ < y_2^+$

$$u^+ = \left(\frac{5.0}{n}\right) 2.303 \log y^+ - 3.05 \tag{5.20}$$

Turbulent Core: $y^+ > y_2^+$

$$u^+ = \frac{G}{n} 2.303 \log y^+ + H/n \tag{5.21}$$

where y_2^+, G, and H are constants to be evaluated from experimental data. Correlation of these equations with experimental data results in G=2.78 and

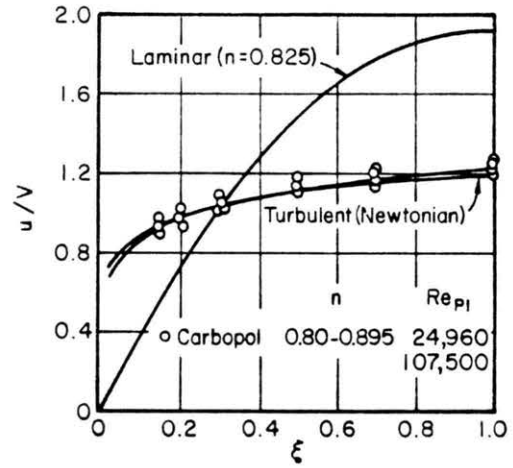

Figure 5-9. Velocity Profiles in Tubes for Power Law Fluids with High n (Mildly Non-Newtonian)

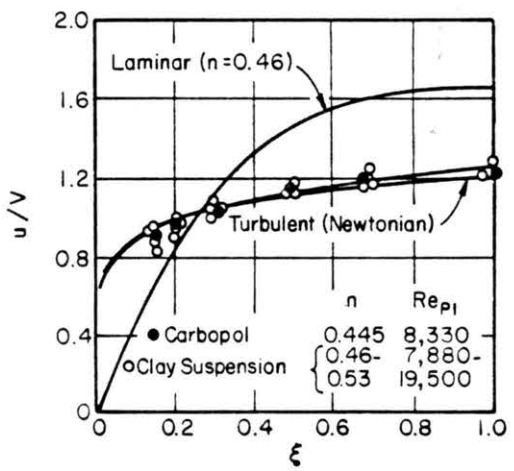

Figure 5-10. Velocity Profiles in Tubes for Power Law Fluids with Low n (Highly Non-Newtonian)

H=3.8, as proposed by Deissler (1951) for Newtonian fluids. Comparison of experimental data with Equations 5.16 and 5.21 by Clapp shows that Clapp's equation suits his data better than does the Dodge and Metzner's relationship (Clapp, 1961).

5.2.2. Polynomial Form of Velocity Profiles

A way to avoid the discontinuity of velocity profiles for different flow regions has been developed by Pai (1957), who used a single polynomial expression for the complex velocity distribution. The velocity distribution is assumed to be represented by three-term power series:

$$\frac{u}{U_m} = 1 + a_1 \left(\frac{r}{R}\right)^{(n+1)/n} + a_2 \left(\frac{r}{R}\right)^{2m} \tag{5.22}$$

The series is limited by the available boundary conditions, which are just sufficient to evaluate the coefficients in a three-term expression. The exponent (n+1)/n on the middle term is chosen to reduce to the known form for power law fluids in the limiting case of laminar flow. m is an exponent to be determined by experiment. By applying the boundary conditions, Pai obtained the expressions for coefficients a_1 and a_2:

$$a_1 = \frac{s-m}{m-(n+1)/2n},$$

$$a_2 = \frac{(n+1)/2n-s}{m-(n+1)/2n}$$

where

$$s = \left[\frac{\rho(U_*)^2}{\eta_p}\right]^{1/n} \left(\frac{R}{2U_m}\right)$$

Equation 5.22 is claimed to give the velocity distribution for power law fluids across the entire pipe, from wall to centerline.

5.2.3. Turbulent Flow of Bingham Fluids or Fluids with a Yield Stress

For hyperconcentrated flows with a yield stress, a "plug" always appears in the laminar regime. As the turbulence in the suspension increases the thickness of the "plug" diminishes until it is down to zero for fully developed turbulent flows. Field and experimental observations show that in this fully developed turbulent flows the logarithmic law of velocity distribution is still applicable (Tomita, 1959; Torrance, 1963; Fei, 1983; etc.). The integration constants in the equation can be determined from experiments. Unfortunately, detail investigations have not been conducted by now.

VI. FLOW RESISTANCE OF HYPERCONCENTRATED FLOWS

Resistance of hyperconcentrated flows has received most attention in the study of hyperconcentrated flows, not only because it is important in analyzing the energy loss or energy dissipation of the flow due to the presence of sediment but also it is the controlling factor in defining the flow regime. Einstein and Chien (1955), Vanoni and Nomicos (1960), Dodge and Metzner (1959), Hedstrom (1952), Montes and Ippen (1973), Dai et. al. (1980), Fei (1985), Chen (1983), etc., have already provided remarkable insights to the problem, although there still exists disagreement on how the sediment in the suspension affects the resistance of the flows. Among these studies, resistance of pipe flows receives the most attention due partly to the handy definition of resistance factor in pipe flows. In this chapter, emphasis then is on the resistance of hyperconcentrated flows in pipes. Nevertheless, most formula from pipe flows are also suitable to flows in open channels, which is similar to the Newtonian flows in pipes and in open channels.

The coefficient used to measure the resistance of Newtonian and non-Newtonian flows is the Fanning friction factor defined as the ratio of the wall shear stress, τ_w, to the kinetic energy per unit volume of fluids, $\rho V^2/2$. Since the wall shear stress is a measure of the energy gradient or energy loss of the flow, then the friction factor is considered to be the dimensionless quantity indicative of the kinetic energy loss of the flows,

$$f = \frac{\tau_w}{\rho V^2/2} \tag{6.1}$$

or

$$f = 2\left(\frac{U_*}{V}\right) \tag{6.2}$$

where V is the cross-sectional average velocity and U_* is the friction velocity defined as $\sqrt{\frac{\tau_w}{\rho}}$. The commonly used friction factor in civil engineering, however, is the Darcy-Weisbach resistance coefficient, f_D, defined as

$$\tau_0 = \frac{f_D}{4} \rho \frac{V^2}{2} \tag{6.3}$$

or

$$f_D = \frac{8\tau_0}{\rho V^2} \tag{6.4}$$

where τ_0 is the shear stress on the channel bed or boundary.

Either Darcy-Weisbach's or Fanning's friction factor will be used in this report whenever it is convenient. Nevertheless, these two friction factors are exchangeable since the Fanning's friction factor is one-fourth of the Darcy-Weisbach's friction coefficient.

VI-1. Resistance of Laminar Hyperconcentrated Flows

The friction factor of non-Newtonian fluids can be obtained simply by integrating the velocity distribution over the cross-section of the pipe or channel. For time-independent non-Newtonian fluids, this friction factor can be eventually represented as a function of Reynolds number, Hedstrom number, Yield number and other specific parameters for that particular fluids. The following lists typical results for Bingham plastics, pseudoplastics (or dilatants), yield-pseudoplastics, which are typical types of fluids in hyperconcentrated flows in civil engineering.

6.1.1. Power Law Fluids (pseudoplastic or dilatant)

$$f_D = \left[\frac{64}{Re_{p1}}\right]\left(\frac{1}{8}\right)\left[\frac{2+6n}{n}\right]^n \tag{6.5}$$

and $$f_D = 64/Re_{p2} \tag{6.6}$$

where Re_{p1} and Re_{p2} are alternate forms of what may be called the "power law Reynolds number", defined as

$$Re_{p1} = \frac{D^n V^{2-n} \rho}{\eta_p}, \tag{6.7}$$

and $$Re_{p2} = Re_{p1}\, 8\left(\frac{n}{2+6n}\right)^n \tag{6.8}$$

6.1.2. Bingham-plastic Fluids

$$f = \frac{16\eta}{DV\rho}\left[1 - \frac{4\chi}{3} + \frac{\chi^4}{3}\right] \tag{6.9}$$

where $\chi = \frac{\tau_y}{\tau_w} = \frac{4L\tau_y}{D\Delta P}$. Equation 6.9 can be rearranged to either a friction-Bingham Reynolds number-yield number, or a friction-Bingham Reynolds number-Hedstrom number form. The results are

$$\frac{1}{Re_B} = \frac{f}{16} - \frac{Y}{6Re_B} + \frac{16Y^4}{3f^3 Re_B^4} \tag{6.10}$$

or $$\frac{1}{Re_B} = \frac{f}{16} - \frac{He}{6\, Re_B^2} + \frac{16He^4}{3f^3 Re_B^8} \tag{6.11}$$

Equations 6.10 and 6.11 can be plotted as of f versus Re_B at constant values of Y or f versus Re_B at constant values of the Hedstrom number He, which are shown in Figures 6-1 and 6-2.

6.1.3. Yield-pseudoplastic Fluids

Equation 5.5 can be integrated over the cross-section to obtain the average velocity of the flow as

$$\frac{2V}{D} = \frac{8Q}{\pi D^3} = \frac{(1/\eta_p)^{1/n}}{\tau_w^3} \left[\tau_w - \tau_y\right]^{(1+n)/n}$$

$$\times \left[\frac{(\tau_w-\tau_y)^2}{(1+3n)/n} + \frac{2\tau_y(\tau_w-\tau_y)}{(1+2n)/n} + \frac{\tau_y^2}{(1+n)/n}\right] \qquad (6.12)$$

where τ_w is the wall shear stress equal to (- DdP/4dL). Unfortunately the complexity of Equation 6.12 is such that it cannot easily be converted to friction factor form. But we may see that

$$f_D = \Phi\left(\frac{D^n V^{2-n} \rho}{\eta_p}, \frac{D\tau_y}{V\eta_p}, \text{ terms involving n}\right) \qquad (6.13)$$

6.1.4. The Metzner and Reed Generalized Approach

The Metzner and Reed Generalized approach has been introduced in the last section of chapter II. Further analysis indicated (Metzner and Reed, 1955) that the friction factor of hyperconcentrated flow can be written as a function of a generalized Reynolds number, in a form similar to that for Newtonian fluids. The result can be represented by;

$$f = 16/Re_{MR} \qquad (6.14)$$

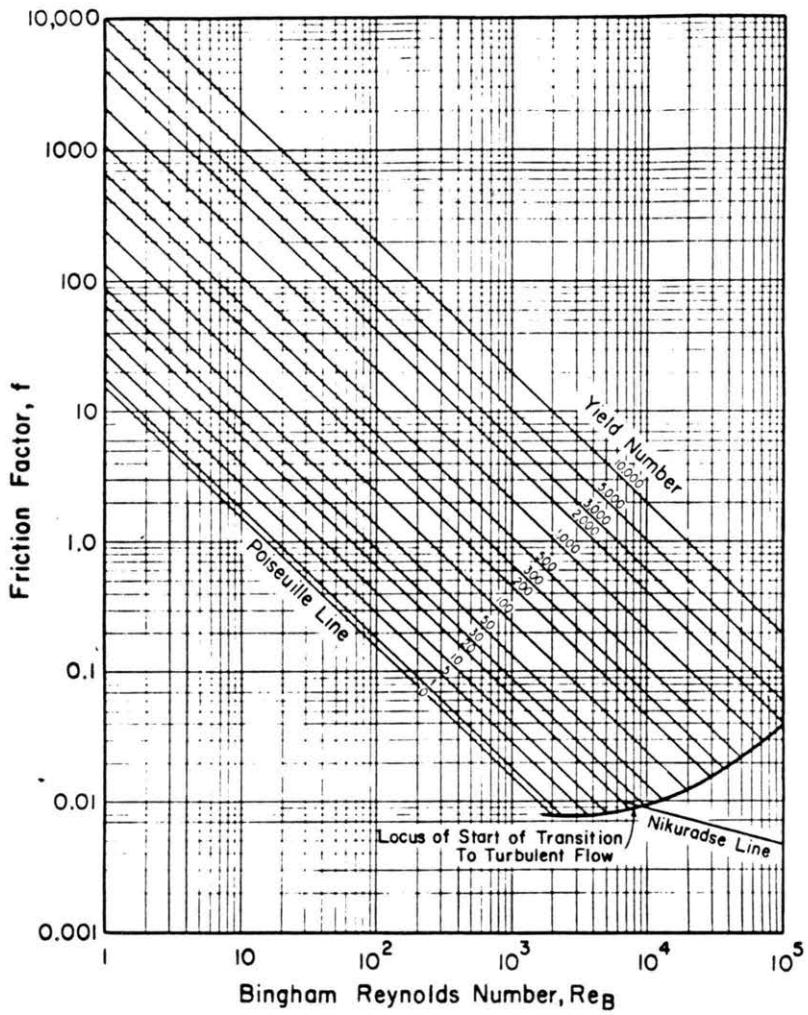

Figure 6-1. Friction Factors for Laminar Flow of Bingham Plastics-Yield Number Form (after Govier and Aziz, 1972)

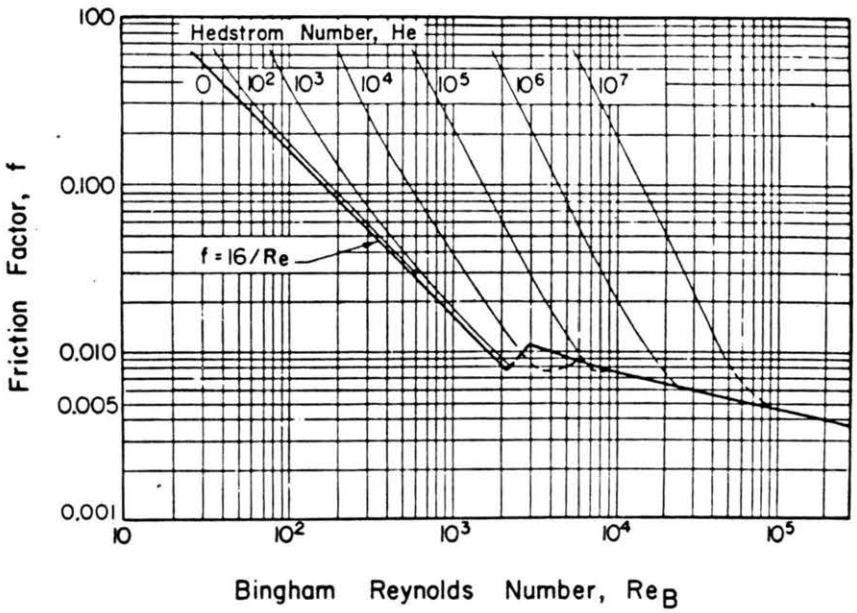

Figure 6-2. Friction Factors for Laminar Flow of Bingham Plastics-Hedstron Number Form (after Govier and Aziz, 1972)

where Re_{MR} is the generalized Reynolds number defined as

$$Re_{MR} = D^{n'} V^{2-n'} \rho / \beta \tag{2.17}$$

in which $\beta = K' 8^{n'-1}$

Equation 6.14 has been compared with experimental data from Metzner and Reed. Figure 6-3, taken from them, illustrates the conformity of data from a variety of non-Newtonian fluids over an intermediate range of Re_{MR}. Metzner and Reed (1955) also demonstrated the relationship between n',K', and β and the actual rheological properties of the different types of fluids. For a Newtonian fluid,

$$n' = 1; \quad \beta = \mu; \quad K' = \mu$$

For a power law pseudoplastic,

$$n' = n; \quad K' = \eta_p \left[\frac{1+3n}{4n}\right]^n; \quad \beta = \eta_p \left[\frac{1+3n}{4n}\right] 8^{n-1}$$

For a Bingham plastic,

$$n' = (1-4\chi/3+\chi^4/3)/(1-\chi^4);$$

$$K' = \tau_w \left[\frac{\eta}{\tau_w(1-4\chi/3+\chi^4/3)}\right]^{n'}$$

$$\beta = 8^{n'-1} \tau_w \left[\frac{\eta}{\tau_w(1-4\chi/3+\chi^4/3)}\right]^{n'}$$

The generalizations of Metzner and Reed are of great value in instances where the rheological behavior of the fluid is not adequately described by one of the simpler constitutive equations, or when one is involved in the

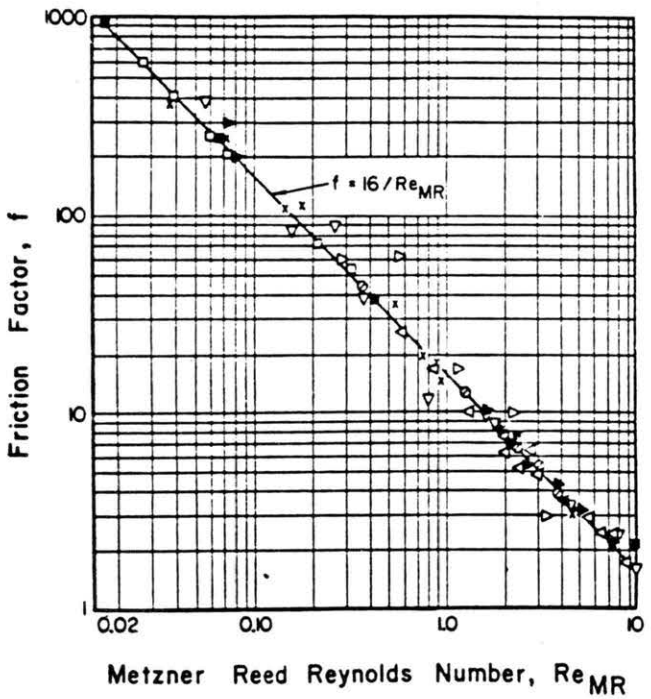

Figure 6-3. Friction Factors for Laminar Flow of Non-Newtonian Fluids in General (after Metzner and Reed, 1955)

direct scale-up from data taken in a small diameter pipe. For the simple cases of the power law pseudoplastic (or dilatant) and the Bingham plastic, however, previously derived relations are at least equally convenient.

6.1.5. Chen's Equation for Open Channel Laminar Flows

For hyperconcentrated flows of yield-pseudoplastic type in open channel, Chen (1983) developed a relationship between the friction factor and the Yield number, the generalized Reynolds number, and the Hedstrom number. The result can be simply expressed as

$$f_D = c/Re_{pl} \tag{6.15}$$

where the "constant" c and the generalized Reynolds number Re_{pl} are defined respectively as;

$$c = \frac{8}{(r_o/R)^{1+n}} \left[\frac{(1+n)/n}{1-(r_o/R)n/(2n+1)}\right]^n \tag{6.16}$$

$$Re_{pl} = \frac{\rho V^{2-n} R^n}{\eta_p} \tag{6.17}$$

in which R is the hydraulic radius of the flow, and r_o is the fictitious space coordinate corresponding to the yield-stress, r_o/R is called the yield-stress index by Chen. Further analysis leads to the following expressions

$$\left[1 - \frac{8He^{1/(2-n)}}{f\ Re_{pl}^{2/(2-n)}}\right]^{(n+1)} \left[1 + \frac{n}{1+n} \frac{8He^{1/(2+n)}}{f\ Re_{pl}^{2/(2-n)}}\right]^n = \left(\frac{2n+1}{n}\right) \frac{8}{f\ Re_{pl}} \tag{6.18}$$

where He is the Hedstrom number defined as

$$He = \frac{c}{8}\left[1 - \frac{r_0}{R}\right]^{2-n} Re_{pl}^{n} \tag{6.19}$$

Equation (6.18) has been claimed to give good agreement with experimental and field data (Chen, 1983).

VI-2. Transition From Laminar to Turbulent Flows

Regardless of the type of non-Newtonian fluid, laminar flow gives way to turbulent flow at sufficiently high values of the Reynolds number. This critical Reynolds number, intuitively, varies for different fluids. For the past few centuries, various criteria have been proposed for defining the end of laminar flow regime (Ryan and Johnson, 1959; Hanks and Christiansen, 1962; Hanks, 1963; Metzner and Park, 1964; Metzner and Reed, 1955; Meter and Bird, 1964; etc.). These criteria consist generally of empirical modifications, specifications, and generalizations of the conventional Reynolds number on the one hand and alternative criteria arising from manipulation of the basic equations of motion on the other.

For Bingham-plastic fluids, the parameters defining the flow regime include Bingham Reynolds number, the Yield number, and Hedstrom number. They are defined as

$$Re_B = DV\rho/\eta = \frac{\text{Inertial}}{\text{Viscous}}, \tag{6.20}$$

$$Y = He/Re_B = \tau_y D/(V\eta) = \frac{\text{Yield}}{\text{Viscous force}}, \tag{6.21}$$

and

$$He = \tau_y D^2 \rho/\eta^2 = Re_B \cdot Y \tag{6.22}$$

respectively, where V is the mean velocity of the flow, D is the diameter of the pipe. Hanks (1963) shows that the transition from laminar to turbulent flow occurs at a critical value of Re_B given by

$$(Re_B)_c = \frac{He}{8\chi_c}\left[1 - \frac{4}{3}\chi_c + \frac{1}{3}\chi_c^4\right] \tag{6.23}$$

where χ_c is the critical value of χ defined by the relation

$$\chi_c/(1-\chi_c)^3 = \frac{He}{16,800} \tag{6.24}$$

Hanks and Pratt (1967) solve these equations for $(Re_B)_c$ and χ_c in terms of He and obtain the results shown in Figures 6-4 and 6-5 taken from their work. The predictions of Figures 6-4 and 6-5 are extensively confirmed by data of Caldwell and Babbitt (1941), Wilhelm, Wroughton, and Loeffel (1939), Alves, Boucher, and Pigford (1952), and others. The relationship of Figure 6-4 may also expressed in terms of the yield number, Y. This is shown in Figure 6-6.

Neglecting the small last term on the right hand, Equation 6.23 can be changed into the following Equation 6.25

$$\frac{DV\rho}{\eta\left(1+\frac{D\tau_y}{6\eta V}\right)} = 2,100/[(1-\chi_c)^3(1+ Y/6)^2] \tag{6.25}$$

Further calculation indicates that

$$(1-\chi_c)^3(1+ Y/6)^2 \approx 1.0$$

Then Equation 6.25 becomes

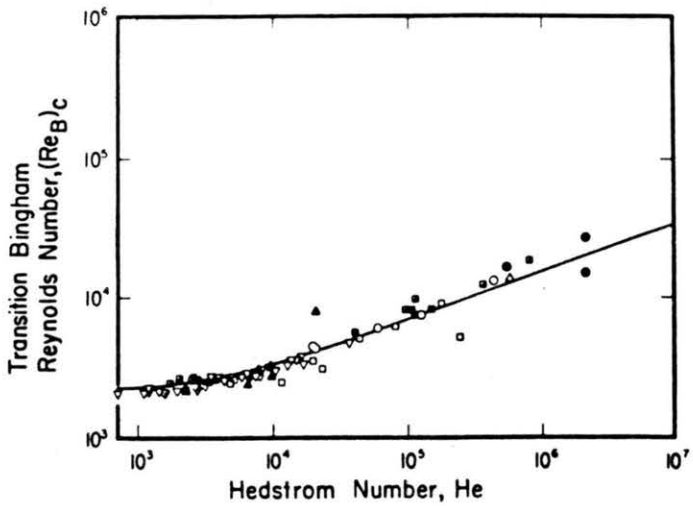

Figure 6-4. Variation of Transition Reynolds Number with Hedstrom Number of Flow of Bingham Plastics. Solid Curve Calculated from Eqs. 6.22 and 6.24 (after Hanks and Pratt, 1967)

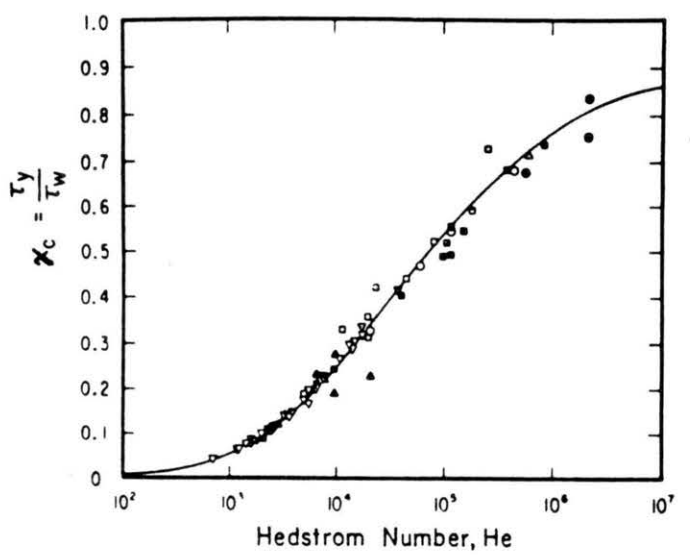

Figure 6-5. Variation of $\chi_c = (\tau_y/\tau_w)_c$ with Hedstrom Number for Laminar Flow of Bingham Plastics. Solid Curve Calculated from Eq. 6.24 (after Hanks and Pratt, 1967)

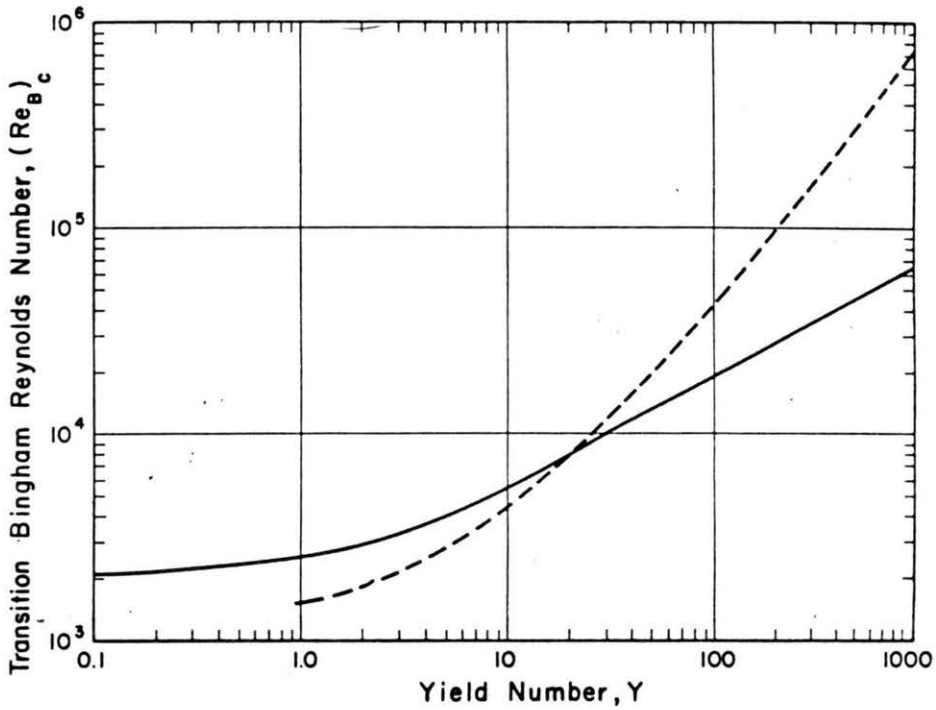

Figure 6-6. Transition Bingham Reynolds Number

_____ $Y = \frac{He}{Re_B}$, Hanks and Pratt (1967)

------- Extrapolated from f-Re-Y lines of Fig. 6-1

$$DV\rho/\left[\eta(1+\frac{D\tau_y}{6\eta V})\right] \approx 2,100 \tag{6.26}$$

which is of the same criteria for Newtonian fluids, with μ replaced by μ_e, the so-called effective viscosity defined as

$$\mu_e = DV\rho/\left[\eta(1 + \frac{D\tau_y}{6\eta V})\right]$$

For pseudoplastic fluids, Ryan and Johnson (1959) proposed the criteria to define the end of laminar flow as

$$(Re_p)_2 = \frac{6464n}{(1+3n)^2(\frac{1}{2+n})^{(2+n)/(1+n)}} \tag{6.27}$$

A generalized critical Reynolds number for all time-independent fluids is given by Metzner and Reed (1955) based on the generalized rheological model they developed (Equation 2.15). Similar to Newtonian flows in pipes, a Fanning friction factor f is defined as a function of the Metzner and Reed generalized Reynolds number,

$$f = \frac{16}{Re_{MR}} \tag{6.28}$$

where the generalized Reynolds number for non-Newtonian fluids is defined as in Eq. (2.17)

$$Re_{MR} = \frac{D^{n'}V^{2-n'}\rho}{\beta} \tag{2.17}$$

with which Equation 6.28 is analogy to the well known result for laminar flow of Newtonian fluids.

Metzner and Reed were able to correlate almost all the available published data for time-independent non-Newtonian fluids on the conventional plot of friction factor versus Reynolds number, their results being shown in Figure 6-7, 6-8 and 6-9 for high, medium and low Reynolds number ranges, respectively. From these figures, it is considered that stable laminar flow in tubes ends when the generalized Reynolds number reaches about 2100. The later work of Dodge and Metzner (1962) led to the generalized f-Re_{MR} chart shown in Figure 6-10. This plot indicates that laminar flow ends at generalized Reynolds numbers which increase slowly as n' decreases. In the limiting case of n'=0 there is no change in velocity profile with increasing Reynolds number.

In cases where n' and K' are not constants, the following rearrangement of the generalized Reynolds number may facilitate calculation:

$$Re_{MR} = \frac{D^{n'}V^{2-n'}\rho}{K'8^{n'-1}} = \frac{DV\rho}{K'(8V/D)^{n'-1}} \qquad (6.29)$$

VI-3. Steady-State Turbulent Flows

The theoretical or semi-empirical formulae for friction factor in hyperconcentrated turbulent flows in pipes generally resemble the counterparts for a Newtonian fluid in pipes. In a smooth wall pipe, the friction factor depends only on the rheological properties of the fluids and the flow Reynolds number, while in a fully rough wall the friction factor is a function of relative roughness of wall as well as the rheological properties of the fluids. In a partially rough wall the friction factor depends on both Reynolds number and relative roughness as well as the rheological properties of the flow. In the past few decades a number of advances have been made in our understanding of the turbulent pipe flow of power law pseudoplastics and Bingham plastics, some of this work is

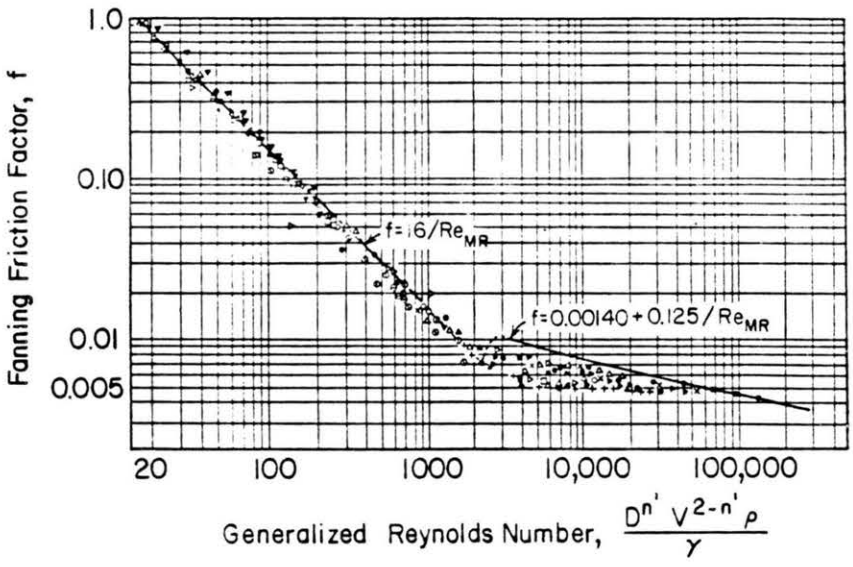

Figure 6-7. Friction Factor -- Generalized Reynolds Number Correlation for Time-Independent Non-Newtonian Flow in Tubes (High Range of Re_{MR})

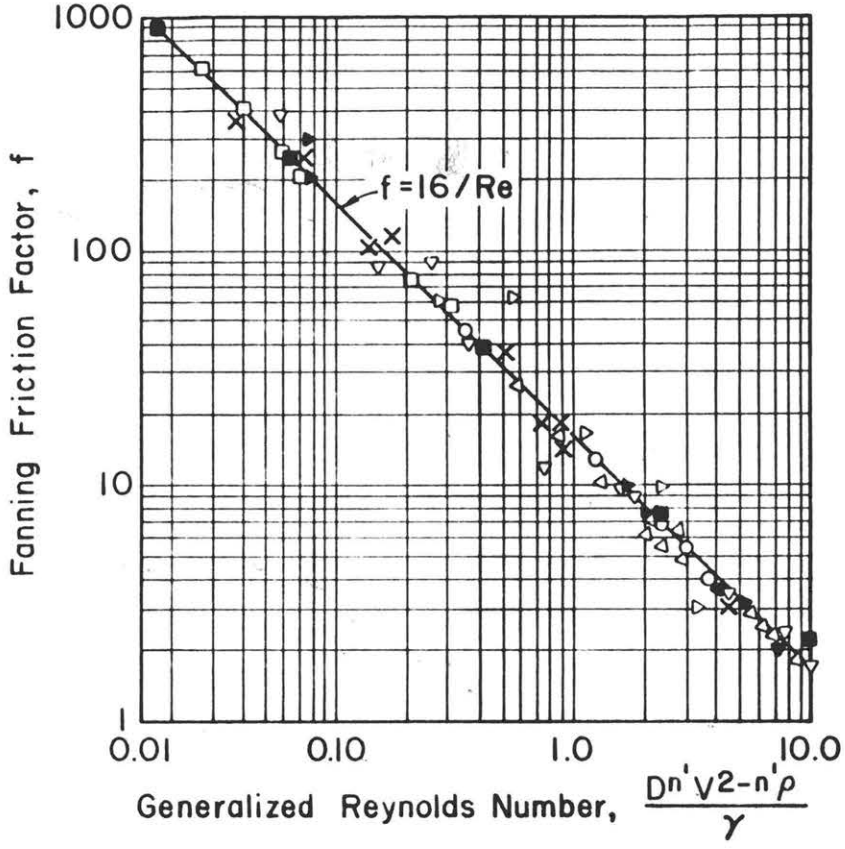

Figure 6-8. Friction Factor - Generalized Reynolds Number Correlation for Time-Independent Non-Newtonian Flow in Tubes (Medium Range of Re_{MR})

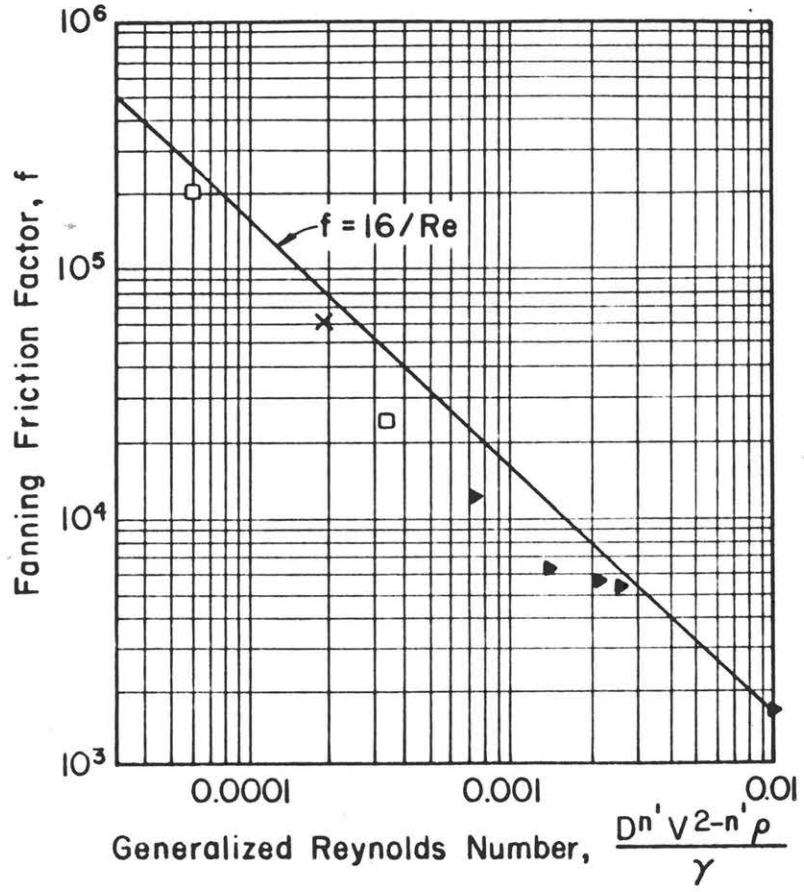

Figure 6-9. Friction Factor - Generalized Reynolds Number Correlation for Time-Independent Non-Newtonian Flow in tubes (Low Range of Re_{MR})

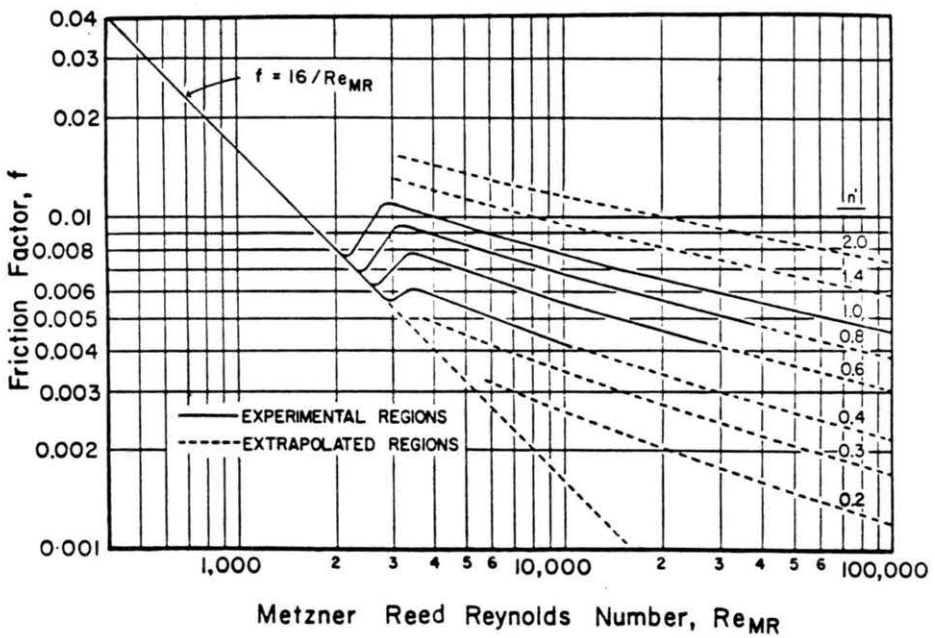

Figure 6-10. Friction Factor Relationships for Newtonian and Non-Newtonian Fluids (after Dodge and Metzner, 1962)

applicable also to the turbulent flow of other time-independent viscous non-Newtonians. Among these significant contributions of Dodge and Metzner (1959), Tomita (1959), Shaver and Merrill (1959), Clapp (1961), Torrance (1963), Thomas (1963), Daido(1970), and Dai et al. (1980) will be discussed in this section.

6.3.1. Resistance of Hyperconcentrated Flows in Smooth Pipes

The Shaver and Merrill Empirical Formula

An empirical formula similar to the Blasius's equation was developed by Shaver and Merrill (1959), who expressed the friction factor for a pseudoplastic fluid as

$$f_D = \frac{0.316}{n^{5} Re_{p2}^{\epsilon}} \tag{6.30}$$

where Re_{p2} is defined in Equation 6.8 and the exponent ϵ is defined as

$$\epsilon = \frac{2.63}{(10.5)^n}$$

Equation 6.30 was claimed applicable approximately in the range of $750 < Re_{p2} < 25,000$. Later inspection of Shaver and Merrill's experimental data indicates that Shaver and Merrill's equation is more favored to the viscoelastic fluids instead of pseudoplastics (Govier and Aziz, 1972).

The Dodge and Metzner Relations

Dodge and Metzner (1959) carried out a semi-theoretical analysis of the turbulent flow in smooth pipes of time-independent viscous non-Newtonian fluids described by the power law. Applying the techniques of dimensional

analysis for the power fluid, as Millikan (1939) has done for Newtonian fluids, they derived the important equation

$$\frac{1}{\sqrt{f}} = A'_{1n} \log\left[Re_{MR} f^{(1-n'/2)}\right] + C'_n \tag{6.31}$$

where $C'_n = A_{1n} \log\left[\frac{1}{8}\left(\frac{2+6n'}{n'}\right)^{n'}\right] + C_n$. The terms A_{1n} and C'_n are functions of n' to be determined experimentally. If $n'=1$, Equation 6.31 reduces to

$$\frac{1}{\sqrt{f}} = A\left(\log \frac{DV\rho}{\mu} \sqrt{f}\right) + C \tag{6.32}$$

which is of the same form as the Nikuradse equation, with A=4.0 and C=-0.4. For the power law fluids, Dodge and Metzner found empirically that

$$A_{1n} = \frac{4.0}{n'^{0.75}} \tag{6.33}$$

and

$$C'_n = -0.4/n'^{1.2} \tag{6.34}$$

This relationship is reflected in graphical form in Figure 6.10 taken directly from Dodge and Metzner. These authors indicate excellent agreement between calculated and experimental friction factors over values of n' from 0.36 to 1.0 and Re_{MR} from 2900 to 36,000 with solid-liquid suspensions and polymeric solutions. They show that non-power law clay suspensions also conform to the correlation provided that the exponent n' is evaluated at a stress corresponding with the wall shear stress.

The Tomita Relation

The Tomita relation is defined as a relation between the modified Fanning friction factor and a modified Reynolds number as follows:

$$\sqrt{1/f_T} = 4\ \ell og(Re_T\sqrt{f_T}) - 0.40 \tag{6.35}$$

where f_T and Re_T are the modified Fanning friction factor and Reynolds number, respectively defined as

$$f_T = \frac{1+2n}{1+3n}\left(\frac{4}{3}\right) f = -\frac{2DdP\ (1+2n)}{3\rho V^2\, dL\ (1+3n)} \tag{6.36}$$

and
$$Re_T = \frac{3}{4}\left(\frac{1+3n}{1+2n}\right) Re_{p2} = \frac{6\lceil(1+3n)/n\rceil^{1-n}}{2^n\lceil(1+2n)/n\rceil}\,\frac{D^n V^{2-n}\rho}{\eta_p} \tag{6.37}$$

for pseudoplastic fluids, and

$$f_T = \frac{f}{1-\chi} \tag{6.38}$$

and
$$Re_T = \frac{DV\rho}{\eta}\left[\frac{(1-\chi)(\chi^4-4\chi+3)}{3}\right] = \frac{(1-\chi)(\chi^4-4\chi+3)}{3}\,Re_B \tag{6.39}$$

for Bingham plastic fluids.

Tomita's relation is based on a similarity consideration and the Prandtl's mixing length theory. The approximate validity of this equation is confirmed by some 40 data points taken with starch pastes and lime slurries for pseudoplastics. For Bingham plastic fluids, this equation is confirmed over the range $2000<Re_T<100{,}000$ by twenty data points covering a good range of diameter, a sevenfold range of yield stress, but only a slight variation in coefficient of rigidity.

The Clapp Relation.

Based on the velocity distribution he derived from the mixing length approach, Clapp (1961) developed the following expression for the friction factor for power law fluids

$$1/\sqrt{f} = \frac{2.69}{n} - 2.95 + \frac{4.53}{n} \log(Re_c f^{1-n/2}) + \frac{0.68(5n-8)}{n} \qquad (6.40)$$

where

$$Re_c = \frac{8\rho V^2}{\eta_p (\frac{8V}{D})^n} = \frac{D^n V^{2-n} \rho}{8\eta_p^{n-1}} \qquad (6.41)$$

Equation 6.40 has been tested against the actual data for n values between .698 and 0.813 and for Re_c values between 5,480 and 42,800, with a maximum deviation of 4%.

The Torrance Relations.

An important analysis has been conducted by Torrance (1963) to the cases of yield-pseudoplastic fluids. By following the method of analysis of Clapp(1961) based on Prandtl's mixing length theory, Torrance obtained the relationship

$$\sqrt{1/f} = \left[(\frac{2.69}{n}) - 2.95\right] + \frac{4.53}{n} \log(1-\chi)$$

$$+ (\frac{4.53}{n} \log Re_c f^{1-n/2}) + \frac{0.68}{n}(5n-8) \qquad (6.42)$$

This general equation is represented graphically in Figures 6-11, 6-12, 6-13, and 6-14. For a power law pseudoplastic, Torrance's equation

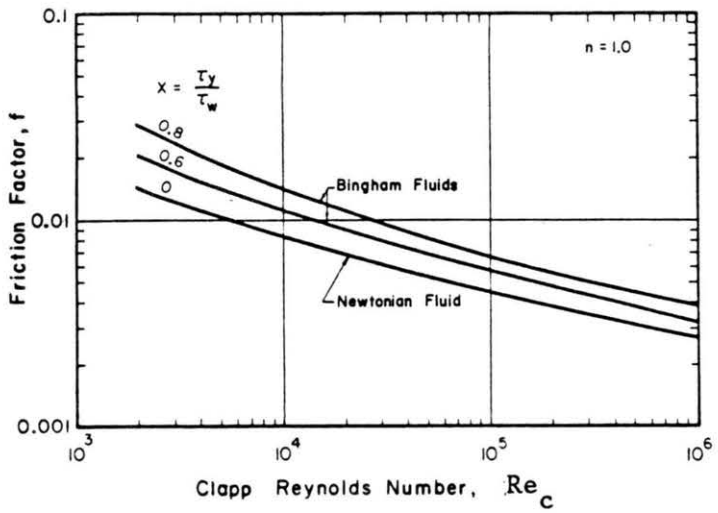

Figure 6-11. Friction Factors for Turbulent Flow of Newtonian and Bingham Fluids -- Torrance Equation

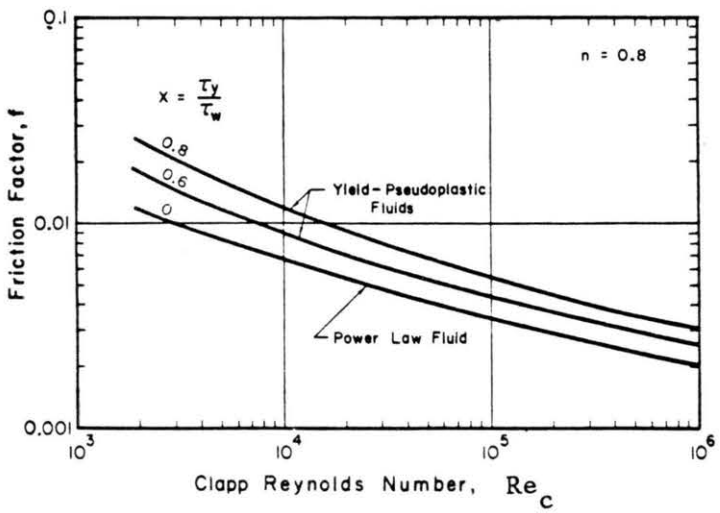

Figure 6-12. Friction Factors for Turbulent Flow of Yield-Pseudoplastic Fluids -- Torrance Equation

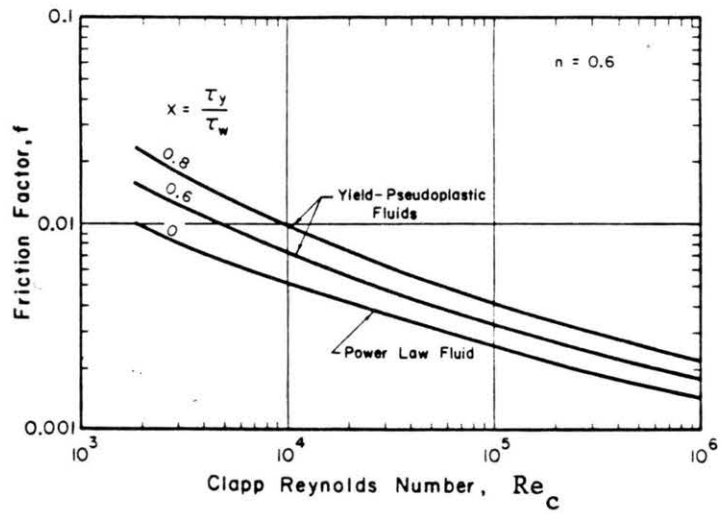

Figure 6-13. Friction Factors for Turbulent Flow of Yield-Pseudoplastic Fluids -- Torrance Equation

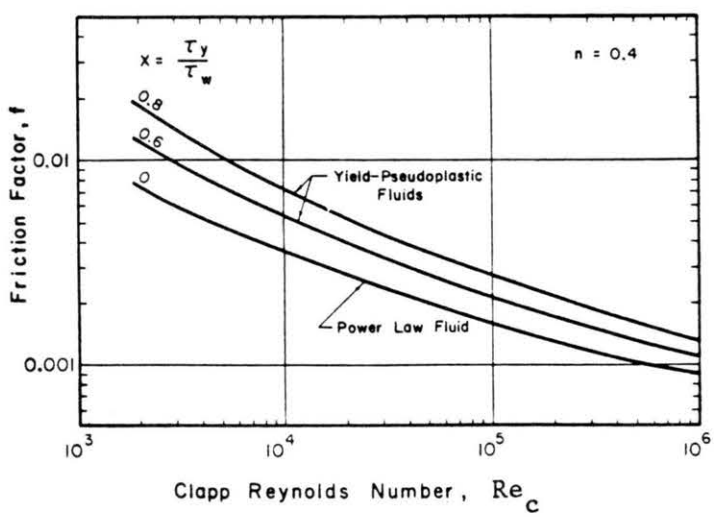

Figure 6-14. Friction Factor for Turbulent Flow of Yield-Pseudoplastic Fluids -- Torrance Equation

simplifies identically to Clapp's equation, i.e., Equation 6.40. For a Bingham plastic fluid, i.e., n=1 and $Re_c=Re_B$, Torrance's equation becomes

$$\sqrt{1/f} = 4.53\ \ell og(1-\chi) + 4.53\ \ell og(Re_B\sqrt{f}) - 2.3 \qquad (6.43)$$

In recent years, many semi-empirical equations have been proposed due to the arising of hyperconcentrated flow analysis, for instance, by Thomas (1963), Daido (1970), Dai et al (1980), Fei (1985). However, those equations are no different from the above discussed equations. Verifications from these authors, nevertheless, solidify the validity of these equations.

6.3.2. Resistance of Hyperconcentrated Flows in Fully Rough Pipes

Resistance of hyperconcentrated turbulent flows in fully rough pipes has yet received much attention so far. It is expected, however, that the friction factor depends no longer on the Reynolds number of the flows. Torrance (1963) extended his analysis on turbulent flow in smooth pipes of yield-pseudoplastic fluids to the fully rough wall turbulent flows in rough pipes which for the power law fluid gives

$$1/\sqrt{f} = \frac{4.07}{n}\ \ell og\ \frac{R}{k} + 6.0 - \frac{2.65}{n} \qquad (6.44)$$

where R is the pipe radius and k is the measure of roughness of the rough pipe. Equation 6.44 is not confirmed by experimental data but would appear suitable for the prediction of friction factors for the fully rough turbulent flows of power law yield-pseudoplastics, Bingham fluids, or simple pseudoplastics in rough pipes. If n=1, Equation 6.44 becomes exactly the same formula for Newtonian fluids. On the other hand, Zhang and Ren (1982)

pointed out that in fully developed turbulent flow in rough pipe the resistance of hyperconcentrated flows is exactly the same as that of a clear water flow.

VII. DISTRIBUTION OF CONCENTRATIONS IN HYPERCONCENTRATED FLOWS

Flowing water has the ability to suspend large quantities of sediment particles depending on the availability of sediment and the transport capacity of the flow. The sediment concentration profiles depends upon the turbulent intensity, viscosity of fluid, particle fall velocity, etc. As suspended sediment concentration increases the gradient of concentration profiles decreases until the profiles become uniform which generally occurs in mud or debris flow.

Sediment concentration profiles can be determined from convection-diffusion equation of sediment, in association with velocity profiles and fall velocity. In the following sections, a brief review will be given.

VII-1. Convection-Diffusion Equation for Sediment Suspension

A well-known convection-diffusion equation was first developed by Schmidt (1925), applying the sediment diffusion in a steady two-dimensional uniform flow. The derived equation is described in Equation 7.1.

$$\epsilon_s \frac{dC}{dy} + C\omega_0 = 0 \tag{7.1}$$

where C is the sediment concentration either by volume or by weight, ω_0 is the settling velocity of sediment particles in still water, and ϵ_s is the diffusion coefficient for sediment. The diffusion coefficient, ϵ_s, is generally a function of y that must be known before Equation 7.1 can be solved for C.

Hunt (1954) also developed a differential equation for the suspension of sediment in two-dimensional steady uniform flow. The result is a little different from Eq. 7.1.

$$\epsilon_s \frac{d C_v}{dy} + C_v \frac{d C_v}{dy} (\epsilon_w - \epsilon_s) + (1 - C_v) C_v \omega = 0 \qquad (7.2)$$

in which ϵ_w = the diffusion coefficient for water such that the rate of flow of water into a unit area normal to the velocity u is $u(1-C_v) - \epsilon_w \frac{\partial(1-C_v)}{\partial x}$; C_v = the sediment concentration by volume, and the other terms are defined previously. Here ω is the particle representative settling velocity in sediment-water mixture. When $\epsilon_w = \epsilon_s$, Eq. 7.2 becomes

$$\epsilon_s \frac{d C_v}{dy} + (1 - C_v) C_v \omega = 0 \qquad (7.3)$$

that was also derived by Halbronn (1949) and which differs from Eq. 7.1 only in that the second member contains the quantity $(1 - C_v)$, which results by taking into account of the continuity of sediment and water. When C_v is negligible compared with unity, Eq. 7.3 becomes the same as Eq. 7.1. in hyperconcentrated flows, however, Eq. 7.3 is considered better suited to describe diffusion of suspension of sediment than Eq. 7.1 because C_v is no longer negligible.

A complete set of diffusion equations for unsteady, nonuniform distribution of sediment in a two-dimensional or three-dimensional steady uniform flow has also been developed so far. The interested readers are referred to the ASCE Sedimentation Engineering Manual (1975), or Qian and Wan (1983) for detail.

VII-2. Equations for Distribution of Suspended Sediment in Turbulent Flows

As long as the diffusion coefficient, ϵ_s, and particle settling velocity, ω_0 or ω, are known, Eq. 7.1 or 7.3 can be integrated easily to obtain the equation for distribution of suspended sediment. Unfortunately,

unique equations describing ω and ϵ_s are still not available, which leads to a great diversity of equations for distribution of suspended sediment (Rouse, 1937; Kalinske, 1943; Ippen, 1971, Karim and Kennedy, 1983; Woo, 1985; etc.).

7.2.1. Rouse's Equation

Based on the following assumptions:

(1) particle settling velocity is not affected by sediment concentration, i.e., $\omega = \omega_0$ is a constant;

(2) velocity profile is described by the universal log-law (Eq. 5.14);

(3) only turbulent shear stress is considered in the rheological model; and

(4) sediment diffusion coefficient, ϵ_s, can be approximated by coefficient for momentum exchange of fluid as

$$\epsilon_s = \beta \epsilon_m \tag{7.4}$$

with β as a numerical constant, Rouse found that

$$\epsilon_s = \beta \kappa U_* \frac{y}{H} (H - y) \tag{7.5}$$

Substituting Eq. (7.5) into Eq. 7.1 and separating the variable and integrating gives

$$\frac{C}{C_a} = \left(\frac{H-y}{y} \frac{a}{H-a}\right)^z \tag{7.6}$$

in which C_a denotes the concentration of sediment with settling velocity ω_0 at the level, y = a, and

$$z = \frac{\omega_o}{\beta \kappa U_*}$$

7.2.2. Karim and Kennedy's Equation

Instead of using log-law velocity distribution to derive the diffusion coefficient for sediment, Karim and Kennedy used a power-law velocity distribution as follows

$$\frac{u}{V} = n_1 \cdot \xi^{n_2} \tag{7.7}$$

where $\xi = y/H$ is the dimensionless depth; coefficients n_1 and n_2 depend on the flow characteristics. It was derived by Zimmermann and Kennedy (1978) that $n_1 = n_2 + 1$ and $n_2 = U_*/\kappa V$, where V is the average flow velocity for open channel flow. From here the diffusion coefficient is derived as

$$\frac{\epsilon_s}{H\ U_*} = \frac{\beta\ U_*}{n_1 n_2\ V} (1 - \xi)\ \xi^{1-n_2} \tag{7.8}$$

Substituting Eq. (7.8) into Eq. (7.1) and separating the variables gives

$$\frac{1}{C} \frac{dC}{d\xi} + \left[\frac{Z_k}{(1-\xi)\ \xi^{1-n_2}} \right] = 0 \tag{7.9}$$

where

$$Z_k = \frac{n_1 n_2\ V\omega_o}{\beta\ U_*^2}$$

Integration of Eq. (7.9) yields

$$\ell n \frac{C}{C_a} = - Z_k \int_a^{\xi} \frac{d\xi}{(1-\xi)\ \xi^{1-n_2}} \tag{7.10}$$

of which the right hand side has been expanded into a series integration to give

$$\frac{C}{C_a} = \exp - Z_k \left[\sum_{j=0}^{\infty} \frac{\xi_a^{j+n_2} - \xi^{j+n_2}}{j+n_2} \right] \tag{7.11}$$

7.2.3. Woo's Modified Equation

In Woo's method (1985), Hunt's diffusion equation (Eq. 7.3) is preferred to Schmidt's formulation because it satisfies continuity of fluid and sediment. On the other hand, the effect of concentration on the fall velocity of particle and increased viscosity of suspension is considered in the derivation. Here, Eq. (4.13) is applied to determine the fall velocity, ω, of the mixture and Eq. (2.10) with neglection of yield stress and dispersive shear stress is used to evaluate shear stress in sediment-laden turbulent flow. Noting

$$\epsilon_m = \ell_m^2 \left| \frac{du}{dy} \right| \tag{7.12}$$

then the total shear stress τ is rewritten as

$$\tau = \rho\ \epsilon_m\ (A\ C_v + 1)\ \frac{du}{dy} + \eta\ \frac{du}{dy}$$

or

$$\tau = \rho\ \epsilon_m\ (1 + A\ C_v)\ \frac{du}{dy} + g(C_v)\ \mu\ \frac{du}{dy} \tag{7.13}$$

where A is a correlation factor = $\frac{\rho_s - \rho}{\rho}$; and $g(C_v)$ is a function of concentration determined from the evaluation of viscosity of mixture in Chapter 3. In Woo's study, Thomas' equation is used to give

$$g(C_v) = 1 + 2.5\ C_v + 10.05\ C_v^2 + 0.00273 \exp\ (16.6\ C_v) \qquad (7.14)$$

On the other hand, the total shear stress τ depends on the unit weight of the suspension γ_m and the energy gradient S_e of the flow,

$$\tau = \int_y^H \gamma_m\ S_e\ dy$$

$$= \int_y^H (1 + A\ C_v)\ \frac{\rho\ U_*^2}{H} \cdot dy$$

$$= \rho\ U_*^2\ (\ 1 - \xi + A \int_\xi^1 C_v\ d\xi) \qquad (7.15)$$

Equating Eqs. (7.13) and (7.15), the diffusion coefficient, ϵ_s, is obtained from the fluid momentum diffusivity, ϵ_m, according to the Reynolds analog ($\epsilon_s = \beta\ \epsilon_m$)

$$\epsilon_s = \beta \left[\frac{U_*^2\ (1 - \xi + A \int_\xi^1 C_v\ d\xi)}{\frac{du}{dy}\ (1 + A\ C_v)} - \frac{\nu\ g(C_v)}{1 + A\ C_v} \right] \qquad (7.17)$$

The vertical distribution of sediments in suspension is then obtained after substituting the turbulent diffusion coefficient (Eq. 7.17) and the representative fall veocity (Eq. 4.13) into the diffusion equation (Eq. 7.3).

$$\frac{d\,C_v}{dy} = \frac{\omega_0}{\beta}\left[\frac{\frac{du}{dy}\,f(C_v)}{\nu\,g(C_v)\,\frac{du}{dy} - U_*^2\,(1 - \xi + A\int_\xi^1 C_v\,d\xi)}\right] \tag{7.18}$$

in which $f(C_v) = C_v(1 - C_v)^{\alpha+1}\,(1 + A\,C_v)$. Equation (7.18) is claimed of general applicability by Woo et al. (1988) and can be solved, provided the velocity profiles is accurately depicted. Woo (1985) gave numerical solutions to both log-law and power-law velocity distributions. For flows with low sediment concentration, a few terms in Eq. (7.18) can be simplified or neglected: (1) $f(C_v) = C_v(1 - C_v)^{\alpha+1}(1 + A\,C_v) \simeq C_v$; (2) $A\int_\xi^1 C_v\,d\xi \simeq 0$. Then Eq. (7.18) reduces to Karim and Kennedy's equation (Eq. 7.9) after viscous shear stress is neglected and power-law velocity profiles is used, while it reduces to Rouse's equation when log-law velocity distribution is used.

7.2.4. Comparison of Sediment Concentration Profiles with Experimental Data

Theoretical sediment concentration profiles from Rouse, Karim and Kennedy, and Woo are compared with flume data collected by Einstein and Chien (1955) including seven runs with local volumetric sediment concentrations between 4% and 23% (Woo et al., 1988). For Woo's method, both log-law and power-law velocity distributions are used. The results are presented in Figures 7-1 and 7-2. It is clear that Woo's method gives excellent results in agreement with the measurements of Einstein and Chien, while Rouse's and Karim and Kennedy's profiles remain far from the observed profiles.

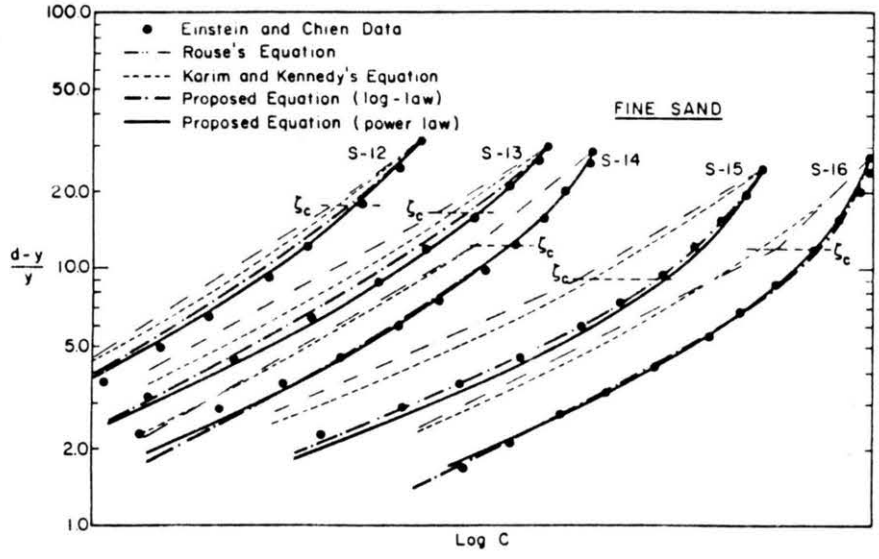

Figure 7-1. Concentration Profiles at Large Concentration of Fine Sands (after Woo et al., 1988)

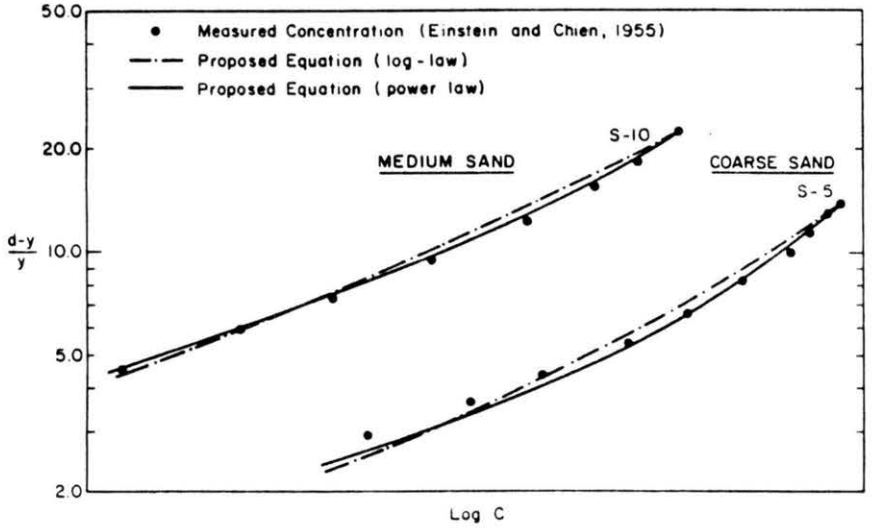

Figure 7-2. Concentration Profiles at Large Concentrations of Medium and Course Sands (after Woo et al., 1988)

VIII. CONCLUSIONS

The physical and kinematic behavior of hyperconcentrations has been delineated in this report with the ultimate objective to summarize recent and past developments in hyperconcentrated flow research. This report, emphasis is the laboratory analysis of hyperconcentrations, and particularly, flow classification, rheological models, settling velocity of particles, velocity profiles and concentration profiles. The following conclusions have been obtained from this study.

The current classifications of hyperconcentrated flows are based on sediment concentration, composition and triggering mechanism, rather than the rheological behavior of the suspension. Many classification schemes are available, but none can satisfactorily describe such a complex flow phenomenon. The rheological behavior of hyperconcentrations should be better understood before promoting a comprehensive classification. Meanwhile, the classification schemes by Beverage and Culbertson (1964) and Pierson and Costa (1984) seem the most appropriate.

Grain movement in hyperconcentrated flows can generally be classified into contact load or bedload, suspended load, and neutral buoyant load. Different from grain movement in ordinary sediment-laden flow, the interaction between particles in the suspension plays an important role in determining the flow kinematics.

Hyperconcentrated flows behave differently from crystal clear water flows and ordinary sediment-laden flows because of the non-Newtonian rheological nature of the suspensions. Therefore, a successful analysis of hyperconcentrated flows depends on the description of the rheological properties of hyperconcentrations. Many rheological models have been proposed to describe the non-Newtonian behaviors of hyperconcentration. The

generalized Metzner and Reed model has been so far very successful in modeling time-independent purely viscous flow, but it has not been tested against flows with high dispersive shear stress. Consequently, the Bingham-plastic model, the yield-pseudoplastic model, and the quadratic model seem most promising at this time.

The rheological properties of hyperconcentrations are generally determined from the rheograms which are obtained by viscometric measurements. Three kinds of commercial viscometers are readily available: the capillary viscometer, the concentric cylindrical viscometer, and the cone-and-plate viscometer. Concentric cylindrical viscometer seems to be best suited for a wide range of shear rates.

Rheological properties of hyperconcentrations are also formulated as functions of sediment concentration along with several coefficients to be determined by experiments. The most frequently applied empirical formulae are the exponential forms relating yield stress and viscosity versus the concentration, and the Bagnold's equation to calculate the dispersive shear stress.

Settling of sediment particles in hyperconcentration is classified into two categories: settling in mixture of fine and/or coarse particles and collective settling in mixture of coarse particles. In the first category, the available methods to predict the settling velocity include approaches from Plessis and Ansley, Ansley and Smith, Valentik and Whitmore, and Pazwash. These approaches are generally based upon the assumption that the suspension acts as a uniform suspension. In the second category, it is found that Chu's formula is the best to predict the settling velocity of non-flocculated sediment in hyperconcentration.

The effect of hyperconcentrations on the velocity distribution is reflected in the changes of rheological properties. In laminar flows, the

velocity profiles are easily obtained by combining the momentum equation and the rheological equation. The obtained velocity profiles are listed in Tables 5-1 and 5-2. A general phenomenon found here is the "plugging" of flow at the central part of a pipe or the upper part of an open channel, due to the existence of yield shear stress in the suspension. In turbulent flows, theoretical results for the velocity distributions are still impossible, mainly because the effect of sediment concentration on the change of turbulence is not well understood. However, the universal log-law (or its modifications) seem to be applicable to turbulent hyperconcentrated flows unless the flows become a "plug"as a whole.

Resistance of hyperconcentrated flows, expressed as Fanning or Darcy-Weisbach friction coefficients, is obtained by integrating the velocity distribution over the cross-section of the pipe or channel. In laminar flow the friction factor is found always larger in hyperconcentrated flows than in clear-water flows. In turbulent hyperconcentrated flows, the theoretical or semi-empirical formulae for friction factor generally resemble the counterparts for a Newtonian fluid. In a smooth boundary pipe or channel, the friction factor depends on the rheological properties of the suspension and the flow Reynolds number, while in a fully rough wall the friction factor is a function of relative roughness of wall as well as the rheological properties of the fluids. In a partially rough wall, the friction factor depends on Reynolds number, relative roughness, and the rheological properties of the flows. Many empirical or semi-empirical formulae have been developed and reviewed in this report although none of them is considered general.

Concentration profiles in hyperconcentrated flows with low concentration of fine sediments can be obtained by solving the convection-diffusion equation for sediment suspension. In order to achieve this,

accurate prediction of velocity profiles and settling velocity of particle must be available. With relative high sediment concentration in flows, concentration profiles can be well predicted by Rouse' formula, Karim and Kennedy's formula, and also Woo's modified method. Unfortunately, these methods haven't been tested against hyperconcentrated flows with large concentration of fine sediments.

In summary, research on hyperconcentrations is still at its early stage. A great effort must be committed in order to understand the rheology and transport mechanism of hyperconcentration. Since the rheology of hyperconcentrations is so essential in determining other behaviors of the flows, it is suggested that study on rheology must be emphasized first. Perhaps additional researches could then be pursued on the sediment transport mechanism, and on the pulsating phenomenon observed in hyperconcentrations.

REFERENCES

Alves, G.E., D. F. Boucher and R.L. Pigford, 1952. Chem. Eng. Progress, Vol.48, p. 385.

Ansley, R.W. and T.N. Smith, 1967. Motion of spherical particles in Bingham plastics, A.I.Ch.E. Journal, Vol.13, No.6, Nov.

ASCE, 1975. Sedimentation Engineering, ed. V.A. Vanoni, Manuals and Reports on Engineering Practice - No. 54, Chapter II.

Bagnold, R.A., 1954. Experiments on a gravity-free dispersion of large solid spheres in a Newtonian fluid under shear. Proc. of the Royal Soc. of London, Series A, Vol.225, pp. 49-63.

Beverage, J.P. and J.K. Culbertson, 1964. Hyperconcentrations of suspended sediment, Journal of Hydraulic Div., ASCE, Vol.90, No.6, pp. 117-128.

Bingham, E.C., 1922. Fluidity and Plasticity, McGraw-Hill Book Co., New York.

Bradley, J.B. and S.C. Mecutcheon, 1985. The effects of high sediment concentration on transport processes and flow phenomena. International Symposium on Erosion, Debris Flow and Disaster Prevention, Sept. 1985, Japan, pp. 219-225.

Bogue, D.C. and A.B. Metzner, 1963. Ind. Eng. Chem. Fundam., Vol.2, p. 143.

Bruhl, H. and I. Kazanskij, 1976. New results concerning the influence of fine particles on sand-water flows in pipes. Proc. of Hydrotransport, No.4, pp. B2-19-25.

Calderbank, P.H. and M.B. Moo-Young, 1959. Prediction of power consumption in agitation of non-newtonian fluids, Trans. Inst. Chem. Engrg., Vol.37, No.1, pp. 26-33.

Caldwell, D. H. and H.F. Babbit, 1941. Ind. Eng. Phem., Vol.33, p. 249.

Cao, R., et al., 1983. The law of hydraulic resistance in density current with hyperconcentration. Proc. 2nd Int'l Symposium on River Sedimentation, October, 1983, Nanjing, China, pp. 65-66.

Chen, C.L., 1983. On-frontier between rheology and mud flow mechanism, Proc. ASCE, Hydraulic Div. --Specialty Conference, Boston, MA, Aug. 1983, pp. 113-118.

Chen, C.L., 1985. Hydraulic concepts in debris flow simulation. Proc. of the Specialty Conference on Delineation of Landslides, Flash Flood and Debris Flow Hazards in Utah, Logan, Utah, June, 1984, pp. 236-259.

Chu, J., 1983. Basic characteristics of sediment-water mixture with high concentration. Proc. 2nd Int'l Symposium on River Sedimentation, Nanjing, China, 1983, pp. 265-273.

Clapp, R.M., 1961. Conf. on Int'l Developments in Heat Transfer, University of Colorado, Boulder, Col., Proc., p. 652.

Coleman, N.L., 1981. Velocity profiles with suspended sediment. Journal of Hydraulic Research, No.3, pp. 219-225.

Coles, D., 1956. The law of the wake in the turbulent boundary layer. J. Fluid Mechanics, vol.1, pp. 191-226.

Costa, J.E., 1984. Physical geomorphology of debris flows. Development and Applications of geomorphology, (Eds. J.E. Costa and P.J. Fleisher), Springer-Verlag, Berlin, pp. 268-317.

Costa, J.E. and R.D. Jarrett, 1981. Debris flow in small mountain stream channels of colorado and their hydrologic implications, Bulletin of the Association of Engineering Geologists, Vol.XVIII, No.3, pp. 309-322.

Cross, M.M., 1965. Rheology of non-Newtonian fluids-New flow equation for pseudoplastic systems. J. Colloid Sci., Vol.20, pp. 417-437.

Daido, A., 1971. On the occurrence of mud-debris flow, Disaster Prevention Research Institute, Bulletin, Kyoto University, Vol.21, pp. 169-175.

Dodge, D.W. and A.B. Metzner, 1959. A.I.Ch.E. Journal, Vol.5, p. 189.

Dodge, D.W. and A.B. Metzner, 1962. A.I.Ch.E. Journal, Vol.8, p. 143.

Einstein, H.A. and N. Chien, 1955. Effects of sediment concentration near the bed on the velocity and sediment distributions. M.R.D. Sediment Series No.8, Missouri River Division, Corps of Engineers, p. 76.

Engelund, F. and Z. Wan, 1984. Instability of hyperconcentrated flow, J. Hydraulic Engineering, ASCE, Vol.110, No. HY3, pp. 219-232.

Eyring, H.J., 1936. J. Chem. Phys., Vol.4, p. 283.

Fan, J. and G. Dou, 1980. Sediment transport mechanism. Proc. 1st International Symposium on River Seddimentation, Beijing, China, pp. 1167-1177.

Fei, X., 1983. Grain composition and flow properties of heavily concentrated suspension. Proc. 2nd Int'l Symposium on River Sedimentation, Nanjing, China, 1983, pp. 307-308.

Folk, R.L. and W.C. Ward, 1957. Brazos River bar: a study in the significance of grain size parameters, Journal of Sedimentary Petrology, Vol.27, No.1, pp. 3-26.

Frankel, N.A. and A. Acrivos, 1967. On viscosity of concentrated suspension of solid spheres. Chem. Eng. Sci., Vol.22, pp. 847-853.

Ginn, R.F. and A.B. Metzner, 1969. Trans. Soc. Rheol., Vol.13, p. 429.

Govier, G.W. and K. Aziz, 1972. The Flow of Complex Mixtures in Pipes. Van Nostrand Reinhold Company, 1972.

Govier, G.M., et al., 1957. Rheological properties of water suspension of finely subdivided magnetite, galena, and ferrosilicon. Trans. Can. Inst. Mining Met., Vol.60, p. 147,

Grisky, R.G. and R.G. Green, 1971. A.I.Ch.E. Journal, Vol.17, p. 725.

Halbronn, G., 1949. Remarque sue la théorie de L'Austausch appliquée au transport des matériaux suspension, Proc. Int. Assoc. of Hydr. Res., 3rd Meeting, pp. 1-6.

Hanks, R.W., 1963. The laminar-turbulent transition for fluids with a yield stress, Journal of A.I.Ch.E., Vol.9, No.3, pp. 306-309.

Hanks, R.W., 1968. On the theoretical calculation of friction factors for laminar, transitional, and turbulent flow of Newtonian fluids in pipes and between parallel plane walls. Journal of A.I.Ch.E., Vol.14, No.5, pp. 691-695.

Hanks, R.W. and E.B. Christiansen, 1962. Laminar-turbulent transition in nonisothermal flow of pseudoplastic fluids in tubes, A.I.Ch.E. Journal, Vol.8, pp. 467-471.

Hanks, R.W. and D.R. Pratt, 1967. On flow of Bingham plastic slurries in pipes and between parallel plates, Soc. Petrol. Engrs. Journal, Vol.7, No.4, pp. 342-346.

Hedstrom, B.O.A., 1952. Ind. Eng. Chem., Vol. 44, pp. 651-656.

Hershel, W.H. and R. Bulkley, 1926. Measurement of consistency as applied to rubber-benzene solutions, A.S.T.M. Proc., Vol.26, p. 621.

Herzog, R.L. and K. Weissenberg, 1928. Kolloid-Z., Vol.46, p277.

Higgins, J.D., Naik, B., et al., 1983. The Mechanism of Mud Flow. State of Washington Water Research Center.

Hou, H. and Z. Yang, 1983. Effects of fine-sediments on the drag reduction in muddy flow. Proc. 2nd Int'l Symposium on River Sedimentation, Nanjing, China, pp. 47-80.

Hunt, J.N., 1954. The turbulent transport of suspended sediment in open channels, Proc. Royal Society of London, Series A, Vol. 224 (1158), pp. 322-335.

Julien, P.Y. and Y.Q. Lan, 1989. On the rheology of hyperconcentrated flows. J. Hydraulic Engineering, ASCE, (in publication).

Julien, P.Y. and Y.Q. Lan, 1988. Discussion on "Simple model of sediment laden flows, by Parker and Coleman," J. Hydraulic Engrg., ASCE, Vol.14, No.2.

Karim, F. and J.F. Kennedy, 1983. Missouri River computer-based predictors for sediment discharge and friction factors of alluvial streams, MRD Sediment Series, No.29, U.S. Army Corps of Engineers, Missouri River, MO.

Kikkawa, H. and S. Fukuoka, 1969. The characteristics of flow with wash load, Proc. 13th Cong., International Assoc. Hydraulic Research, Vol.2, pp. 223-240.

Krieger, I.M. and S.H. Maron, 1954. J. Appl. Phys., Vol.25, p. 72.

Landel, R.F., B.G. Moser and A.J. Bauman, 1965. Fourth Int. Congress on Rheology, Brown Univ. (1963), Proc. Part 2, p. 663, Interscience Publishers, New York.

Lau, Y.L., 1983. Suspended sediment effects on flow resistance. Journal of Hydraulic Engineering, ASCE, Vol.109, No.5, pp. 757-763.

Lowe, D.R., 1976. Grain flow and grain deposits, Journal of Sedimentary Petrology, Vol.46, March, pp. 188-199.

Meister, B.J. and R.B.Biggs, 1969. Prediction of the first normal stress difference in polymer solutions, A.I.Ch.E. Journal, Vol.15, No.5, pp. 643-653.

Meter, D.M. and R.B. Bird, 1964. Tube flow of non-Newtonian polymer solutions, A.I.Ch.E. Journal, Vol.10, No.6, pp. 878-884.

Metzner, A.B. and M.G. Park, 1964. Turbulent flow characteristics of visco-elastic fluids. Journal of Fluid Mech., Vol.20, pp. 291-303.

Metzner, A.B. and J.C. Reed, 1955. Flow of non-Newtonian fluids-correlation of laminar, transition, turbulent flow regions, A.I.Ch. E. Journal, Vol.1, No.4, pp. 434-440.

Metzner, A.B. and M. Whitlock, 1958. Trans. Soc. Rheol., Vol.2, p. 239.

Mills, A.V., 1983. An Experimental Study of the Rheology of Mud Flows. Master thesis, Washington State University, Washington

Mooney, M.J., 1931. J. Rheology, Vol.2, p. 210.

Montes, J.S. and A.J. Ippen, 1973. Interaction of two-dimensional turbulent flow with suspended particle, Rep. No. 164, Lab, Water Resources and Hydrodynamics, MIT, Jan.

O'Brien, J.S., 1986. Physical processes, rheology and modelling of mudflows. Ph.D. dissertation, Dept. Civil Engineering, Colorado State University.

O'Brien, J.S. and P.Y. Julien, 1984. Physical properties and mechanism of hyperconcentrated sediment flows. Proc. of the Specialty Conference on Delineation of Landslides, Flash Flood and Debris Flow Hazards in Utah, Logan, Utah, June, 1984.

O'Brien, J.S. and P.Y. Julien, 1988. Laboratory analysis of mudlfow properties, J. Hydraulic Engineering, ASCE, Vol.114, No.8, pp. 877-887.

Pai, S.I., 1957. Viscous Flow Theory, Vol.II, Turbulent Flow, (a)p. 36; (b)p. 43, D. Van Nostrand Co., Princeton, New Jersey.

Parker, G. and N.L. Coleman, 1986. Simple Model of sediment laden flows. J. Hydraulic Engineering, ASCE, Vol.112, No.5, pp. 356-375.

Pazwash, H., 1970. Drag forces on bodies moving through aqueous clay suspensions, Ph.D. dissertation, University of Illinois.

Philippoff, W., 1935. Kolloid-Z., Vol.71, p. 1.

Pierson, T.C. and J.E. Costa, 1984. A rheological classification of subaerial sediment-laden flows. Abstracts with Programs, 97th Annual Meeting of the Geological Soc. of America, Vol.16, No.6.

Pierson, T.C. and K.M. Scott, 1985. Downstream dilution of a lahar: transition from a debris flow to hyperconcentrated streamflow, Water Resources Research, AGU, Vol.21, No.10, pp. 1511-1524.

du Plessis, M.P. and R.W. Ansley, 1967. Settling parameters in solid pipelining. J. Pipeline Div., ASCE, Vol.93, July, 1967, pp

Prandtl, L., 1928. E. Angew. Math. Mech. Vol.8, p. 85.

Qian, N. and Z. Wan, 1983. Dynamics of Sediment Movement, Academy Press, China (in Chinese).

Qian, N. and Z. Wan, 1986. A Critical Review of the Research on the Hyperconcentrated Flow in China. IRTCES Publish Series, Int'l Res. Training Center on Erosion and Sedimentation, 1986.

Qian, N. and Z. Wang, 1984. A preliminary study in the mechanism of debris flows. Acta Geographica Sinica, Vol.39, No.1, (in Chinese).

Qian, Y., et al., 1980. Basic characteristics of flow with hyperconcentration of sediment. Proc. 1st Int'l Symposium on River Sedimentation, Beijing, China, pp. 175-184.

Rabinowitsch, B., 1929. E. Physik. Chem., Series A, Vol.145, p. 1.

Reiner, M., 1949. Deformation and Flow, Lewis, London.

Reiner, M., 1960. Deformation, Strain, and Flow, Interscience, New York, p. 246.

Richardson, J.F. and W.N. Zaki, 1954. Sedimentation and fluidizations, part 1. Trans. Inst. Chem. Engrg., Vol. 32, No.1.

Rouse, H., 1937. Modern conceptions of the mechanics of fluid turbulence, Trans. ASCE, 102, pp. 463-543.

Ryan, N.W., and M.M. Johnson, 1959. A.I.Ch.E. Journal, Vol.5, p. 533.

Savage, S.B. ,1979. Gravity flow of cohesionless granular materials in chutes and channels. Journal of Fluid Mechanics, Vol.93, part 1, pp. 53-96.

Savage, S.B. and S. Mckeown, 1983. Shear stresses developed during rapid shear of concentrated suspension of large spherical particles between concentric cylinders. J. Fluid Mechanics, Vol.127, pp. 453-472.

Schlichting, H., 1955. Boundary Layer Theory, McGraw-Hill Book, Co., New York.

Schmidt, W., 1925. Der massenaustausch in freier luft und verwandte erscheinungen, Probleme der Kosmischen Physik, 7, Hamburg, Germany (in German).

Shaver, R.G. and E.W. Merrill, 1959. Turbulent flow of pseudoplastic polymer-solutions in straight cylindrical tubes, American Inst. of Chem. Engrs. Journal, Vol. 5(2), pp. 181-188.

Sisko, A.W., 1958. Flow of lubricating greases, Ind. and Eng. Chem., Vol.50, No.12, pp. 1789-1792.

Skelland, A.H.P., 1967. Non-Newtonian Flow and Heat Transfer. John Wiley and Sons, Inc., New York.

Street, N., 1958. Viscosity of clay suspensions, World Oil, No.107, pp. 151-156.

Takahashi, T., 1978. Mechanical charateristics of debris flow, Journal of Hydraulics Div., ASCE, Vol.104, pp. 1153-1169.

Takahashi, T., 1980. Debris flow on prismatic open channel, Journal of Hydraulics Div., ASCE, Vol.106, No.HY3, pp. 381-396.

Thomas, D.G., 1963. Non-Newtonian suspensions. Ind. and Engr. Chem., Vol.55, No.11, pp.

Tomita, Y., 1959. On fundamental formula of non-Newtonian flow, Bulletin, J.S.M.E., Vol.2, No.7, pp. 469-474.

Tomita, Y., 1961. Analytical Treatment of non-Newtonian fluid flow by introducing concept of boundary layer, Bulletin, J.S.M.E., Vol. 4, No.13, pp. 77-86.

Torrance, B. McK., 1963. Friction factor for turbulent non-Newtonian fluid flow in circular pipes, South African Mechanical Engineer, Vol.13, No.4, pp. 89-91.

Yue, P., 1983. A preliminary research on sediment settling velocity in quiescent sediment-laden mixture. J. Sediment Research, No. 4, pp. 66-74. (in Chinese).

Varnes, D.J., 1958. Landslides type and process, Chap. 3 in Landslides and Engineering Practice, (ed. E. B. Eckel), Highway Research Board Special Report 29, Committee on Landslides Investigations, National Academy of Science - National Research Council Publication 544.

Varnes, D.J., 1978. Slope movement types and processes, landslides: Analysis and control, Trans. Res. Bd. Spec. Rep. 176, Nat. Acad. of Sci., Washington, D.C.

Valentik, L. and R.L. Whitmore, 1965. The terminal velocity of spheres in Bingham plastics, British J. of Applied Physics, Vol.16, pp. 1197-1203.

Vanoni, V.A., 1946. Transportation of suspended sediment by water, Transaction of ASCE, Vol.III, Paper No.2267.

Vanoni, V.A. and G.N. Nomicos, 1960. Resistance properties of sediment laden streams. Trans. Amer. Soc. Civil Engr., Vol.125, pp. 1140-1175.

Wan, Z., 1982. Bed material movement in hyperconcentrated flow, Series Paper 31, Inst. of Hydrodynamics and Hyd. Eng., Tech. Univ. of Denmark, 79 p.

Wilhelm, R.H., D.M. Wroughton and W.F. Loeffel, 1939. Ind. Eng. Chem., Vol.31, p. 622.

Woo, H., 1985. Sediment Transport in Hyperconcentrated Flow, Ph.D. dissertation, Dept. Civil Engineering, Colorado State University.

Woo, H.S., P.Y. Julien and E.V. Richardson, 1988. Suspension of large concentrations of sands, J. Hydraulic Engineering, ASCE, Vol.114, No.8, pp. 888-898.

Xu, M. and D. Wu, 1983. The analysis of settling characteristics of a spherical particle in Bingham fluid. J. Hydraulic Engineering, No. 11, pp. 29-36 (in Chinese).